EXERGY ANALYSIS OF COMBINED FUEL PROCESSOR – FUEL CELL SYSTEM

by

Cüneyt Şeyban

B.S., Chemical Engineering, Yıldız Technical University, 2002

Submitted to the Institute of Graduate Studies in
Science and Engineering in partial fulfillment of
the requirements for the degree of
Master of Science

Graduate Program in Chemical Engineering

Boğaziçi University

2008

ACKNOWLEDGEMENTS

Firstly, I would like to express my truthful gratitude to my thesis supervisors, Prof. Dr. Ahmet Erhan Aksoylu and Prof. Dr. Mahir Arıkol for their guidance and understanding. My respect and admiration in their personality as well as their invaluable way of teaching inspired me all the time. It was a great opportunity for me to learn from their experiences and knowledge. It was a privilege for me to work with Prof. Dr. Aksoylu and Prof. Dr. Arıkol during my MS thesis.

I would like to thanks to Feyza Gökaliler, Burcu Selen-Çağlayan and Eyüp Şimşek for their valuable support, for their everlasting help and for sharing their scientific background with me.

Finally, I think that no words or phrases can be used to thank to my family – closest of the closest and best of the best. This thesis would not have been possible without their everlasting support.

ABSTRACT

EXERGY ANALYSIS OF COMBINED FUEL PROCESSOR – FUEL CELL SYSTEM

Exergy analysis and energy efficiency of a combined fuel processor-fuel cell system was performed. Experimental data were used for the performances of the ATR, WGS and PROX catalytic reactors assuming that the concentrations of the outlet streams obtained at the laboratory experiments can be achieved at the exit of the reactors. The catalyst performance data for IPOX reactor for pure propane, 50% propane – 50% butane and 75% propane – 25% butane feeds at different temperatures have been obtained from experimental works conducted in Catalyst Technology and Reaction Engineering Laboratory. The conversion level of the water-gas shift reactor was assumed as 70% of the equilibrium conversion at the corresponding reactor temperature level. 100% CO selectivity and 100% CO conversion were accepted for preferential oxidation reactor by using the above experimental results.

Output composition from each reactor was based on the experimental data obtained from the experiments. Once mass flow rates were calculated for each stream, energy balances were carried out to calculate unknown outlet temperatures as well as the temperatures of the other units present in the combined system. The fuel cell conversions in the calculations were taken in the range of 75% - 85%. After all the streams in the system were determined, exergy balances were calculated for each unit and also for the whole system. The overall system exergy efficiencies were calculated as a function of IPOX reactor temperature. According to the results of this study, when IPOX reactor output temperature increased, except at 743 K, exergy efficiency of the system increased. Exergy analysis indicated that water-gas shift and preferential oxidation reactors have a minimum impact on the overall exergy of the system. The energy efficiency of the whole system was found sensitive to the methane content and the temperature level of the exhaust stream from the system.

ÖZET

BİRLEŞİK YAKIT ÜNİTESİ-YAKIT PİLİ SİSTEMİNİN EKSERJİ ANALİZİ

Birleşik bir yakıt ünitesi-yakıt pili sisteminin ekserji analizi ve verimlilik hesabı yapılmıştır. ATR, WGS ve PROX katalitik reaktörleri için, laboratuar deneylerinde elde edilen çıkış konsantrasyonlarının reaktör çıkışlarında sağlanabileceği varsayılarak, deneysel veriler kullanılmıştır. IPOX reaktöründe değişik sıcaklıklarda saf propan, %50 propan - %50 bütan karışımı, %75 propan - %25 bütan karışımı beslemeleri için katalizör performansı verileri Katalizör Teknolojisi ve Reaksiyon Mühendisliği Laboratuarı'nda gerçekleştirilen deneysel çalışmalardan elde edilmiştir. WGS reaktörünün dönüşüm oranı, karşılık gelen sıcaklık düzeyindeki denge dönüşüm oranının %70'i olarak alındı. Yukarıdaki deneysel sonuçlar kullanılarak PROX reaktöründe %100 CO seçiciliğinin ve %100 CO dönüşümünün gerçekleştiği kabul edilmiştir.

Her reaktörün çıkış akısının kompozisyonları, deneylerden elde edilen deneysel verilere dayandırılmıştır. Her akı için kütle debileri hesaplandıktan sonra, bilinmeyen çıkış sıcaklıklarını ve birleşik sistemdeki diğer ünitelerin sıcaklıklarını hesaplamak için enerji denklikleri kurulmuştur. Hesaplamalardaki yakıt pili dönüşüm oranları %75 ile % 85 arasında alınmıştır. Sistemdeki tüm akıların belirlenmesinden sonra hem her ünite, hem de tüm sistem için ekserji denklikleri hesaplanmıştır. Tüm sistemin ekserji verimlilikleri IPOX reaktör sıcaklığının fonksiyonu olarak hesaplanmıştır. Bu çalışmanın sonuçlarına gore, 743 K hariç, IPOX reaktörünün çıkış sıcaklığı arttırıldığında sistemin ekserji verimi artmaktadır. Ekserji analizleri göstermiştir ki, WGS ve PROX reaktörleri tüm system ekserjisi üzerinde çok az etkilidir. Tüm sistemin enerji veriminin metan içeriğine ve sistemden çıkış akısının sıcaklığına karşı duyarlı olduğu tespit edilmiştir.

TABLE OF CONTENTS

ACKNOWLEDGEMENTS iii
ABSTRACT iv
ÖZET v
LIST OF FIGURES viii
LIST OF TABLES xiii
LIST OF SYMBOLS xvi
1. INTRODUCTION 1
2. LITERATURE SURVEY 4
2.1. Fuel Cell Operation 4
2.1.1. Proton Exchange/Polymer Electrolyte Membrane Fuel Cells 4
2.2. Storage of Hydrogen 6
2.3. Fuel Processor 6
2.3.1. Fuel Selection 6
2.3.2. Steam Reforming 7
2.3.3. Partial Oxidation 8
2.3.4. Direct Partial Oxidation 8
2.3.5. Indirect Partial Oxidation (IPOX) 9
2.3.6. Water – gas Shift (WGS) Reaction 10
2.3.7. Preferential Oxidation (PROX) 11
2.4. Exergy Analysis 12
3. DESIGN, ANALYSIS & CALCULATION PRODECURE 17
3.1. Design of The FP – FC System 17
3.2. Calculation Method 21
3.3. Calculation of Exergy of The Gas Streams 22
4. RESULTS AND DISCUSSION 24
4.1. The Effect of IPOX Temperature 24
4.2. The Effects of WGS and PROX Units 34
4.3. The Effect of FC Performance 34
4.4. The Effect of Fuel Cell Outlet / Exhaust 38
4.5. The Effect of Hydrocarbon Feed Composition 40

5. CONCLUSIONS …… 41
APPENDIX A: REAL DATA ……..... 43
APPENDIX B: SAMPLE CALCULATIONS ……..... 46
B.1. IPOX reactor calculations ……... 46
B.2. WGS reactor calculations ……..... 50
B.3. PROX reactor calculations ……..... 52
B.4. PEM reactor calculations ……..... 53
B.5. Cooler calculations ……..... 54
B.6. Burner calculations ……... 55
B.7. Heat exchanger 2 calculations ……..... 56
B.8. Evaporator calculations ……..... 57
B.9. Mixer calculations ……..... 57
B.10. Overall system efficiency ……..... 58
APPENDIX C: FUEL PROCESSOR/FUEL CELL OPERATION …….. 59
REFERENCES ..…… 74

LIST OF FIGURES

Figure 3.1. Proposed FP – FC system ……... 18

Figure 4.1. The overall system exergy efficiency as a function of IPOX reactor temperature for 50% propane – 50% butane feed …….. 25

Figure 4.2. The overall system exergy efficiency as a function of IPOX reactor temperature for 75% propane – 25% butane feed …….. 25

Figure 4.3. Hydrogen amount at the exit of the IPOX reactor as a function of temperature for 50% propane – 50% butane feed …….. 26

Figure 4.4. Hydrogen amount at the exit of the IPOX reactor as a function of temperature for 75% propane – 25% butane feed …….. 27

Figure 4.5. Exergy efficiency as a function of hydrogen amount at the IPOX outlet for 50% propane – 50% butane feed ……... 27

Figure 4.6. Exergy efficiency as a function of hydrogen amount at the IPOX outlet for 75% propane – 25% butane feed ……... 28

Figure 4.7. H_2 amount at the fuel cell inlet as a function of the H_2 amount at the exit of IPOX for 50% propane – 50% butane feed …….. 28

Figure 4.8. H_2 amount at the fuel cell inlet as a function of the H_2 amount at the exit of IPOX for 75% propane – 25% butane feed …….. 29

Figure 4.9. Hydrogen amount at the fuel cell inlet as a function of IPOX temperature for 50% propane – 50% butane feed …… 30

Figure 4.10. Hydrogen amount at the fuel cell inlet as a function of IPOX temperature for 75% propane – 25% butane feed ……... 30

Figure 4.11. The relation between H_2 production and CH_4 production for 50% propane – 50% butane feed …… 31

Figure 4.12. The relation between H_2 production and CH_4 production for 75% propane – 25% butane feed ……. 31

Figure 4.13. CH_4 amount at the PEM exit as a function of IPOX temperature for 50% propane – 50% butane feed ……. 32

Figure 4.14. CH_4 amount at the PEM exit as a function of IPOX temperature for 75% propane – 25% butane feed ……. 32

Figure 4.15. The electricity production as a function of IPOX temperature for 50% propane – 50% butane feed ……. 33

Figure 4.16. The electricity production as a function of IPOX temperature for 75% propane – 25% butane feed ……. 33

Figure 4.17. Electricity production as a function of H_2 production in IPOX for 50% propane – 50% butane feed ……. 35

Figure 4.18. Electricity production as a function of H_2 production in for 75% propane – 25% butane feed …… 35

Figure 4.19. The relation between H_2 conversion within the FC and system efficiency at 663 K ……..... 37

Figure 4.20. The relation between H_2 conversion within the FC and system efficiency at 723 K 37

Figure 4.21. The relation between H_2 conversion within the FC and system efficiency at 643 K ……..... 37

Figure 4.22. The relation between H_2 conversion within the FC and system efficiency at 683 K …….. 38

Figure 4.23. The relation between H_2 conversion within the FC and system efficiency at 703 K ……... 38

Figure 4.24. The impact on the overall system efficiency of the CH_4 amount at the fuel cell outlet / exhaust for 50% propane – 50% butane feed …… 39

Figure 4.25. The impact on the overall system efficiency of the CH_4 amount at the fuel cell outlet / exhaust for 75% propane – 25% butane feed ……... 40

Figure B.1. Known flow rates and temperatures …… 47

Figure C.1. Fuel processor/fuel cell operation for pure propane feed at 663 K IPOX temperature …….. 60

Figure C.2. Fuel processor/fuel cell operation for pure propane feed at 723 K IPOX temperature …….. 61

Figure C.3. Fuel processor/fuel cell operation for 50% propane – 50% butane feed at 623 K IPOX temperature ……. 62

Figure C.4. Fuel processor/fuel cell operation for 50% propane – 50% butane feed at 643 K IPOX temperature ……. 63

Figure C.5. Fuel processor/fuel cell operation for 50% propane – 50% butane feed at 663 K IPOX temperature ……. 64

Figure C.6. Fuel processor/fuel cell operation for 50% propane – 50% butane feed at 683 K IPOX temperature …… 65

Figure C.7. Fuel processor/fuel cell operation for 50% propane – 50% butane feed at 703 K IPOX temperature ……. 66

Figure C.8. Fuel processor/fuel cell operation for 50% propane – 50% butane feed at 723 K IPOX temperature ……. 67

Figure C.9. Fuel processor/fuel cell operation for 50% propane – 50% butane feed at 743 K IPOX temperature ……..... 68

Figure C.10. Fuel processor/fuel cell operation for 75% propane – 25% butane feed at 643 K IPOX temperature ……..... 69

Figure C.11. Fuel processor/fuel cell operation for 75% propane – 25% butane feed at 663 K IPOX temperature ……... 70

Figure C.12. Fuel processor/fuel cell operation for 75% propane – 25% butane feed at 683 K IPOX temperature ……... 71

Figure C.13. Fuel processor/fuel cell operation for 75% propane – 25% butane feed at 703 K IPOX temperature ……... 72

LIST OF TABLES

Table 4.1. The overall system exergy efficiency as a function of IPOX reactor temperature for pure propane …….. 25

Table 4.2. Hydrogen amount at the exit of the IPOX reactor as a function of temperature for pure propane …….. 26

Table 4.3. Exergy efficiency as a function of hydrogen amount at the IPOX outlet for pure propane …….. 27

Table 4.4. H_2 amount at the fuel cell inlet as a function of the H_2 amount at the exit of IPOX for pure propane ……. 28

Table 4.5. Hydrogen amount at the fuel cell inlet as a function of IPOX temperature for pure propane 29

Table 4.6. The relation between H_2 production and CH_4 production for pure propane……. 30

Table 4.7. CH_4 amount at the PEM exit as a function of IPOX temperature for pure propane ……..... 32

Table 4.8. The electricity production as a function of IPOX temperature for pure propane……. 33

Table 4.9. Electricity production as a function of H_2 production in IPOX for pure propane …… 34

Table 4.10. The total electricity generation and the overall system exergy efficiency 36

Table 4.11. The impact on the overall system efficiency of the CH_4 amount at the fuel cell outlet / exhaust for pure propane …….. 39

Table A.1. Feed inputs for pure propane, 50% propane - 50% butane and 75% propane - 25% butane at different temperatures …….. 44

Table A.2. Reactor outputs for pure propane, 50% propane - 50% butane and 75% propane - 25% butane at different temperatures ……. 45

Table B.1. c_p^h and h_d^o values for mixture components for T=723 …..... 48

Table B.2. c_p^h and h_d^o values (T=661 K) for a trial value of inlet temperature of IPOX …….. 48

Table B.3. E_0 and c_P^E values for T=723 K …… 49

Table B.4. E_0 and C_P^E values for T=661 K ……..... 49

Table B.5. h_d^0, c_p^h values for T=523 K and WGS reactant and product flow rates ... 51

Table B.6. c_p^E values for T=523 K ……..... 52

Table B.7. h_d^0, c_p^h,c_p^E values for T=398 K and PROX reactant and product flow rates 52

Table B. 8. Values of c_p^h and c_p^E for T = 349 K 53

Table B.9. c_p^h and c_p^E (for T=431 K) values of components of the mixture 55

Table B.10. c_p^h and c_p^E values for T=1208 K 55

Table B.11. c_p^h and c_p^E values (for T=1161 K) for mixture components 56

Table B.12. c_p^h and c_p^E values (for T=702 K) of output stream..... 57

Table C.1. Exergy efficiencies of all system units 59

Table C.2. Reference environment according to Kotas 73

LIST OF SYMBOLS / ABBREVIATIONS

c_p^E	Mean isobaric exergy capacity.
c_p^h	Mean isobaric heat capacity for enthalpy of components
C_PVAPA	Constant in the ideal gas
C_PVAPB	Constant in the ideal gas
C_PVAPC	Constant in the ideal gas
C_PVAPD	Constant in the ideal gas
E	Exergy
E_0	Standard chemical exergy
E_{eff}	Exergy efficiency of the unit
E_H	The exergy of exhaust stream
E_{ke}	Kinetic exergy
E_{pe}	Potential exergy
E_{phy}	Physical exergy
E_R	The exergy of waste heat
H	Enthalpy
h_d^o	Ideal gas standard enthalpy of formation
K	Equilibrium constant
n_i	Flow rate of the i-th component in the mixture
P	Mechanical condition
Q	Enthalpy difference
s	Specific entropy
T	Reaction temperature; thermal condition
x_i	The mole fraction of the i-th component in the mixture
μ_{i00}	The chemical potential of species i evaluated in the reference medium
μ_{io}	The chemical potential of species i evaluated at To and Po
μ	Physicochemical equilibrium
$E_i^{\Delta T}$	Molar thermal component of specific exergy
Max Ψ	Maximum exergy efficiency

ΔG_0	Gibbs function of reaction
ΔH_0	Enthalpy of reaction
Ψ	The rational efficiency of the system

AC	Activated carbon
AC1	Acid-washed with HCl
AC2	Acid-washed and air oxidized
AC3	Acid-washed and HNO3 oxidized
AFC	Alkaline Fuel Cells
ATR	Autothermal reforming
BUR	Burner reactor
CATREL	Catalyst Technology and Reaction Engineering Laboratory
CHP	Combined heat-and-power generation
FC	Fuel cell
FP	Fuel processor
H.E.	Heat exchanger
IPOX	Indirect Partial Oxidation
LPG	Liquefied propane gas
MCFC	Molten Carbonate Fuel Cells
PAFC	Phosphoric Acid Fuel Cells
PEMFC	Proton/Polymer Electrolyte Membrane Fuel Cell
PROX	Preferential Oxidation
SOFC	Solid Oxide Fuel Cells
SR	Steam reforming
STP	Standard condition
TOX	Total oxidation
WGS	Water Gas Shift

1. INTRODUCTION

Fuel cells are highly advantageous in clean and efficient power generation due to the fact that they operate at zero emission level when pure hydrogen is utilized as the fuel. They achieve direct conversion of chemical energy into electrical power without any heat generation step. That is the reason why, they operate much more efficiently than internal combustion engines (Avcı, 2003). Fuel cells are planned to be utilized in a vast range of markets, small scale portable/leisure applications to large scale stationary power generation, in addition to their potential utilization in powering vehicles (Ralph and Hards, 1998). Small-scale combined heat and power generation is based on fuel cells up to 250 kW (Avcı *et al*., 2002).

A wide variety of fuel cells operating with different fuels and electrolytes are under investigation, but the Proton/Polymer Electrolyte Membrane Fuel Cell (PEMFC) fuelled by hydrogen appears to be the most promising one for both vehicular and small scale combined heat-and-power (CHP) facilities due to its compactness, modularity, high power density and fast response (Ahmed and Krumpelt, 2001; Ralph, 1999).

Hydrogen storing or production is necessary for having hydrogen on-site as continuous hydrogen availability is needed for PEMFC operation. However, the current level of non-pressurized hydrogen storage technology can not meet the targeted storage specifications for vehicular/small scale residential applications. Furthermore, there are difficulties associated with the availability and distribution of hydrogen. That's the reason why, compact and efficient catalytic devices that are called fuel processors have been preferred in order to provide the conversion of much more readily available hydrocarbon fuels to hydrogen (Avcı, 2003).

A fuel processor basically consists of three catalytic reactions for hydrogen production from hydrocarbon fuels. These reactions are:

i) reforming of hydrocarbon fuels to hydrogen by means of steam reforming, direct or indirect partial oxidation,

ii) water-gas shift reaction that is used for eliminating carbon monoxide and enhancing the hydrogen concentration,

iii) preferential oxidation, where it is aimed to decrease carbon monoxide concentration in the reformer product to levels less than 10 ppm, which warrants steady operation of PEMFC without any loss of facility (Selen, 2003).

Hydrogen produced by the fuel processor is sent to a fuel cell which is actually an electrochemical energy conversion device. This device converts the chemical energy of hydrogen and oxygen into electrical energy, with waste heat and liquid water as by-products (Hussain *et al*., 2005).

In this study, an exergy analysis of an integrated fuel processor-fuel cell system for mobile and small scale stationary applications has been presented. The fuel processor consists of Indirect Partial Oxidation (IPOX), Water Gas Shift (WGS) and Preferential Oxidation (PROX) reactors, an evaporator, a burner and heat exchangers. Pure propane or mixtures of propane and n-butane with ranging compositions were utilized as input to the fuel processor. As the fuel cell, the Proton Exchange Membrane (PEM) was selected due to its high efficiency and low operating temperature. In the analysis of small-scale stationary applications, a heat exchanger can be used in order to cool PEMFC down to desired operating temperature, whereas car radiator can be utilized in mobile applications.

Exergy method of analysing energy systems integrates the first and second laws of thermodynamics, with exergy defined as the maximum amount of work which can be obtained when a system or flow of matter is brought to equilibrium with a preferential reference medium reversibly. Determination of the parameters to be varied and their respective ranges in the exergy analysis was based on the results of previous experimental work conducted in Catalyst Technology and Reaction Engineering Laboratory (CATREL) of Boğaziçi University.

The catalyst performance data for IPOX reactor for different feeds have been taken from studies conducted by Selen-Çağlayan (2003) and Gökaliler (2005) on Pt-Ni bimetallic catalyst with pure propane, 50% propane – 50% n-butane and 75% propane – 25% n-butane feeds. For WGS part, 70% of the equilibrium condition at the given

temperatures was assumed. For PROX reactor, data were taken from studies conducted by Şimşek (2006) on Pt-Sn/AC (Pt-Sn catalyst supported on activated carbon) system.

The aim of this study is to perform an exergy analysis on a combined Fuel Processor-Fuel Cell system to be used in small scale applications in order to understand the effect of operating parameters on overall system efficiency.

Section 2 gives some information about fuel cell operation, fuel processor and exergy analysis. Section 3 includes design and analysis of Fuel Processor - Fuel Cell system and also calculation method. In Section 4, the impacts of indirect partial oxidation temperature, water-gas shift and preferential oxidation units, fuel cell performance, fuel cell outlet / exhaust and hydrocarbon feed composition on the Fuel Processor - Fuel Cell system are investigated and the results are indicated. Finally, the major conclusions are given in Section 5.

2. LITERATURE SURVEY

2.1. Fuel Cell Operation

An electrochemical conversion device that is called fuel cell converts the chemical energy into electrical energy and water, producing waste heat and by-products which are pollutants. Various reactions arise in this cell depending on the electrolyte type and the fuel. It is a clean, quiet and efficient process (Selen, 2003) since conversion takes place via an electrochemical process.

In a fuel cell, oxygen, which comes from air, enters through the catalytic cathode. Hydrogen, which is usually utilized as the fuel, is fed to the anode. Hydrogen molecules split into protons and electrons where some heat is produced and then proton and electrons move towards the cathode so as to react with oxygen (Selen, 2003).

Fuel cell operation should be held at temperatures higher than 333 K to sustain reaction kinetics and lower than 373 K since the membrane (electrolyte) needs to be humidified to conduct protons which migrate as hydrated species (Avcı, 2003). High temperature cells are convenient to use in stationary applications rather than in mobile applications because of their high operating temperatures which in turn lets them operate at higher efficiencies in electricity production (Selen, 2003).

2.1.1. Proton Exchange / Polymer Electrolyte Membrane Fuel Cells (PEMFC)

Fuel cells are classified according to their electrolytes and operation temperatures. Some fuel cells operate at low temperature such as PEMFC, Phosphoric Acid Fuel Cells (PAFC) and Alkaline Fuel Cells (AFC). On the other hand, there are also high temperature fuel cells such as Molten Carbonate Fuel Cells (MCFC) and Solid Oxide Fuel Cells (SOFC).

High temperature fuel cells can use both carbon monoxide and hydrogen as fuel, so fuel processing can be achieved in less steps. On the other hand, due to relatively low

operation temperature of PEMFC, the Pt-anode is prone to deactivation by carbon monoxide impurity; that is the reason why PEMFC needs essentially CO-free (max 10 ppm) hydrogen. Thus, the fuel processors must have suitable catalysts and operation parameters for decreasing CO-level that guarantees stable operation of PEMFC (Song, 2002).

Investigations show that energy-efficient and convenient catalysts, and processes for reforming fuels are essential for all combined fuel processor-fuel cell systems. Active and robust (non-pyrophoric) catalysts for WGS, active and selective catalysts for PROX at low temperature for fuel processors and carbon monoxide-tolerant anode catalysts for fuel cells have led to implementation of low temperature fuel cells, especially PEMFC for practical uses (Song, 2002).

PEMFCs operate at temperatures between 343-363 K and utilize polyperflourosulfonic acid as the membrane. High operation temperature is not essential in order to reach high efficiency because electrochemical processes in fuel cells are not governed by Carnot's Law (Mert *et al.*, 2007). They are suitable for a variety of applications such as transportation, small-scale stationary combined heat and power generation due to their compactness, modularity, energy efficiency, high power density, fast start-up and reduced corrosion (Selen, 2003).

Most of the fuel cells are currently manufactured using expensive techniques and materials. To begin with, they include catalytic anode and cathode units where platinium-based catalysts are found to satisfy the best combination of fast kinetics and required stability, especially in the low temperature ranges (Avcı, 2003).

The acceptance of FP - PEMFC as a stationary cogeneration system might become faster than that of FC vehicles for a variety of reasons. These reasons are;

a) the required capacity for an immobile system is much smaller than for a mobile system,

b) a fuel-supply infrastructure already exists (Nagata, 2005).

It is obvious that PEM possesses the highest power density compared with the conventional energy production technologies, like combustion. Due to this fact, the manifold applications in the stationary sector speak in favour of PEM. They range from small-scale applications in the watt range, over decentralised applications in power-heat cogeneration, and up to applications in emergency power supply (Pokojski, 2000).

Fuel cell-based Combined Heat and Power Generation (CHP) systems allow electricity generation and heat production in a decentralised, quiet, efficient and environmentally friendly way, so these systems are quite attractive for stationary energy generation. Accordingly, a mathematical model of the FC/CHP unit was developed in order to allow for the prediction of system performance and operating parameters under off-design condition by Gigliucci et al., (2004).

2.2. Storage of Hydrogen

For supplying hydrogen to the fuel cell, one of the alternatives is chemical storage in liquid fuels. Using pressured cyclinders, cryogenic methods, metal hydrides and carbon nanotubes can be cited as the storage methods which are expensive, need excessive volume and weight and are far from satisfying the ideal performance except carbon nanotubes (Trimm and Önsan, 2001). The current technology have not yet reached the targeted specifications for storing hydrogen under low pressure (Avcı *et al*., 2003; Özkara and Aksoylu, 2003).

2.3. Fuel Processor

2.3.1. Fuel Selection

Both hydrocarbon and alcohol fuels can be utilized as fuels for reforming on-site or on-board. Alcohol fuels are ultra clean and sulfur-free. They can be reformed at lower temperatures. However, hydrocarbon fuels have higher energy density (Song, 2002). The liquid fuel should fulfill the following criteria: i) Being liquefiable at a moderate pressure; ii) Being easily available at refuelling stations; iii) Having high hydrogen/carbon ratio; iv) Being inexpensive (Jacobs *et al*., 2003).

Hydrogen is the most suitable fuel for a low temperature fuel cell like PEMFC. However, natural gas (CH_4) and liquefied propane gas (LPG) for stationary applications, and liquid hydrocarbon fuels (C_nH_m) and methanol (MeOH) and other alcohols for mobile applications can be also utilized as hydrogen source (Song, 2002).

For mobile and portable use, Liquefied petroleum gas (LPG) is a promising hydrocarbon fuel due to being stored in liquid phase and easily transported. Due to its low sulphur content, it is harmless from environmental point of view. Furthermore, it is not expensive and it has high power density. Propane and n-butane are major constituents of LPG (Selen, 2003).

There are three possible reforming reactions in a fuel processor. They are steam reforming, direct and indirect partial oxidation.

2.3.2. Steam Reforming

It is utilized widespread and is very cheap. This process is highly endothermic and it consists of reaction of hydrocarbons with steam in order to produce hydrogen and carbonoxides.

$$C_nH_m + n\ H_2O = n\ CO + (1/2\ m + n)\ H_2 \qquad (2.1)$$

Steam reforming reaction gives the highest quantity of hydrogen in the product stream. That's the reason why, it is quite favourable for PEM. However, steam reforming has some disadvantages such as it needs high catalyst loadings, large reactors and considerable heat input (Avcı *et al*., 2002).

In the study of Avcı et al.(2004), hydrogen via n-butane steam reforming has been searched on Ni/δ-Al_2O_3 and Pt-Ni/δ-Al_2O_3 catalyst. It was shown that Pt-Ni/δ-Al_2O_3 possessed superior performance in terms of preferential hydrogen production that is responsible for lower carbon dioxide and methane formation.

Steam reforming of methanol was also widely investigated since hydrogen conversion is much easier than other hydrocarbons (Tsai and Yoshimura, 2001; Iwasa *et*

al., 1998; Breen and Ross, 1999; Ledjeff-Hey *et al.,* 1998). At low temperatures, more than 99% conversion was reached because of the fact that the process was less endothermic (Joensen and Rostrup-Nielsen, 2001).

2.3.3. Partial Oxidation

In spite of the fact that steam reforming is the most convenient process in terms of maximal hydrogen throughput, it is not preferable because of its high energy and quite high temperature demand. On the other hand, Partial Oxidation possesses all of the properties to provide the needs of fuel cell applications so as to generate motive power. It is faster than steam reforming. In addition, it does not require bigger amounts of catalysts. Partial oxidation occurs in two routes which are: i) direct partial oxidation which contains only one step, ii) indirect partial oxidation which consists of total oxidation and steam reforming reactions.

2.3.4. Direct Partial Oxidation

Direct Partial Oxidation is the reaction of the fuel with an oxygen quantity insufficient for complete combustion (Brown, 2001).

This oxidation contains only one step where hydrocarbons react with oxygen and as a result, carbon monoxide and hydrogen are produced. This reaction is favoured at high temperatures (approximately 1023 K). It is faster than indirect partial oxidation, but it occurs under oxygen deficient conditions and generates less heat than total oxidation (TOX) (Ma, 1995).

$$C_nH_m + ½m\ O_2 = m\ CO + ½n\ H_2 \qquad (2.2)$$

High activity and selectivity levels in partial oxidation of methane have been reached over $Ni/AlPO_4$ between 773-1173 K (Choudhary *et al*., 1998).

In the study of Hohn and Schmidth (2001), the significance of heat transfer on direct oxidation has been determined. Furthermore, the positive impact of the alumina on methanol partial oxidation has been worked in the study of Alejo *et al*., (1997). The

addition of alumina to the Cu-Zn based catalyst has increased the catalyst stability, whereas the activity of the catalyst was found to depend only on the copper metal area.

O'Conner *et al.,* (2000) have studied the direct oxidation of cyclohexane, n-hexane, isooctane, toluene and commercial gasoline over Rh-coated monoliths. It was shown that the fuel conversion exceeded 95% and synthesis gas yielded above 90%. Direct conversion of commercial gasoline gave 80% of carbon monoxide selectivity, but catalyst was poisoned because of the sulphur content.

2.3.5. Indirect Partial Oxidation (IPOX)

Steam reforming is an endothermic and partial oxidation is an exothermic reaction. Accordingly, when the fuel is treated with a mixture of steam and oxygen simultaneously, over a suitable catalyst both of the reactions proceed leading to an energy efficient process which is called as indirect partial oxidation.

$$C_nH_m + n\ H_2O = n\ CO + ((1/2)\ m + n)\ H_2 \quad (2.3)$$

$$C_nH_m + (n + (1/4)\ m)\ O_2 = n\ CO_2 + (1/2)\ m\ H_2O \quad (2.4)$$

This operation which is autothermal is generally run in an adiabatically operating fixed-bed reactor. In other words, heat is provided by the exothermic TOX and is utilized by the endothermic SR. This process can also be referred to as autothermal reforming (ATR) and generates a mixture of CO, CO_2 and H_2.

IPOX is a promising technology for production of hydrogen from hydrocarbon fuels, as it does not have significant disadvantages like slow response, considerable heat input or output, higher catalyst loadings, larger reactors, mass transfer limitations and low efficiency (Çağlayan *et al*., 2005).

Total oxidation and steam reforming performance of Pt-Ni bimetallic catalyst has been investigated in a series of papers for propane and n-butane feeds. The results of initial work gave significant clues such that if a bimetallic catalyst, like Pt-Ni, would be utilized in IPOX, the heat produced by the TOX reaction (exhothermic), catalyzed mostly by Pt,

would be transferred via using the catalyst itself as a micro heat exchanger to Ni sites, which mostly catalyze the steam reforming reaction (endothermic) (Çağlayan *et al.,* 2005). As a result of this study, it was shown that S/C = 3 (steam to carbon ratio), C/O_2 = 2.7 (carbon to oxygen ratio) and W/F = 0.51 $g_{cat}h/mol$ (residence time) hydrocarbon for IPOX of propane on the basis of high hydrogen productivity and selectivity between 623-748 K were optimal conditions. For every hydrocarbon feed, the bimetallic Pt-Ni/γ-Al_2O_3 catalysts are very convenient during the 12 hour stability tests. Also, an enhancement in the steam/carbon ratio contributes to ca. 10% increase in hydrogen production from propane in IPOX (Selen, 2003).

In one study, indirect partial oxidation (IPOX) of propane was studied over bimetallic 0.2 wt.% Pt-15 wt.% Ni/δ-Al_2O_3 catalyst in order to investigate the influences of S/C, C/O_2 and W/F ($g_{cat}h/mol$ HC) on the hydrogen production activity, selectivity and product distribution. It was found that the Pt-Ni bimetallic system possessed superior performance than the monometallic catalysts (Çağlayan *et al.,* 2005). Recently, Gökaliler studied the power law type kinetics of ethanol steam reforming and indirect partial oxidation of propane/n-butane mixture with the purpose of hydrogen production over a bimetallic 0.2wt%Pt-15wt%Ni/δ-Al_2O_3 catalyst. In addition, hydrogen production from LPG was also investigated. In this study, the fuel flexibility of the bimetallic system was also investigated. Here, LPG possesses a composition of 50% propane – 50% n-butane. It was shown that higher steam/carbon ratios contributed to greater hydrogen production rates with only one exception and increasing the n-butane percentage in the fuel increases the activity and the selectivity of the process (Gökaliler, 2005).

2.3.6. Water-gas Shift (WGS) Reaction

WGS reaction is one of the major steps for production of hydrogen that this reaction both enhances the amount of hydrogen and reduces the carbon monoxide concentration in the reforming output. It is clear that the majority of the carbon monoxide is removed by WGS reaction:

$$CO + H_2O = CO_2 + H_2, \quad \Delta H = -41.2 \text{ kj/mol} \quad \Delta G = -28.6 \text{ kj/mol} \qquad (2.5)$$

WGS is a critical step in fuel processors for preliminary carbon monoxide clean- up and additional hydrogen generation prior to the further elimination of CO (Ghenciu, 2002). Since fuel cells operate at 353 - 373 K and are poisoned by even trace amounts of carbon monoxide present in the hydrogen fuel, a further carbon monoxide reduction is crucial for stable fuel cell performance.

Since this reaction is slightly exothermic, a cooler is utilized so as to decrease water-gas shift exit temperature down to the operation temperature of preferential oxidation.

This reaction is usually carried out in two modes: i) high temperature (623 – 673 K) water-gas shift over mixtures of Fe/Cr oxides (Hakkarainen *et al.,* 1994; Li *et al.,* 1999), ii) low temperature (453 – 523 K) water-gas shift over mixtures of Cu/Zn oxides (Lima *et al*., 1998; Karyobkina *et al*., 2003; Kepinski *et al*., 2000).

The WGS reactor currently represents the largest volume of any catalyst in a fuel processor because of the slow kinetics at temperatures in which the equilibrium is favourable (Natesakhawat *et al*., 2006).

Performance of chromium-free iron-based catalysts in the high temperature WGS reaction, the impact of different catalysts preparation variables and praparation methods have been searched in the study of Natesakhawat *et al*., (2006). Equilibrium conversion of carbon monoxide was found to be 73%, 78% and 82% at 350 C, 400 C and 450 C, respectively. In this study, 70% conversion was adopted as a conservative value by taking work of Natesakhawat *et al*.,'s results into consideration during the exergy calculations of FP – FC combined system.

2.3.7. Preferential Oxidation (PROX)

CO is harmful for the PEMFC anode catalysts, so CO concentration within the hydrogen-rich flux is removed by means of PROX reaction.

In the preferential oxidation reaction, carbon monoxide is selectively oxidized in the presence of water vapor, CO_2 and hydrogen by means of utilizing stoichiometric amounts

of oxygen. PEMFC's reaction occurs at a temperature range of 333 – 363 K, so PROX reaction should be studied at low temperature (Avcı *et al*., 2002).

$$CO + O_2 = CO_2 \quad (2.6)$$

$$H_2 + O_2 = H_2O \quad (2.7)$$

In the work of Özkara and Aksoylu (2003), PROX in a hydrogen-rich gas flow was studied over Pt-Ce and Pt-Sn catalysts supported on activated carbon (AC). This catalyst possesses high activity and selectivity between 353 – 473 K temperature range which is the temperature interval essential for guaranteeing convenient operation of Pt-anode of PEMFC without being poisoned.

In a following study, the influence of carbon dioxide and water in the feed stream on preferential low temperature CO oxidation activity of the same catalysts was investigated by Şimşek (2005). In this work, three species of untreated and oxidized activated carbons, which are i) Acid-washed with HCl (AC1) ii) Acid-washed and air oxidized (AC2) iii) Acid-washed and HNO3 oxidized (AC3) are utilized as catalyst support.

The results of this study show that Pt-SnO_x catalyst supported on AC3, the HNO_3-oxidized activated carbon support, gave 100% carbon monoxide conversion in the presence of carbondioxide or carbondioxide plus water in the feed. Additionally, Pt-CeO_x supported on AC2, the air-oxidized activated carbon support, gave almost 100% CO conversion in hydrogen-rich feed streams containing carbondioxide plus water (Şimşek *et al.,* 2005).

2.4. Exergy Analysis

Exergy analysis (Availability analysis) which is also known as thermodynamic second law analysis is a proven method for system design, analysis, process-evaluation and improvement. This analysis, which is also regarded as a primary tool in addressing the impact of energy resource utilization on the environment (Hussain *et al*., 2005), is based on both the first and the second laws of thermodynamics, whereas energy analysis is based on only the first law of thermodynamics (Mert *et al.,* 2007).

The first law of thermodynamics tackles the quantity of energy in which enegy can not be created or destroyed, whereas the second law tackles the quality of energy (Çengel and Boles, 2002). Thus, exergy describes the quality of energy in addition to quantity.

The Exergy Technique is an alternative, relatively new method based on the concept of exergy, loosely defined as a universal measure of the work potential or quality of various forms of energy in relation to a given medium. It provides a meaningful and exact representation of process efficiencies within a system. An exergy balance applied to a process or a whole plant indicates that how much of the usable work potential, or exergy, supplied as the input to the system has been consumed (irretrievably lost) by the process. The loss of exergy, or irreversibility, supplies a generally applicable quantitative measure of process efficiency. Analysing multi-component plants declares the total plant irreversibility distribution among the plant components, pinpointing those contributing most to overall plant inefficiency (Kotas, 1984). Hence, exergy analysis is a significant and effective method of utilizing the conservation of mass and energy principles together with the second law of thermodynamics for the design and analysis of thermal systems (Mert *et al*., 2007) and energy conversion processes (Cownden *et al*., 2001).

The concept of irreversibility is firmly based on the two main laws of thermodynamics unlike the traditional criteria of performance. The exergy balance for a control region, from which the irreversibility rate of a steady flow process can be calculated, has its origins in combining the steady flow energy equation (First Law) with the expression for the entropy production rate (Second Law). In spite of the fact that the Second Law is not utilized explicitly in the Exergy Technique, its application to process analysis shows the practical implications of the Second Law. Working with various forms of irreversibilities and their impact on plant performance, gives a better and more useful understanding of the Second Law than working with its statements and corollaries (Kotas, 1984).

A system in equilibrium with its surroundings does not have exergy due to having no capability in order to lead to any change with respect to its reference environment. At this point, the system exergy has been completely destroyed. Accordingly, every system not in

equilibrium with its reference environment possesses exergy. The exergy consumption of a process is due to entropy production because of irreversibilities (Hussain *et al.*, 2005).

For exergy analysis, defining the reference environment is essential. Then, exergy will be calculated as the maximum work which can be obtained when equilibrium is established with this reference environment. There are two forms of equilibrium:

i) Restricted equilibrium where only thermal (T) and mechanical (P) conditions of equilibrium are satisfied.

ii) Unrestricted equilibrium where in addition to thermal and mechanical conditions, physicochemical equilibrium (μ) condition is also satisfied.

A system in restricted equilibrium is said to be in an environmental state whereas a system in unrestricted equilibrium is said to be in a dead state. The environmental state is usually defined as STP (298 K and 1 Atm) whereas complete definition of dead state requires selection of reference substances for each element and their compositions in the solid, liquid or gas state (Kotas, 1984). The reference environment adopted in this work is that of Kotas and details are given in Appendix C.

The specific total exergy (2.8) can be determined with the following formulation where nuclear, magnetism, electricity and surface tension influences are absent (Mert *et al*., 2007):

$$E = E_0 + E_{pe} + E_{phy} + E_{ch} \tag{2.8}$$

in which, E_0 is kinetic exergy, E_{pe} is potential exergy and E_{phy} (2.9) is physical exergy which is defined as the maximum amount of work obtainable when the stream of substance is brought from its initial state to the environmental state defined by Po and To, by physical processes including only thermal interaction with the environment (Kotas, 1984).

$$E_{phy} = (H - h_d^{\,0}) - T_0(s - s_0) \tag{2.9}$$

where ‘H’ is specific enthalpy and ‘s’ is specific entropy. The subscript ‘0’ stands for the reference environment (restricted).

E_{ch} (2.10) is chemical exergy which is defined as the maximum amount of work obtainable when the substance under consideration is brought from the environmental state to the dead state by processes including heat transfer and exchange of substances only with the medium (Kotas, 1984). It is equal to:

$$E_{ch} = \sum x_i (\mu_{io} - \mu_{i00}) \quad (2.10)$$

where x_i is the mole fraction, μ_{io} is the chemical potential of species i evaluated at To and Po and μi_{00} is the chemical potential of species i evaluated in the reference medium (unrestricted).

Unlike energy, exergy is not generally conserved but destroyed by irreversibilities within a system. There are two types of irreversibility which are internal and external. Friction, expansion, mixing and chemical reaction lead to internal irreversibilities. On the other hand, external irreversibilities occur because of heat transfer through a finite temperature difference. Exergy is lost when the energy associated with a material or energy flow is rejected to the environment (Colpan *et al*., 2007).

Hussain et al. have dealt with the thermodynamics modeling of a polymer electolyte membrane (PEM) fuel cell power system for transportation applications. It was found that the difference between the gross stack power and net system power enhances with the increase of external load (current density) and in the fuel stack, minimization of the irreversibility rate is needed in order to increase the performance of the system (Hussain *et al*., 2005).

Haynes *et al*. (2002) and Hussain *et al.* (2004) have studied low temperature PEM fuel cell for transportation applications. Moreover, Cownden *et al.* (2001) have performed exergy analysis of hydrogen fuel cell power for bus transportation. Their studies demonstrated the usefulness of thermodynamic analysis in determining the irreversibilities in various system components, but did not rigorously address the operating characteristics

of PEM fuel cell for minimizing irreversibilities and maximizing the performance of the system.

Kazim (2004) has performed exergy analysis of a PEM fuel cell at specified voltages of 0.5 and 0.6 V. At various operation conditions, exergy efficiencies of the PEM fuel cell were reported. It was shown that PEM fuel cell voltages play an important role in the exergy efficiency of the cell operation. The lower the cell voltage, the greater is the mass flow rates required for reactions and products to operate the fuel cell so as to generate motive power. Furthermore, if the fuel cell operating temperature is enhanced from 298 K to 373 K, a maximum increase in the exergy efficiency of 2,5% can be obtained.

Delsman *et al.* (2006) have performed exergy analysis for a methanol processor integrated with a PEM, for use as a portable power generator. They demonstrated that the calculated overall exergetic efficiency of the fuel processor (FP) – fuel cell (FC) system is higher than that of typical combustion engines and rechargeable batteries.

In another work, an exergy analysis of a solid polymer fuel cell power system for transportation applications has been studied. It was shown that the largest destruction of exergy within the system occurs inside the fuel cell stack (Cownden *et al.,* 2001).

3. DESIGN, ANALYSIS & CALCULATION PRODECURE

3.1. Design of The FP – FC System

A fuel processor is a system that has three catalytic reactions in series, namely autothermal reforming (ATR), WGS and PROX, which produce CO-free hydrogen from hydrocarbons. In a combined fuel processor - fuel cell system, the hydrogen is fed to the fuel cell, the system is energetically optimized via using heat exchangers and burners wherever necessary. A fuel processor efficiency can go up to 70% for pure hydrogen generation.

The proposed FP-FC combined system, including all streams, reactors, heat exchangers, mixers and burners is given in Figure 3.1. For avoiding dehydration of the fuel cell and reducing carbon monoxide concentration, excess water is provided to the system (Delsman *et al*., 2001). This water firstly enters a vaporizer. Then a hydrocarbon fuel like propane or n-butane (the molar ratio of steam to carbon is 5:1 for the propane – n-butane mixture; 3:1 for the pure propane), oxygen and nitrogen (which come from air) are mixed with evaporated water. Then, this mixture reacts in the IPOX at various temperatures using a Pt-Ni bimetallic catalyst.

In our FP – FC system, firstly, water, which is at 298 K temperature and 1 Atm pressure, is evaporated in the vaporizer by means of heat provided by the burner effluent. Whenever heat exchanger 2 is utilized as explained below, burner effluent reaches the evaporator after passing through this heat exchanger. Then, a hydrocarbon fuel, oxygen and nitrogen coming from air and steam are mixed. These components are at 298 K temperature except water due to the fact that water is at 383 K at the outlet of the evaporator. The system operates at atmospheric pressure. Exit temperatures of these mixtures are calculated in the temperature range of 349 – 356 K. Exit temperature is found as 349 K for pure propane feed, 352 K for 50% - 50% propane – n-butane mixture and 356 K for 75% propane – 25% n-butane.

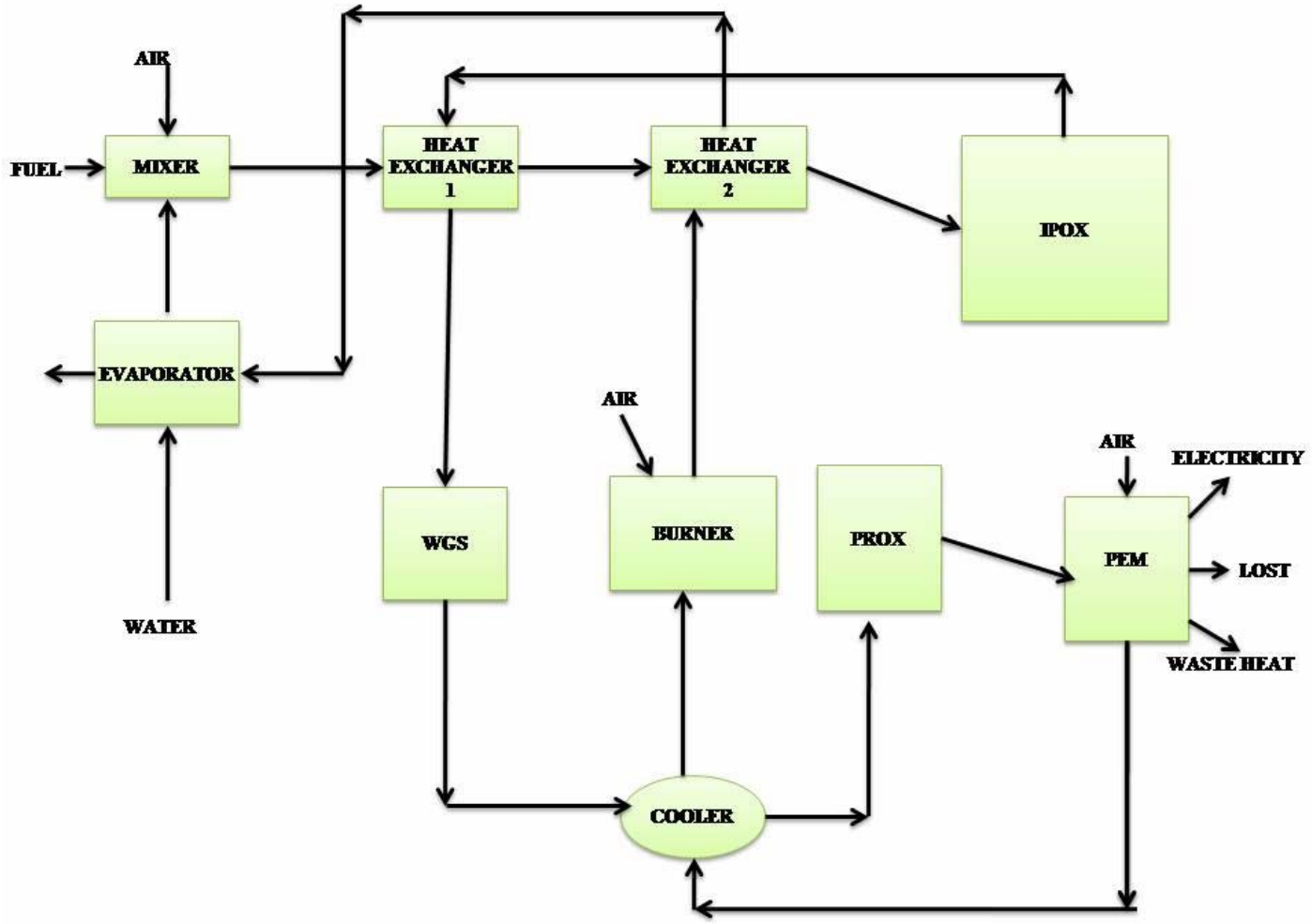

Figure 3.1. Proposed FP-FC system

They are sent to heat exchanger 1 in order to enhance temperature because IPOX reactions occur at a definite temperature interval. Outlet stream of mixer is heated by output stream coming from IPOX reactor. However, sometimes heat exchanger 1 does not supply sufficient temperature increase. At this point, in addition to heat exchanger 1, heat exchanger 2 must be utilized, and outlet stream from heat exchanger 1 enters heat exchanger 2 before entering IPOX reactor.

IPOX reactions are carried out in the temperature range of 623 – 743 K in this system. For various feed mixtures, authothermal conditions are taken into account during IPOX. In IPOX reactions, bimetallic Pt–Ni/&-Al_2O_3 catalyst is preferred since IPOX runs efficiently over this catalyst (Ma and Trimm, 1996). Main IPOX reactions are:

$$C_3H_8 + 3H_2O \rightarrow 3CO + 7H_2 \quad (3.1)$$

$$C_3H_8 + 5O_2 \rightarrow 3CO_2 + 4H_2O \quad (3.2)$$

$$C_4H_{10} + 4H_2O \rightarrow 4CO + 9H_2 \quad (3.3)$$

$$C_4H_{10} + 6.5O_2 \rightarrow 4CO_2 + 5H_2O \quad (3.4)$$

$$CO + H_2O \rightarrow CO_2 + H_2 \quad (3.5)$$

$$CO + H_2 \rightarrow CH_4 + H_2O \quad (3.6)$$

where propane and n-butane are generally spent completely and CO, CO_2, H_2 and CH_4 components occur as a result of these reactions. Output stream of IPOX supplies heat to heat exchanger 1 and it leaves heat exchanger 1 at 523 K temperature. Output flux of H.E.1 is sent to WGS reactor which operates at 523 K. In this reactor, the following reaction occurs:

$$CO + H_2O \leftrightarrow CO_2 + H_2 \quad (3.7)$$

Here, conversion changes between 65% and 67%. This conversion value is based on 70% of the thermodynamical equilibrium conversion (Natesakhawat *et al*., 2006).

Between WGS and PROX reactors, a cooler is utilized so as to reduce the shift converter exit temperature down to the operating range (between 353 K – 473 K) of the PROX unit (Avcı *et al.,* 2002). Here, output stream of WGS is cooled by means of heat which is obtained from output flux of PEM. In this system, input temperature of PROX is decreased to 398 K by the cooler because preferential carbon monoxide oxidation catalyst possesses high activity and selectivity between 353 and 473 K as mentioned before (Özkara and Aksoylu, 2003).

As the carbon monoxide presence is harmful for PEMFC, the CO content must be reduced to <10 ppm. Hence, CO conversion must be better than 99.99% so as to reach a 10 ppm CO level. The most significant requirements for PROX are high CO oxidation activity at low temperature and high CO selectivity against the undesired hydrogen in order to prevent the reduction of overall fuel efficiency (Şimşek *et al*., 2005).

In PROX reactor, CO and hydrogen react with oxygen and CO is consumed completely. Here, the reactions are:

$$CO + ½\ O_2 \rightarrow CO_2 \qquad (3.8)$$

$$H_2 + ½\ O_2 \rightarrow H_2O \qquad (3.9)$$

In PEM reactor, only hydrogen reacts with oxygen which comes from both output stream of PROX and air. Generally, hydrogen conversion is taken as 75% (Avcı et al., 2002), but this value can change and increase to 80% or 85%. PEMFC's operating temperature is less than 393 K, usually between 343 – 363 K due to the limitation on the temperature imposed by the polymer and water balance (Song, 2002). In our system, the operation temperature of the PEM reactor is selected as 349 K.

Working principle:

$$\text{Overall cell reaction: } H_2 + O_2 \rightarrow H_2O(l) + \text{electrical work} + \text{heat} \qquad (3.10)$$

60% of the heat of reaction is produced as electricity, with the remaining 40% being rejected as heat (Lattner *et al.,* 2003). 20% of the total heat generated by the fuel cell is

assumed to be lost via convection and radiation from the fuel cell stack, while the remainder is taken to be removed at the radiator in mobile applications (Cownden *et al.,* 2001). For stationary applications, heat exchanger replaces the radiator.

After output stream of PEMFC passes from cooler, this flux reaches burner. In the burner, unreacted hydrogen and hydrocarbons fuels like CH_4, C_3H_8 and C_4H_{10} are combusted completely:

$$CH_4 + 2O_2 \rightarrow CO_2 + 2H_2O \quad (3.11)$$

$$H_2 + ½\ O_2 \rightarrow H_2O \quad (3.12)$$

$$C_3H_8 + 5O_2 \rightarrow 3CO_2 + 4H_2O \quad (3.13)$$

$$C_4H_{10} + 6.5O_2 \rightarrow 4CO_2 + 5H_2O \quad (3.14)$$

In this system, output temperatures of burner are very high, ranging from 1000 K to 1300 K. However, when this flow is sent to the evaporator, these high values decrease to 600 – 1000 K before discharge to the environment.

As explained above, the heat integration of the system consists of two heat exchangers, a cooler and a catalytic burner reactor (BUR) where unconverted hydrogen, propane n-butane and methane originating from the exit flux of PEM are combusted in order to provide heat necessary for the vaporizer, cooler and heat exchangers. Sometimes oxygen is insufficient so as to combust this substances. In this situation, approximately 10% excess air is utilized.

3.2. Calculation method

In order to investigate the performance of the proposed FP – FC combined system for different hydrocarbon fuels and for different operating conditions, a simple mathematical model based on mass and energy balances around each unit was developed. In this simple model, input mass flow rates to the mixer were known and output mass flow

rates from the other units were calculated in a sequential manner using simple mass balances.

Output flow rates from each reactor were based on conversion data obtained from actual experiments. For example, the amounts of the feed mixture to IPOX reactor and conversions obtained in this reactor were based on experimental results obtained for Pt-Ni/Al_2O_3 catalysts. Similar approach has also been adopted for WGS and PROX reactions, utilizing data from (Selen-Çağlayan, 2003; Gökaliler, 2005; Natesakhawat *et al*., 2006; Şimşek, 2006).

Once mass flow rates were calculated for each stream in the system, energy balances are employed to calculate unknown outlet temperatures whenever necessary. This required a trial and error procedure, utilizing isobaric heat capacity data acquired from tables of Kotas (1984). Details of the calculational procedure and information on different parameters investigated are provided in Appendices A & B.

When all the streams in the system are completely defined in terms of flow rate, composition and temperature, exergy balances are easily calculated for each unit and for the entire process as explained below.

3.3. Calculation of Exergy of The Gas Streams

The general expression (3.15) utilized for calculating the exergy rate of the fuel gas is (Kotas, 1984):

$$E = \sum x_i E_i^{\Delta T} + nRT_0 \ln(P/P_0) + n[\sum x_i E_{0,i} + RT_0 \sum x_i \ln x_i] \qquad (3.15)$$

where x_i is the mole fraction of the i-th component in the mixture and n is number of total moles of the mixture. Each component at P_0, T_0 has at this point molar exergy $E_{0,i}$ while its flow rate per mole of mixture is x_i. The mixture is provided at a steady state P_0, T_0. In this work, P_0: 1 atm and T_0: 298 K were taken and standard chemical exergy (E_0) values were found Kotas' tables (Kotas, 1984). Moreover, $E_i^{\Delta T}$ (3.16) is molar thermal component of specific exergy (Kotas, 1984):

$$E_i^{\Delta T} = (T-T_0)*c_p^{E} \quad (3.16)$$

where c_p^{E} is mean isobaric exergy capacity. c_p^{E} values were found by utilizing Kotas' tables at T=298 K and P= 1 Atm. In this formulation, last term was negligible and P/P_0 is equal to 1 because of environmental pressure is 1 Atm, so $nRT_0In(P/P_0)$ is equal to zero.

After exergy values were calculated for each stream, exergy efficiencies of each unit were calculated. Lastly, after these values were obtained, all of the system's exergy efficiency (3.17) was calculated by means of:

$$\Psi = \text{Electricity} / \text{Exergy Input} \quad (3.17)$$

where Ψ is efficiency. Also, maximum possible exergy efficiency (3.18) was also calculated by:

$$\Psi_{max} = (\text{Electricity} + E_R + E_H) / \text{Exergy Input} \quad (3.18)$$

where E_R is the exergy of waste heat and E_H is the exergy of exhaust stream.

4. RESULTS AND DISCUSSION

In the exergy analysis of the FP - FC system, the results of the following experimental studies have been utilized for the reactors present in the processor part; i) for reformer, the results of IPOX tests performed over Pt–Ni/Al_2O_3 catalysts for pure propane and LPG feeds (Selen-Çağlayan, 2003; Gökaliler, 2005), ii) for WGS unit, the results of WGS tests performed over Fe – based catalysts which were reported by Özkan's group (Natesakhawat et al., 2006), and iii) for PROX unit, the results of PROX tests performed over Pt – Sn / AC catalysts (Şimşek, 2006) were used.

The flow rates were adjusted in a way that the exergy input values are equal in given conditions.

It should be noted that fuel cell conversion was taken as 85% for finding the overall exergy efficiency trends. The results are summarized below:

4.1. The Effect of IPOX Temperature

i) Due to the fact that Pt – Ni system showed very high efficiency in the temperature range of 623 – 743 K, this temperature interval was taken into account for IPOX reactor. It is clear that IPOX unit performance has a dominant effect in the overall performance of the fuel processor part. This is the reason why, the overall system exergy efficiency results are first studied as a function of IPOX reactor temperature. As obviously seen here, when IPOX reactor output temperature increased, except at 743 K, exergy efficiency of the system increased. These trends obtained as a function of IPOX reactor temperature were similar for pure propane, 50% propane – 50% butane and 75% propane – 25% butane feeds. This increase was demonstrated to be valid not only for 85% fuel cell conversion but also 80% and 75% conversion levels. For all hydrocarbon feeds, increase in IPOX temperature for the range tested in this study led to an increase in overall system exergy (Figures 4.1, 4.2 and Table 4.1).

Table 4.1. The overall system exergy efficiency as a function of IPOX reactor temperature for pure propane

IPOX reactor temperature (K)	663	723
overall system exergy efficiency	14.15	18.86

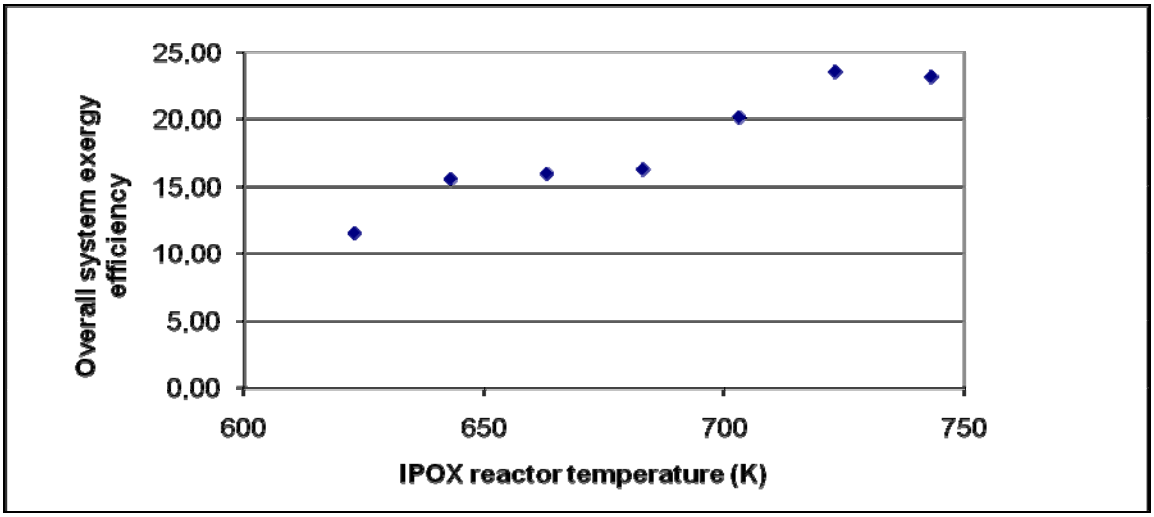

Figure 4.1. The overall system exergy efficiency as a function of IPOX reactor temperature for 50% propane – 50% butane feed

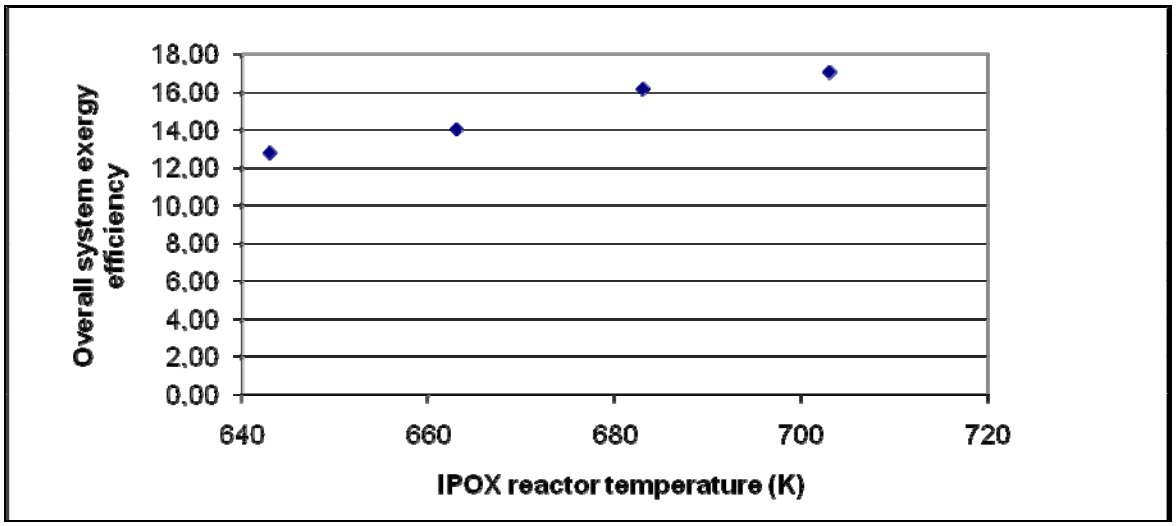

Figure 4.2. The overall system exergy efficiency as a function of IPOX reactor temperature for 75% propane – 25% butane feed

ii) Considering the fact that hydrogen amount at the exit of the IPOX reactor shows an increasing trend as a function of temperature (Figures 4.3, 4.4 and Table 4.2), which is parallel to exergy efficiency - IPOX temperature trends (Figures 4.5, 4.6 and Table 4.3), one can safely claim that the dominant parameter that determines overall system efficiency in general is the hydrogen amount at the exit of the IPOX reactor for each hydrocarbon feed. High H_2 levels suppress CH_4 amount all through the system.

iii) As a result of the fact that WGS reactor operates at constant temperature, 523 K, and at 70% of the equilibrium conversion, the increased H_2 amount at the exit of IPOX reactor directly reflects itself as enhanced H_2 amount at the fuel cell inlet (Figures 4.7, 4.8 and Table 4.4).

Table 4.2. Hydrogen amount at the exit of the IPOX reactor as a function of temperature for pure propane

IPOX reactor temperature (K)	663	723
Hydrogen amount at the exit of the IPOX reactor (μmol/s)	24.01	32.26

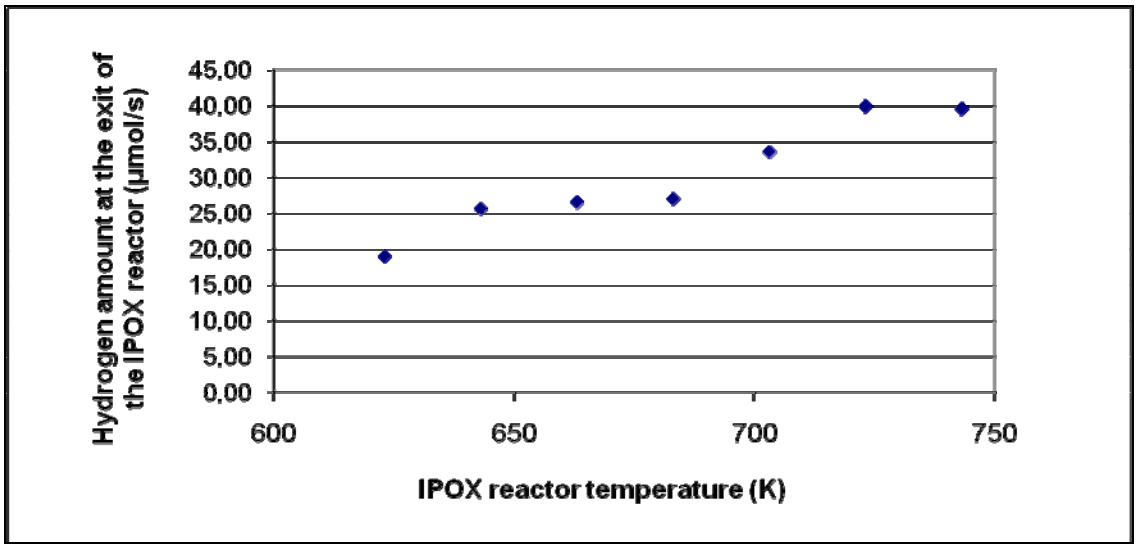

Figure 4.3. Hydrogen amount at the exit of the IPOX reactor as a function of temperature for 50% propane – 50% butane feed

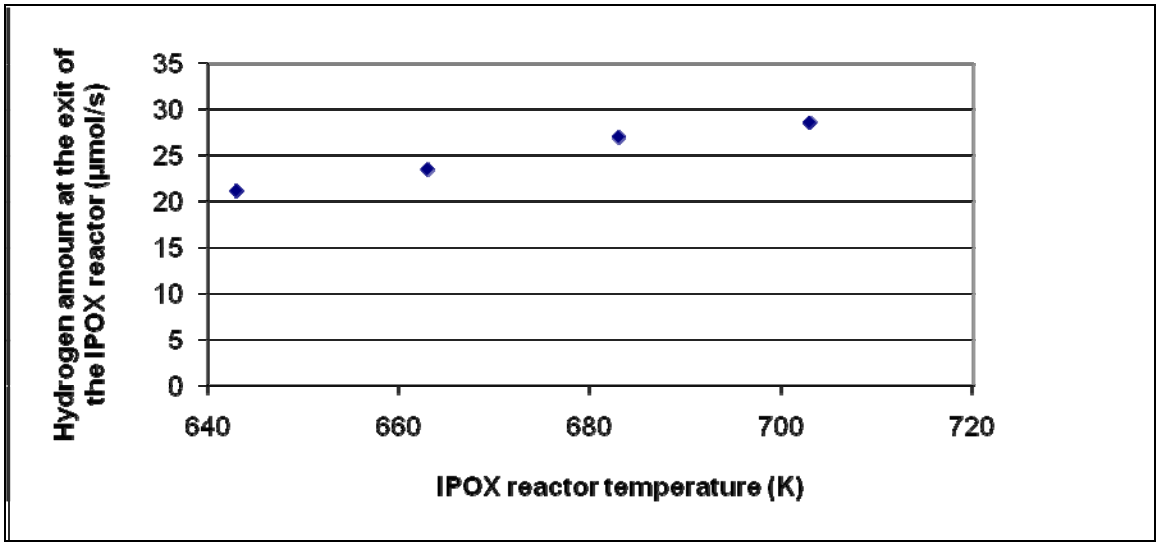

Figure 4.4. Hydrogen amount at the exit of the IPOX reactor as a function of temperature for 75% propane – 25% butane feed

Table 4.3. Exergy efficiency as a function of hydrogen amount at the IPOX outlet for pure propane

Hydrogen amount at the exit of the IPOX reactor (µmol/s)	24.01	32.26
% exergy efficiency	14.15	18.86
IPOX reactor temperature (K)	663	723

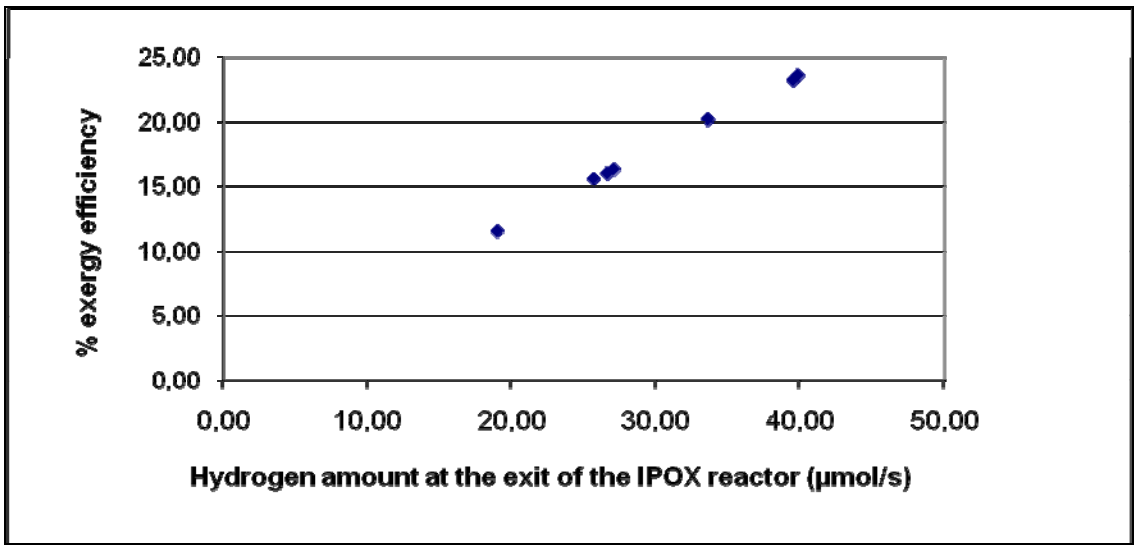

Figure 4.5. Exergy efficiency as a function of hydrogen amount at the IPOX outlet for 50% propane – 50% butane feed

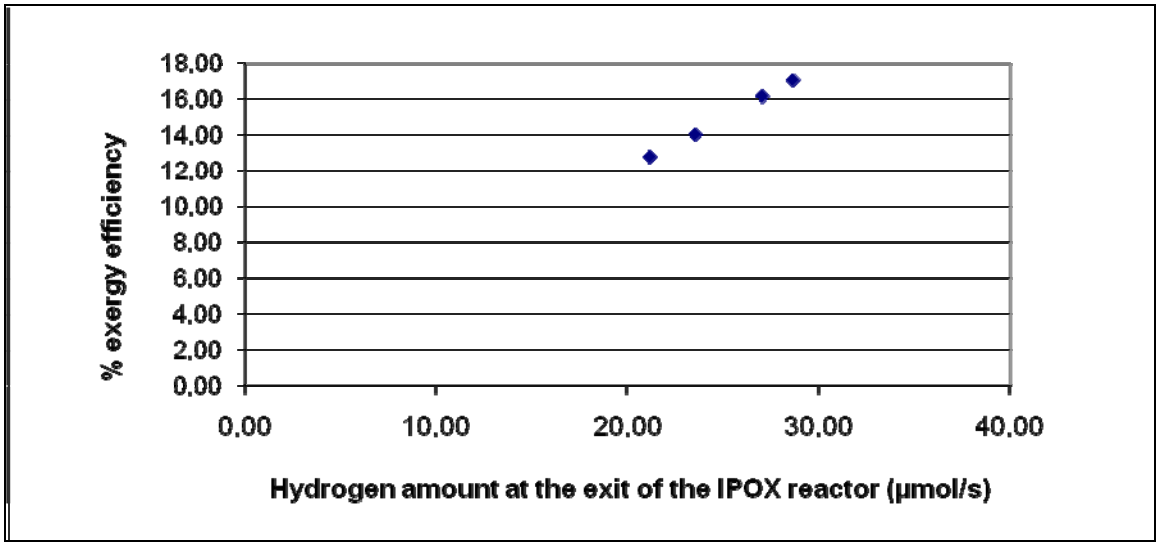

Figure 4.6. Exergy efficiency as a function of hydrogen amount at the IPOX outlet for 75% propane – 25% butane feed

Table 4.4. H_2 amount at the fuel cell inlet as a function of the H_2 amount at the exit of IPOX for pure propane

Hydrogen amount at the exit of the IPOX reactor (µmol/s)	24.01	32.26
Hydrogen amount at the fuel cell inlet (µmol/s)	24.26	32.84
IPOX reactor temperature (K)	663	723

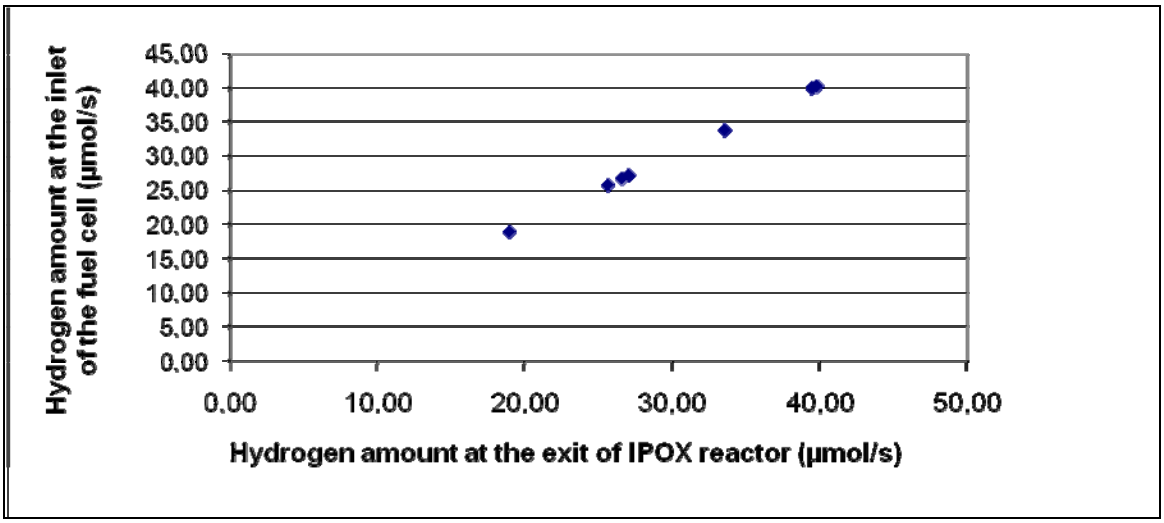

Figure 4.7. H_2 amount at the fuel cell inlet as a function of the H_2 amount at the exit of IPOX for 50% propane – 50% butane feed

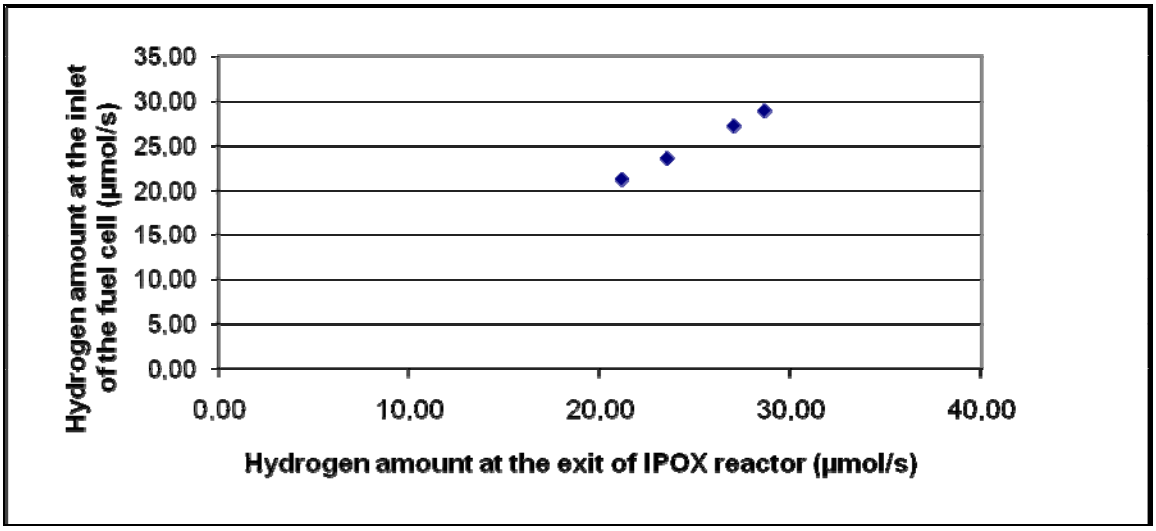

Figure 4.8. H_2 amount at the fuel cell inlet as a function of the H_2 amount at the exit of IPOX for 75% propane – 25% butane feed

As a consequence, increase in IPOX temperature led to an increase hydrogen amount at the fuel cell inlet (Figures 4.9, 4.10 and Table 4.5).

iv) Coming from the nature of the IPOX reaction which is the simultaneous steam reforming (SR) and total oxidation (TOX) as well as the performance specifications of the catalyst used, which determines the extent of main reactions, SR and TOX, and the side reactions, ie. WGS, methanation, etc., high hydrogen amount in general led to low CH_4 levels at the fuel cell outlet (Figures 4.11, 4.12 and Table 4.6).

Table 4.5. Hydrogen amount at the fuel cell inlet as a function of IPOX temperature for pure propane

IPOX reactor temperature (K)	663	723
Hydrogen amount in the fuel cell inlet (µmol/s)	24.26	32.84

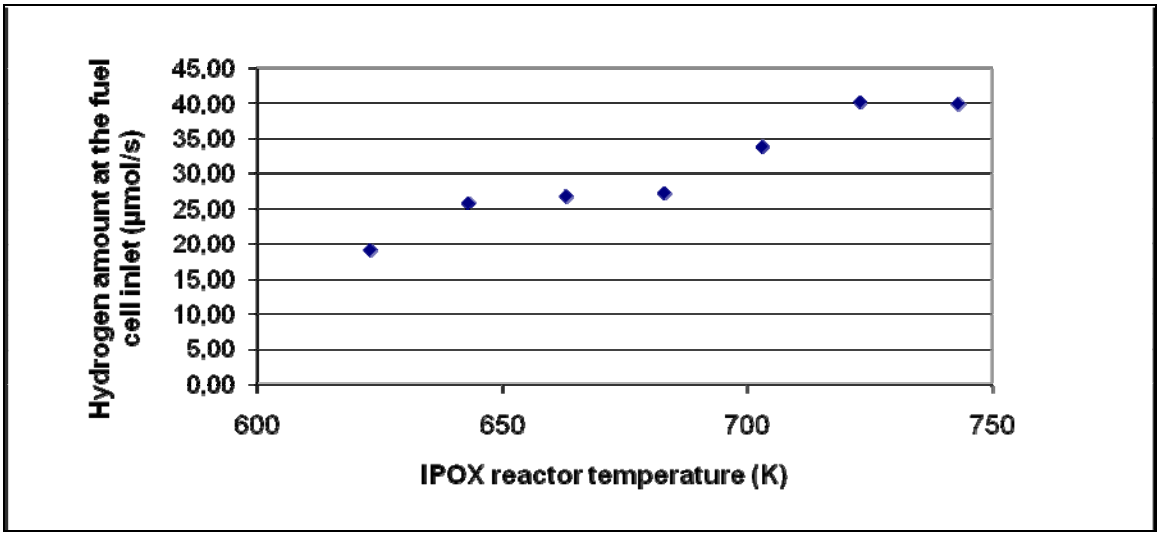

Figure 4.9. Hydrogen amount at the fuel cell inlet as a function of IPOX temperature for 50% propane – 50% butane feed

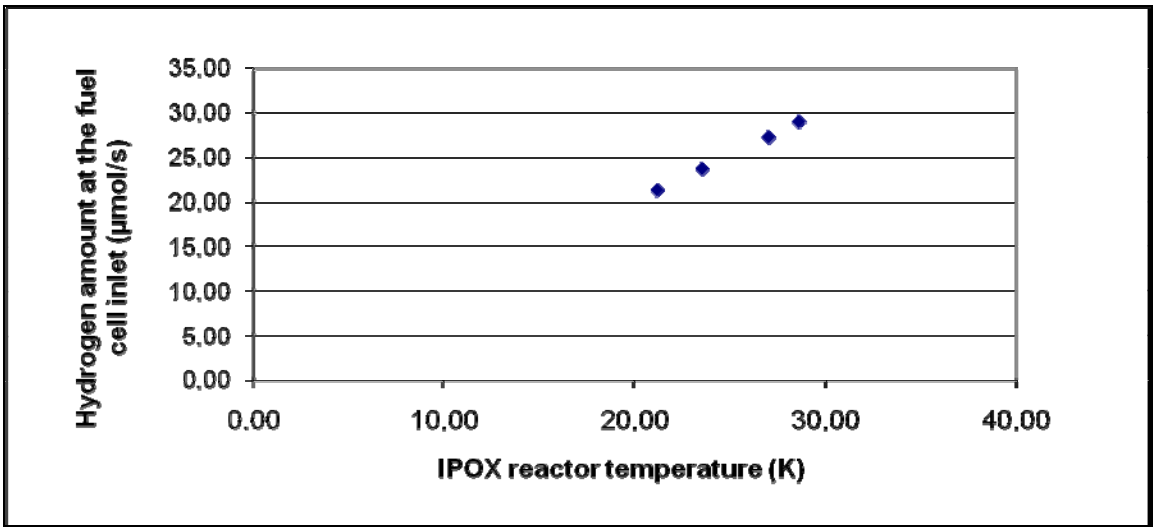

Figure 4.10. Hydrogen amount at the fuel cell inlet as a function of IPOX temperature for 75% propane – 25% butane feed

Table 4.6. The relation between H_2 production and CH_4 production for pure propane

Hydrogen amount at the exit of IPOX reactor (µmol/s)	24.01	32.26
Methane amount at the PEM exit (µmol/s)	12.98	10.75
IPOX reactor temperature (K)	663	723

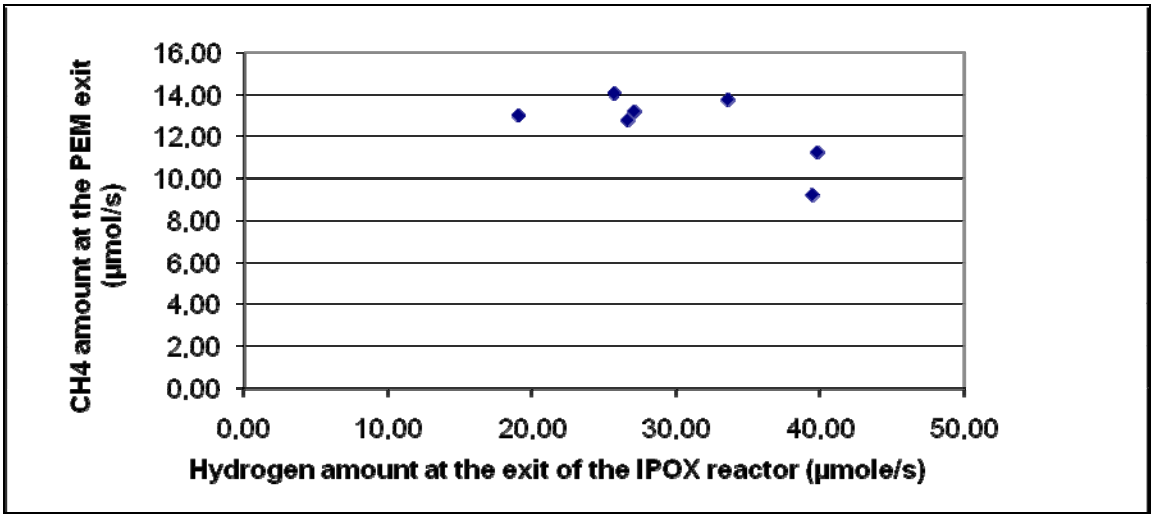

Figure 4.11. The relation between H_2 production and CH_4 production for 50% propane – 50% butane feed

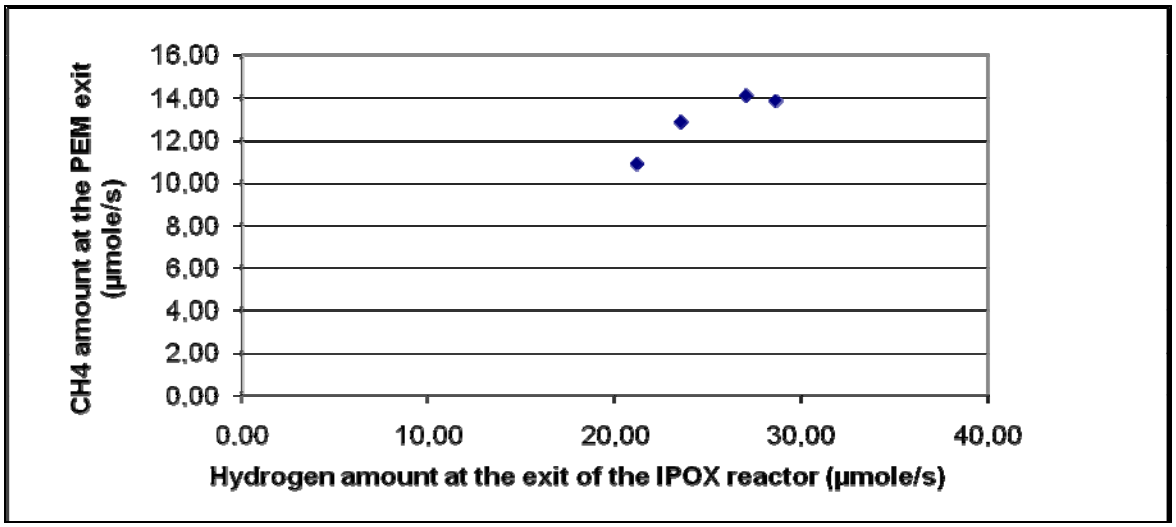

Figure 4.12. The relation between H_2 production and CH_4 production for 75% propane – 25% butane feed

The unexpected trend observed for 75% propane – 25% butane feed in Figure 4.12 may come from the selectivity characteristics of the Pt – Ni catalyst for WGS and methanation side reactions.

Figures 4.13, 4.14 and Table 4.7 show CH_4 production as a function of IPOX temperature.

v) The electricity production is very sensible to hydrogen amount and, as a consequence, IPOX reactor temperature (Figures 4.15, 4.16 and Table 4.8).

Table 4.7. CH_4 amount at the PEM exit as a function of IPOX temperature for pure propane

IPOX reactor temperature (K)	663	723
Methane amount at the PEM exit (µmol/s)	12.98	10.75

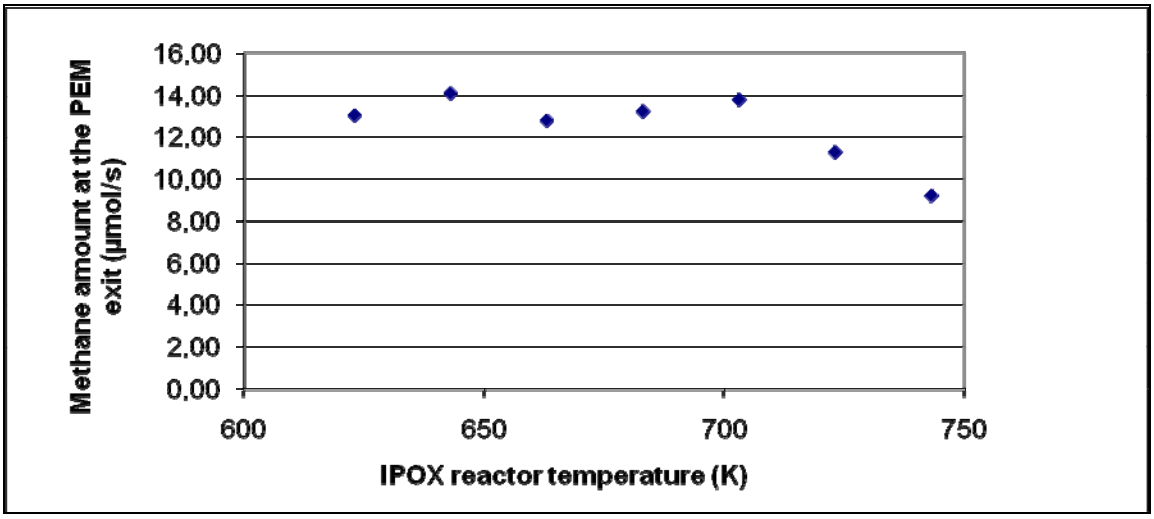

Figure 4.13. CH_4 amount at the PEM exit as a function of IPOX temperature for 50% propane – 50% butane feed

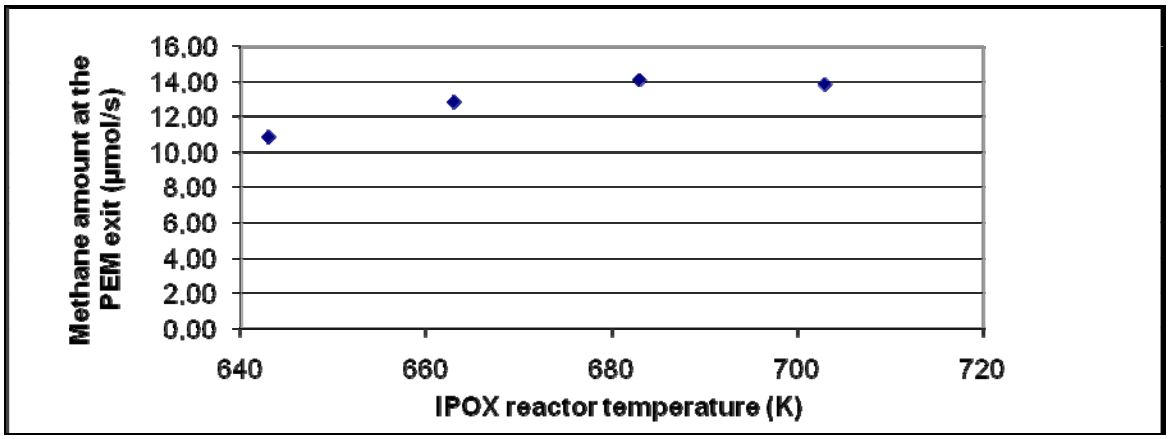

Figure 4.14. CH_4 amount at the PEM exit as a function of IPOX temperature for 75% propane – 25% butane feed

Table 4.8. The electricity production as a function of IPOX temperature for pure propane

IPOX reactor temperature (K)	663	723
Electricity production (j/s)	3.018	4.021

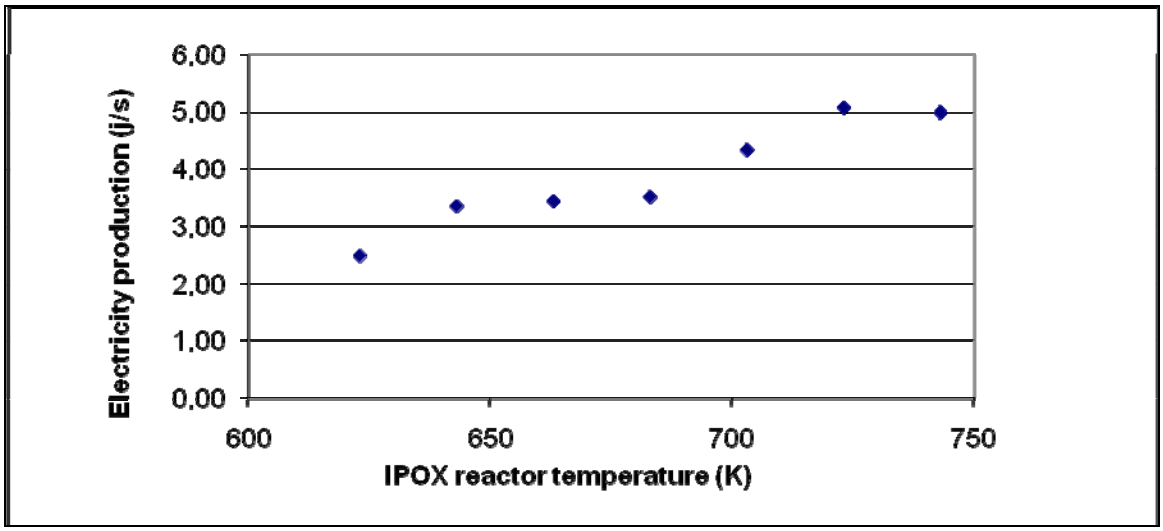

Figure 4.15. The electricity production as a function of IPOX temperature for 50% propane – 50% butane feed

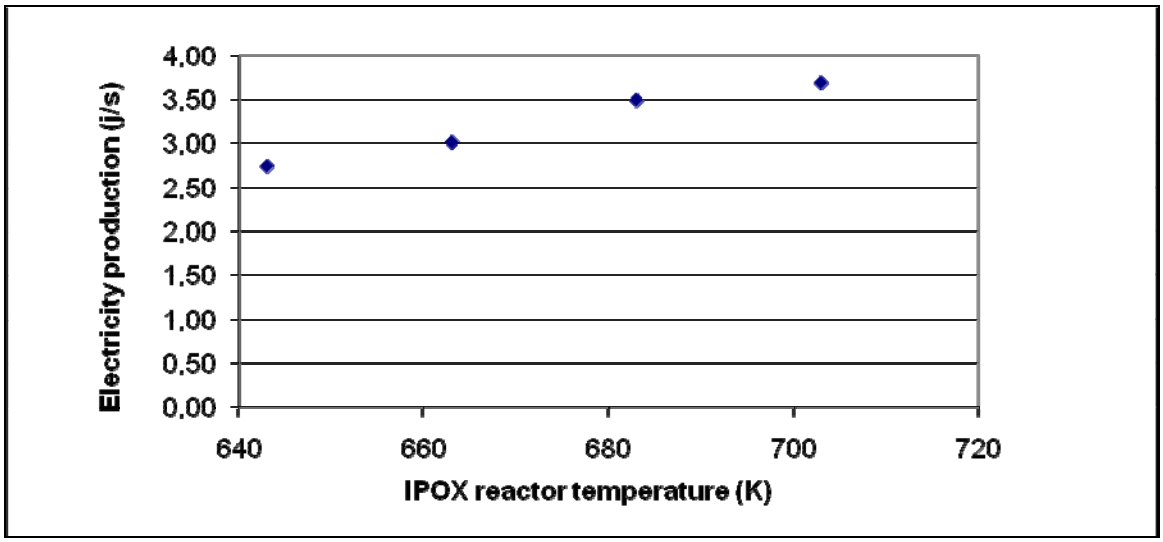

Figure 4.16. The electricity production as a function of IPOX temperature for 75% propane – 25% butane feed

4.2. The Effect of WGS and PROX Units

i) The WGS unit has a limited effect on the overall performance of the FP – FC system. This is reasonable considering the facts that a) the conversion at the WGS unit is taken as 70% of the thermodynamic conversion level, which was reported at the literature for Fe-based catalyst at 523 K, without taking the inert compositions in the inlet stream into account. b) the WGS unit temperature was taken as constant at 523 K.

ii) In the PROX unit, CO conversion was taken as 100%, as the experimental results indicated for Pt–Sn/AC catalyst at 125 C. But, the converted amount of CO is very limited, so its contribution to the exergy efficiency of the FP – FC system, is practically negligible.

iii) The WGS reactor is assumed to be operating at 70% of its equilibrium conversion level at 523 K. Additionaly, the hydrocarbons present in the feed to WGS unit are considered as inerts for the reaction. Thus, the hydrogen amount at the exit of the IPOX unit dominantly determines the changes of hydrogen amount at the inlet of the fuel cell [Figures 4.7, 4.8 and Table 4.4).

4.3. The Effect of FC Performance

i) The fuel cell conversion in the calculations were taken between 75% - 85%. In the figures, the electricity production of the FC unit is reported for its 85% conversion efficiency. Since fuel cell electricity production is a direct function of H_2 amount in the FC feed for constant feed composition (Figures 4.17, 4.18 and Table 4.9), the results clearly show an increase in the electricity production as a function of IPOX reactor temperature for all three hydrocarbon feeds (Figures 4.15, 4.16 and Table 4.8).

Table 4.9. Electricity production as a function of H_2 production in IPOX for pure propane

Hydrogen production in IPOX (μmol/s)	24.01	32.26
Electricity production (j/s)	3.018	4.021
IPOX reactor temperature (K)	663	723

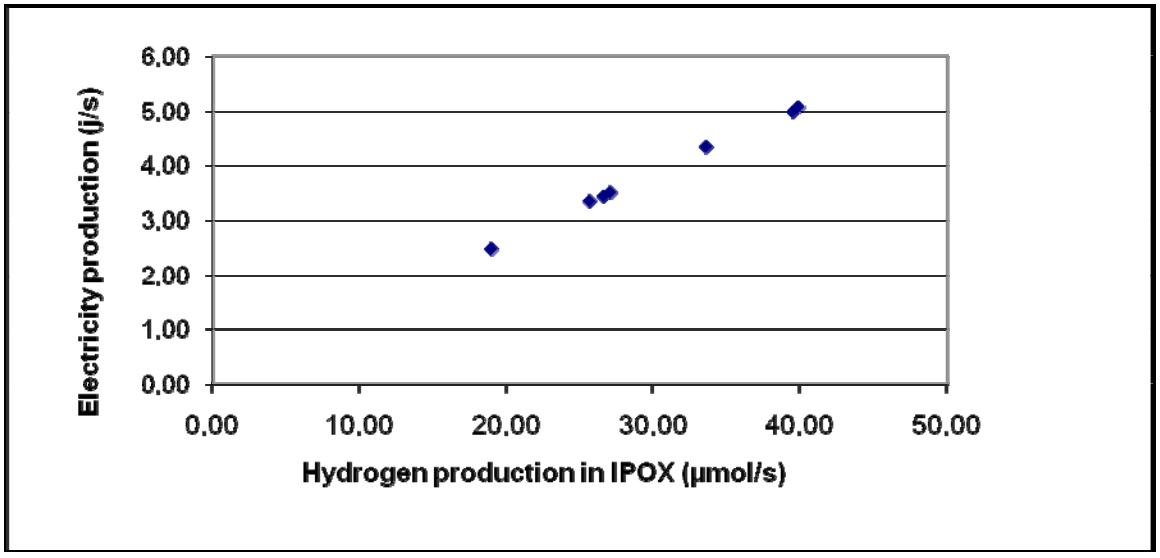

Figure 4.17. Electricity production as a function of H_2 production in IPOX for 50% propane – 50% butane feed

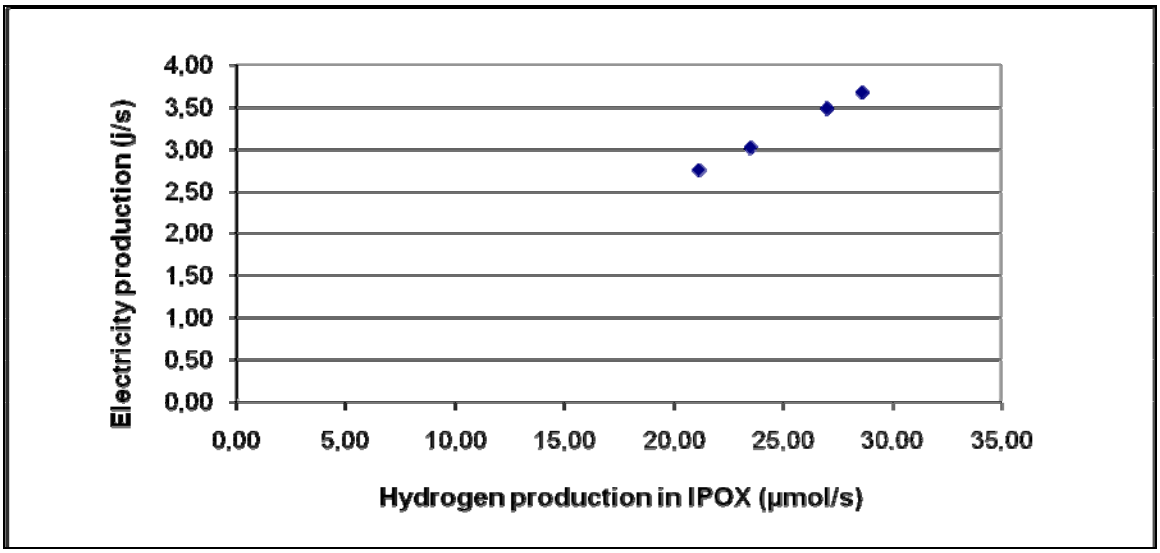

Figure 4.18. Electricity production as a function of H_2 production in for 75% propane – 25% butane feed

ii) In PEM fuel cell, when conversion is increased from 75% to 80% or 85%, increase of the total electricity generation and the overall system exergy efficiency are shown in Table 4.10. Furthermore, maximum exergy efficiency values are shown in the same table. Accordingly, exergy efficiency of the system which is proportional to FC electricity generation increases with hydrogen conversion at 643, 663, 703 and 723 K (Figures 4.19, 4.20, 4.21, 4.22, 4.23 and Table 4.10);

Table 4.10. The total electricity generation and the overall system exergy efficiency

IPOX T	FEED	Total electricity generation (j/s)	Total electricity generation (j/s)	Total electricity generation (j/s)	Overall system exergy efficiency	Overall system exergy Efficiency	Overall system exergy efficiency	Maximum exergy efficiency	Maximum exergy efficiency	Maximum exergy efficiency
(K)		75%	80%	85%	75%	80%	85%	75%	80%	85%
663	pure	2.665	2.841	3.018	12.50	13.33	14.15	41.87	41.87	41.74
723	pure	3.544	3.782	4.021	16.62	17.74	18.86	40.97	41.00	40.92
623	50%-50%	2.213	2.352	2.491	10.29	10.93	11.58	32.02	32.11	32.17
643	50%-50%	2.974	3.162	3.350	13.82	14.70	15.57	39.31	39.35	39.43
663	50%-50%	3.049	3.243	3.438	14.17	15.08	15.98	37.14	37.18	37.26
683	50%-50%	3.111	3.310	3.508	14.46	15.38	16.31	38.36	38.48	38.52
703	50%-50%	3.847	4.093	4.340	17.88	19.03	20.17	41.27	41.39	41.47
723	50%-50%	4.482	4.775	5.068	20.83	22.20	23.56	41.21	41.40	41.65
743	50%-50%	4.405	4.696	4.987	20.48	21.83	23.18	37.58	37.92	38.35
643	75%-25%	2.440	2.595	2.750	11.35	12.07	12.79	37.33	37.36	37.39
663	75%-25%	2.677	2.849	3.021	12.45	13.25	14.05	36.81	36.94	36.92
683	75%-25%	3.089	3.287	3.485	14.36	15.28	16.20	41.72	41.72	41.73
703	75%-25%	3.258	3.468	3.678	15.15	16.12	17.10	41.21	41.17	41.19

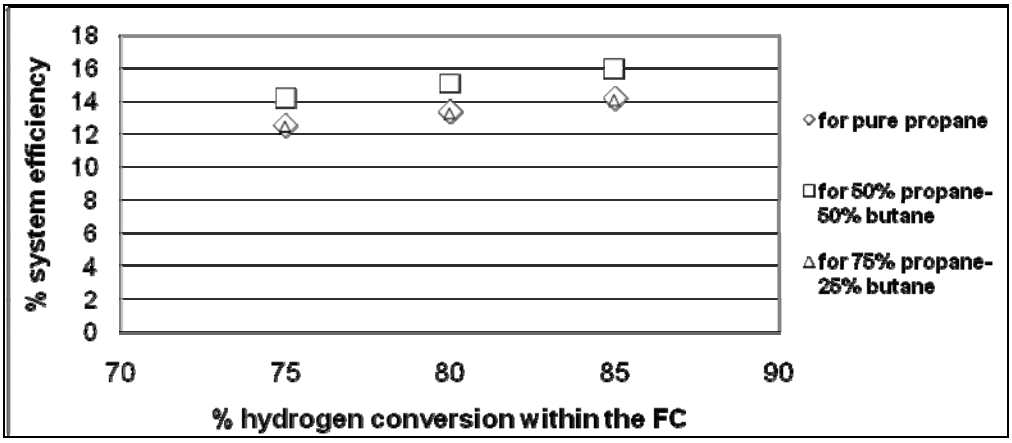

Figure 4.19. The relation between H_2 conversion within the FC and system efficiency at 663 K

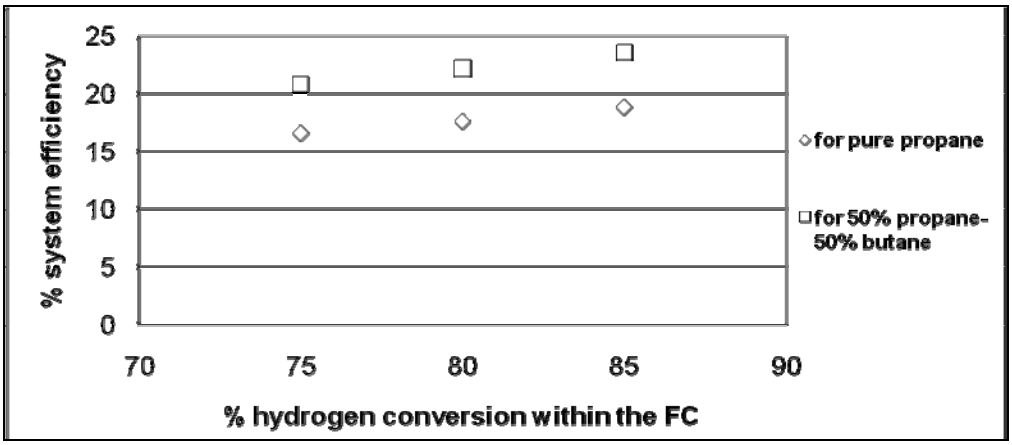

Figure 4.20. The relation between H_2 conversion within the FC and system efficiency at 723 K

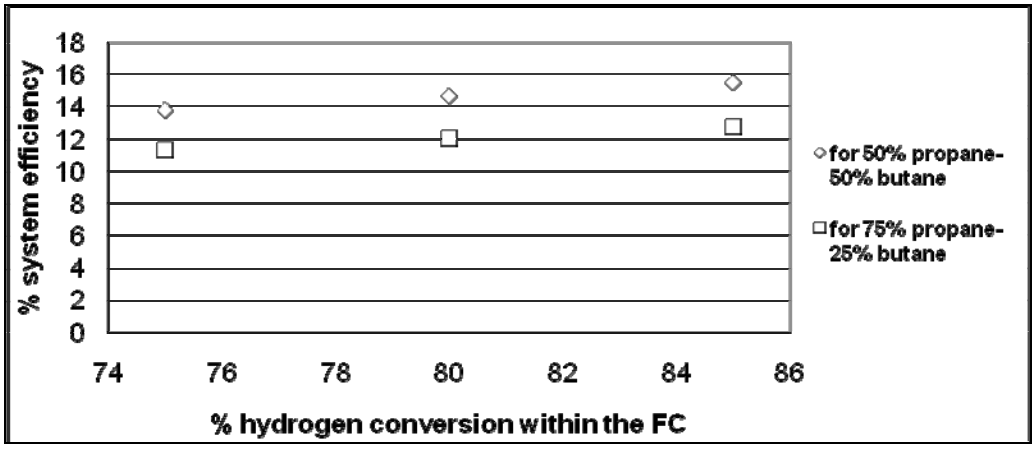

Figure 4.21. The relation between H_2 conversion within the FC and system efficiency at 643 K

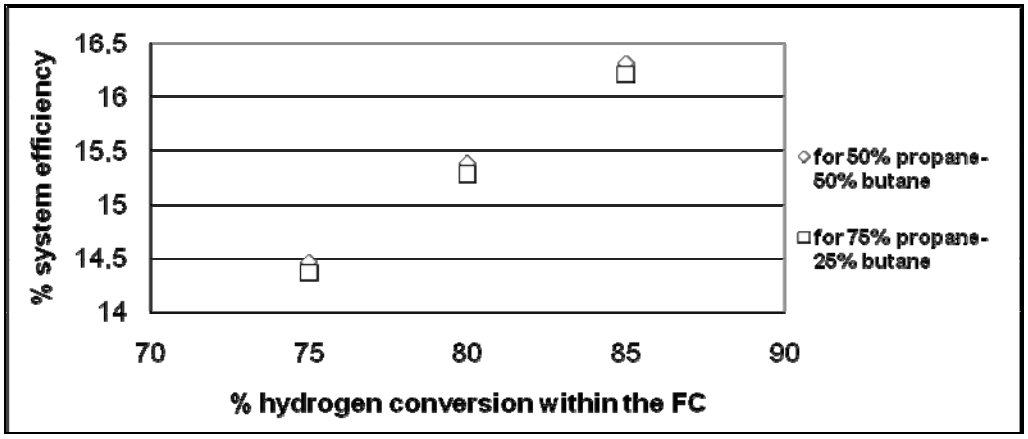

Figure 4.22. The relation between H_2 conversion within the FC and system efficiency at 683 K

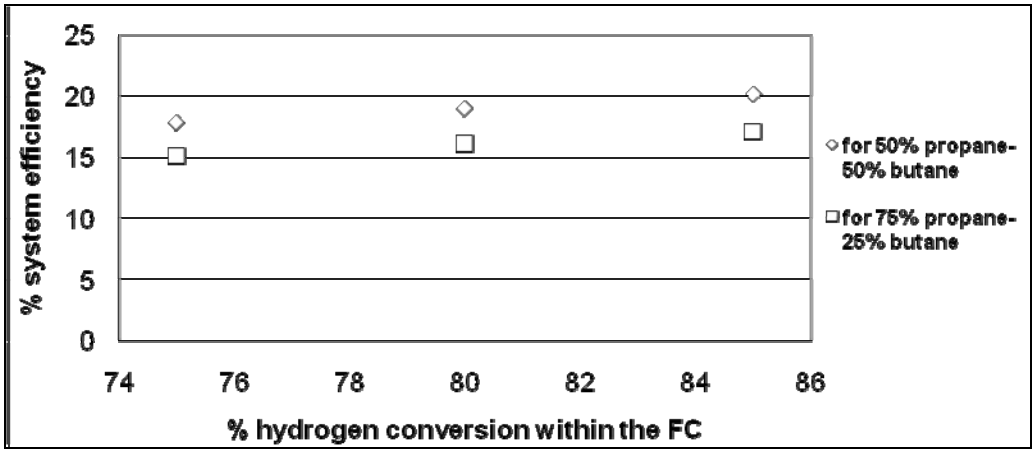

Figure 4.23. The relation between H_2 conversion within the FC and system efficiency at 703 K

4.4. The Effect of Fuel Cell Outlet/Exhaust

The exhaust, which is the effluent of the last evaporator, leaves the FP – FC system at very high temperatures led by the insufficient utilization/conversion of methane within the system. Methane was produced in IPOX and it was not consumed anywhere till the Burner. In general, the methane amount at the fuel cell outlet/exhaust has a negative effect on the overall system efficiency (Figure 4.24 and Table 4.11). The only exception to this trend is shown in Figure 4.25 for 75% propane – 25% butane feed. The unexpected result may stem from the relatively higher temperature levels of the purge stream from the evaporator, compared to those calculated for 50% C_3H_8 – 50% C_4H_{10} feed, leading high exergy losses which shadows the effect of methane amount on the efficiency.

The results of this study clearly show that either the methane production activity of the IPOX catalyst should be limited or rejected methane should be mixed to the fresh feed prior to the IPOX unit. Since the experimental data for mixed feed tests are not available, the calculations considering recycle of the rejected stream could not be performed. It is clear that if the fuel cell outlet is utilized through a recycle to the fresh feed, output temperature of system could be less than the ones obtained in this study. In the future, exergy analysis of the FP – FC system will be performed by using experimental IPOX values which will be obtained for the HC feed containing CH_4 presenting recycled stream.

Table 4.11. The impact on the overall system efficiency of the CH_4 amount at the fuel cell outlet / exhaust for pure propane

Methane amount at the PEM exit (µmol/s)	12.98	10.75
% exergy efficiency	14.15	18.86
IPOX reactor temperature (K)	663	723

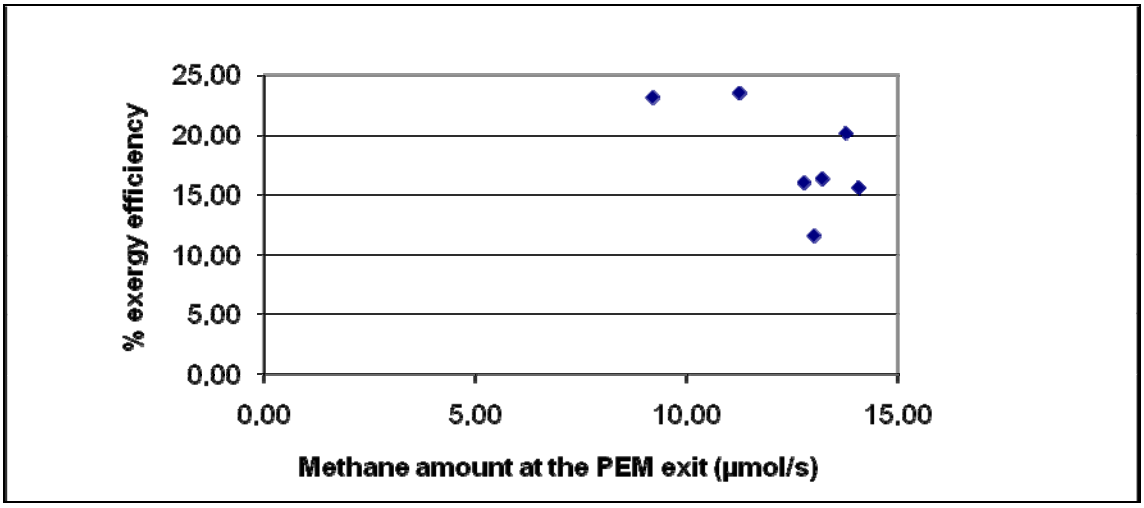

Figure 4.24. The impact on the overall system efficiency of the CH_4 amount at the fuel cell outlet / exhaust for 50% propane – 50% butane feed

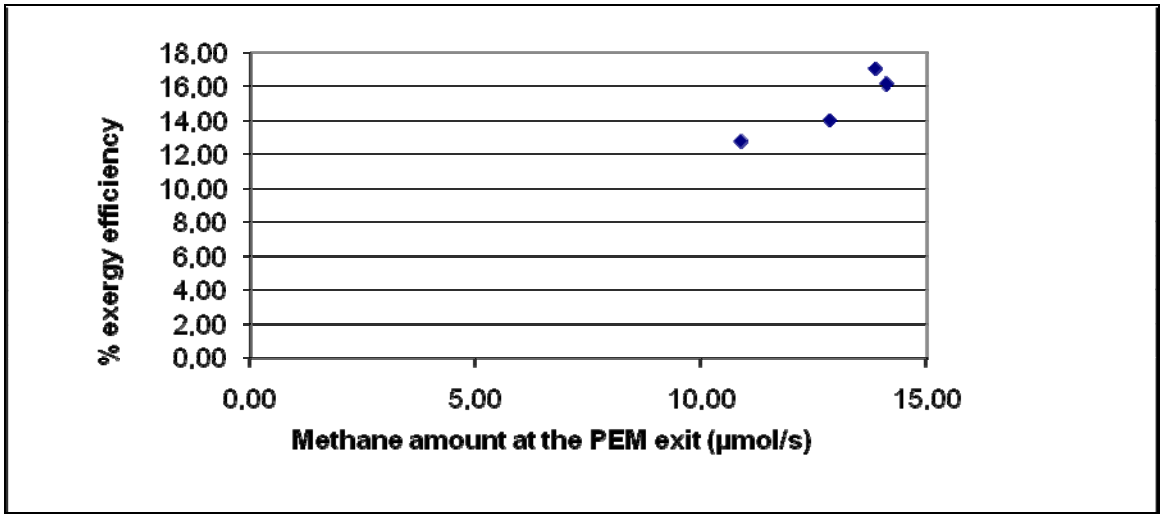

Figure 4.25. The impact on the overall system efficiency of the CH_4 amount at the fuel cell outlet / exhaust for 75% propane – 25% butane feed

4.5. The Effect of Hydrocarbon Feed Composition

A comparison of exergy efficiency values obtained for different feed compositions show that exergy efficiency of the 50% propane – 50% butane feed is higher than the other feeds. This is partly due to the higher enthalpy of butane, which leads to enhanced IPOX performance in hydrogen production. It should be noted that in the IPOX tests had been conducted previously, the catalyst suffers from severe coke deposition when pure butane was used as the hydrocarbon feed. Thus, the hydrocarbon feed composition should be optimized such as to exploit the beneficial effects of butane on IPOX performance while guaranteeing that there is no coke deposition which leads to severe stability problems.

5. CONCLUSIONS

The major aim of this study was to present an exergy analysis of an integrated fuel processor-fuel cell system for mobile and small scale stationary applications. Pure propane or mixtures of propane and n-butane, with compositions ranging from pure propane to equimolar propane-butane mixture, were used as the fuel to the fuel processor, which has series of catalytic reactors, ie. Indirect Partial Oxidation, Water Gas Shift and Preferential Oxidation reactors, and mixing and heat exchanging units. A Proton Exchange Membrane (PEM) was preferred as the fuel cell. Determination of the parameters to be varied and their respective ranges in the exergy analysis was based on the results of previous experimental work carried out in Catalyst Technology and Reaction Engineering Laboratory (CATREL) of Boğaziçi University. Conclusions that can be drawn from this work indicate that the targeted objectives are satisfied. The major conclusions are given as follows:

● When IPOX reactor output temperature increased from 623 K to 743 K, exergy efficiency of the system increased. For all hydrocarbon feeds, increase in IPOX temperature for the range tested in this study caused an increase in overall system exergy.

● Hydrogen amount at the IPOX outlet stream demonstrates an increasing trend as a function of temperature as the parallel to exergy efficiency - IPOX temperature trends.

● The electricity production which is produced by PEM was shown to be very sensible to hydrogen amount and, as a consequence, IPOX reactor temperature.

● Due to the fact that the conversion at the WGS unit was taken as 70% of the thermodynamic conversion level without taking the inert compositions in the inlet stream into account and the WGS unit temperature was taken as constant at 523 K, the WGS unit showed that it had a limited impact on the overall performance of the FP – FC system.

● The results show that either the methane production activity of the IPOX catalyst should be suppressed and/or a fraction of the rejected gas mixture from the fuel cell should be recycled and mixed to the fresh hydrocarbon feed prior to the IPOX unit.

● Due to the higher enthalpy of butane, which leads to enhanced IPOX performance in hydrogen production, exergy efficiency of the 50% propane – 50% butane feed is higher than the other feeds. On the other hand, it has been known from the experimental studies that the ATR catalyst suffers from severe coke deposition when pure butane was used as the hydrocarbon feed; thus, the fresh hydrocarbon feed composition should be optimized considering both the stability of the catalyst and energy efficiency of the combined system.

APPENDIX A: REAL DATA

Real data used in this study for IPOX reactor are summarized below:

For pure propane and 75% propane – 25% n-butane feeds, these real data were obtained from works of Çağlayan. At different temperatures, feed inputs and reactor outputs are indicated in Table A.1 & Table A.2. The attention should be focused on C/O ratio and steam/C ratio where these ratios are shown C/O ratio: 2.7 and S/C ratio: 3 for pure propane feed, but for 75% propane – 25% n-butane C/O ratio is similar, whereas S/O ratio is taken as 5. In this work, other data which are achieved by Gökaliler are also used. In these data, flow rates of propane and n-butane are equal and C/O ratio: 2.12, S/O ratio: 5 as seen in Table A.1 & Table A.2.

Table A.1. Feed inputs for pure propane, 50% propane - 50% butane and 75% propane - 25% butane at different temperatures

Feed	$C : O_2$	S : C	Total Flow (ml/min)	W / F (min)	Cat.Weight (g)	T (K)	Feed inputs (μmol/s)				
							C_3H_8	C_4H_{10}	H_2O	O_2	N_2
Pure	2.70	3	293	0.51	0.15	663	14.94	-	134.1	16.57	62.33
						723	13.16	-	118.2	14.60	54.90
50% - 50%	2.12	5	133.7	1.12	0.15	623	2.722	2.722	95.26	8.986	33.80
						643	2.360	2.360	82.38	7.772	29.24
						663	2.472	2.472	86.51	8.610	30.70
						683	2.399	2.399	83.96	7.921	29.80
						703	2.151	2.151	75.29	7.102	26.72
						723	2.212	2.212	77.37	7.299	27.46
						743	2.434	2.434	85.19	8.036	30.23
75% - 25%	2.70	5	293	0.51	0.15	643	7.120	2.373	154.3	11.43	42.99
						663	6.937	2.312	150.3	11.13	41.88
						683	6.786	2.262	147.0	10.89	40.97
						703	6.994	2.331	151.5	11.22	42.23

Table A.2. Reactor outputs for pure propane, 50% propane - 50% butane and 75% propane - 25% butane at different temperatures

Feed	$C : O_2$	S : C	Total Flow (ml/min)	W / F (min)	Cat.Weight (g)	T (K)	Reactor outputs (μmol/s)							
							C_3H_8	C_4H_{10}	H_2O	H_2	CH_4	CO	CO_2	O_2
Pure	2.70	3	293	0.51	0.15	663	-	-	116.9	36.88	19.94	1.277	23.39	1.188
						723	-	-	98.07	43.64	14.55	2.425	22.51	0.9240
50% - 50%	2.12	5	133.7	1.12	0.15	623	-	-	90.74	12.23	8.390	0.2450	10.42	0.7040
						643	-	-	73.60	14.29	7.840	0.3060	8.332	3.679
						663	-	-	78.24	15.56	7.479	0.3640	9.460	2.656
						683	-	-	75.18	15.36	7.503	0.3800	8.911	3.209
						703	-	-	63.53	17.09	7.016	0.4720	7.570	5.178
						723	-	-	64.66	20.83	5.892	0.7170	8.866	4.431
						743	-	-	73.74	22.74	5.306	0.9060	10.83	2.481
75% - 25%	2.70	5	293	0.51	0.15	643	1.046	0.4070	143.3	22.21	11.43	0.4200	14.24	2.455
						663	0.3250	0.0290	137.8	24.05	13.14	0.4790	15.35	1.786
						683	0.2040	0.0260	129.3	27.03	14.12	0.6000	13.97	5.502
						703	0.0340	0.0020	132.9	29.51	14.30	0.9170	14.98	5.090

APPENDIX B: SAMPLE CALCULATIONS

In this section, sample calculations for 50% n–butane - 50% propane feed with IPOX reactor operating at 723 K are presented. Flow sheet providing information on known flow rates and temperatures is shown in Figure B.1.

B.1. IPOX reactor calculations

Based on experimental measurements, the species and amounts contained in the outlet stream from the IPOX reactor are 4.431 μmol/s of O_2, 27.46 μmol/s of N_2, 64.65 μmol/s of H_2O, 8.866 μmol/s of CO, 20.83 μmol/s of H_2 and 5.892 μmol/s of CH_4.

As clearly seen above, propane and n-butane are completely consumed. On the other hand, CO, CO_2, H_2 and CH_4 are produced in addition to O_2, N_2 and H_2O.

The exit gas temperature of IPOX will be also calculated from the energy balance assuming the process to be adiabatic.

The enthalpy of each stream (B.1) can be expressed in terms of its chemical and physical components:

$$H = \sum n_i h_d^o + \sum n_i (T-T_0) c_p^h \qquad (B.1)$$

where n_i is flow rates of each components, h_d^o is ideal gas standard enthalpy of formation, T is reaction temperature, T_0 is 298 K and c_p^h is mean isobaric heat capacity for enthalpy of components. The energy balance:

$$H_{out} = H_{in} \qquad (B.2)$$

Values of h_d^o and c_p^h for different components of the mixture can be obtained from tables of Kotas.

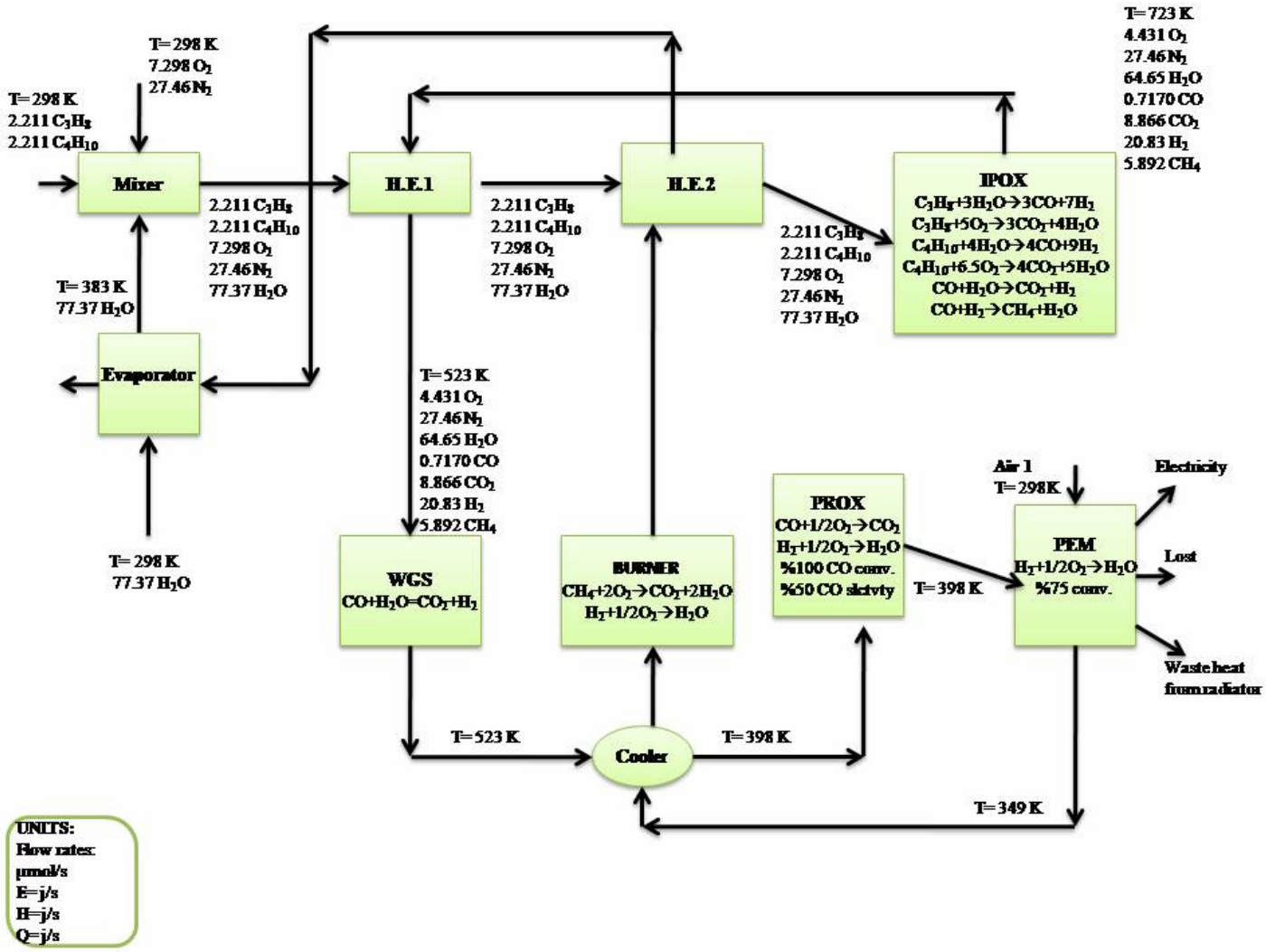

Figure B.1.Known flow rates and temperatures

The following table gives values of c_p^h for T=723 K and values of h_d^o for the components of the mixture and $H_{(T=723\ K)}$ = -17.70 j/s is found from the tabulated values.

Table B.1. c_p^h and h_d^o values for mixture components for T=723 K

T=723 K	H_2O	O_2	N_2	H_2	CH_4	CO	CO_2
n_i (μmol/s)	64.66	4.431	27.46	20.83	5.892	0.7164	8.866
h_d^0 (kj/kmol)	-241814	0	0	0	-74520	110530	393510
c_p^h(kj/kmol*K)	35.33	31.56	30.26	29.45	47.32	30.20	45.44

Values of c_p^h extracted from tables of Kotas for a trial value of inlet temperature of IPOX can be used in the energy balance to calculate this temperature by iteration.

Table B.2. c_p^h and h_d^o (T=661 K) values for a trial value of inlet temperature of IPOX

T=661 K	H_20	O_2	N_2
n_i (μmol/s)	77.37	7.298	27.46
h_d^0 (kj/kmol)	-241814	0	0
c_p^h(kj/kmol*K)	34.99	31.17	30.09

And also $h_d^o + (T-T_0)c_p^h$ values of C_3H_8 and C_4H_{10} found this formulation (Sinnott *at al.*,1983):

$$H - n_i h_d^o = n_i \int c_p dT = n_i \int (C_P VAPA + (C_P VAPB)*T + (C_P VAPC)*T^2 + (C_P VAPD)*T^3) dT \quad (B.3)$$

where h_d^o = -104680 kj/kmol for C_3H_8 and h_d^o = -125790 kj/kmol for C_4H_{10}. In this formulation, c_p unit is j/mol*K and temperature unit is Kelvin. C_PVAPA, C_PVAPB, C_PVAPC and C_PVAPD are constants in the ideal gas. These constants are -4.224, 0.3062, $1.586*10^{-4}$, $3.214*10^{-8}$ for C_3H_8; and -9.487, 0.3313, $-1.108*10^{-4}$, $-2.821*10^{-9}$ for C_4H_{10}.

The flow rates of C_3H_8 and C_4H_{10} respectively:

$$n_{(C3H8)} = 2.211\ \mu mol/s$$

$$n_{(C4H10)} = 2.211\ \mu mol/s$$

From the tabulated values:

$$H_{(T=661\ K)} = -17.67\ j/s \text{ and}$$

$$-17.70 + 17.67 = -0.0257\ j/s$$

Since this difference is negligible, T=661 K is found as the inlet temperature of IPOX.

The exergy efficiency of the process can now be calculated using the exergy balance for every unit.

Exergy values can be evaluated from the expression (Kotas, 1984):

$$E = \sum x_i E_i^{\Delta T} + nRT_0 In(P/P_0) + n[\ \sum x_i E_{0,i} + RT_0 \sum x_i Inx_i\ ] \qquad (B.4)$$

To calculate E requires the following data on E_0 and c_P^E (for every temperature) from the tables of Kotas.

Table B.3. E_0 and c_P^E values for T=723 K

T=723 K	H_2O	O_2	N_2	H_2	CH_4	CO	CO_2
n_i (μmol/s)	64.65	4.431	27.46	20.83	5.892	0.7164	8.866
E_0 (kj/kmol)	11710	3970	720	238490	836510	275430	20140
c_p^E (kj/kmol)	13.49	12.27	11.55	11.21	18.95	11.52	17.81

Table B.4. E_0 and c_P^E values for T=661 K

T=661 K	H_20	O_2	N_2
n_i (μmol/s)	77.37	7.298	27.46
E_0 (kj/kmol)	11710	3970	720
c_p^E (kj/kmol)	12.17	11.07	10.48

Also, $(T-T_0)c_P^E$ values for C_3H_8 and C_4H_{10} are calculated by means of this formulation (Sinnott *et al.*, 1983):

$$E - n_iE_0 = n_i[(H-h_d^0) - (s - s_0)] + nRT_0\sum x_i Inx_i \quad (B.5)$$

$$s - s_0 = \int(C_PVAPA/T + C_PVAPB + C_PVAPC*T + C_PVAPD*T^2)dT \quad (B.6)$$

where $E_0 = 2163190$ kj/kmol (for propane) and $E_0 = 2818930$ kj/kmol (for n-butane).

In IPOX reactor, exergy values are:

$$E_{(T=661\ K)} = 12.25 \text{ j/s and } E_{(T=723\ K)} = 11.34 \text{ j/s}$$

and exergy efficiency of the process is found by (B.6):

$$E_{eff} = E_{out} / E_{in} \quad (B.7)$$

Here; $E_{eff} = 11.34 / 12.25 = 0.9260$

B.2. WGS reactor calculations

Outlet stream of IPOX provides heat to heat exchanger 1 and it abandons heat exchanger 1 at 523 K. Then, it is sent to WGS reactor. In this reactor, this reaction occurs:

$$CO + H_2O \leftrightarrow CO_2 + H_2 \quad (B.8)$$

Here, 70% of equilibrium conversion at specified temperature is utilized regardless of hydrocarbon feed composition. Conversion at thermodynamic equilibrium is found by (Levenspiel, 1962):

$$R*In(K_2/K_1) = \Delta\alpha*In(T_2/T_1) + (\Delta\beta/2)*(T_2-T_1) + (\Delta\gamma/3)*(T_2^2-T_1^2) + [-\Delta H_0 + \Delta\alpha*T_0 + (\Delta\beta/2)*T_0^2 + (\Delta\gamma/3)*T_0^3]*(1/T_2-1/T_1) \quad (B.9)$$

$\Delta G_0 = -28630$ j/mol at $T_1 = 298$ K and by using (B.8):

$$\Delta G_0 = -RTInK \quad (B.10)$$

K_{298} = 104366.937 value is found. This expression allows us to find the variation of the equilibrium constants, hence conversion, with temperature.

$$K_{523} = 89.49$$

$$K_{523} = [[CO_2]_0 + [CO]_0*X]*[[H_2]_0 + [CO]_0*X] / [[CO]_0*(1-X)]*[H_2O]_0 - [CO]_0*X] \quad (B.11)$$

where $[CO_2]_0$ = 8.866 μmol/s; $[CO]_0$ = 0.7170 μmol/s; $[H_2]_0$ = 20.83 μmol/s;

$[H_2O]_0$ = 64.66 μmol/s.

For WGS reaction, equilibrium conversion is 0.95 and 70% of equilibrium conversion is 0.6650 at 523 K. The composition of the products of WGS reaction are 4.431 μmol/s of O_2, 27.46 μmol/s of N_2, 64.18 μmol/s of H_2O, 0.2402 μmol/s of CO, 9.343 μmol/s of CO_2, 21.30 μmol/s of H_2 and 5.892 μmol/s of CH_4. Here, enthalpy values of inlet and outlet streams are calculated as explained before.

Table B.5. h_d^0, c_p^h values for T=523 K and WGS reactant and product flow rates

T=523 K	H_2O	O_2	N_2	H_2	CH_4	CO	CO_2
n_{in} (μmol/s)	64.65	4.431	27.46	20.83	5.892	0.7164	8.865
n_{out} (μmol/s)	64.18	4.431	27.46	21.30	5.892	0.2402	9.343
h_d^0 (kj/kmol)	-241814	0	0	0	-74520	110530	393510
c_p^h(kj/kmol*K)	34.22	30.06	29.73	29.11	41.89	29.70	42.46

And then by using these values, H_{in} = -18.65 j/s and H_{out} = -18.67 j/s are found. By utilizing energy balance, enthalpy difference (B.12) is found:

$$Q = H_{out} - H_{in} = -0.0181 \text{ j/s} \quad (B.12)$$

Exergy values of inlet and outlet streams of WGS reactor are calculated by means of using exergy formulation again.

Table B.6. c_p^E values for T=523 K

T=523 K	H_2O	O_2	N_2	H_2	CH_4	CO	CO_2
n_i (µmol/s)	64.65	4.431	27.46	20.83	5.892	0.7164	8.866
c_p^E (kj/kmol)	8.740	7.870	7.620	7.450	11.11	7.610	11.15

These values are obtained from the tables of Kotas as mentioned before. As a result of exergy balance:

$$E_{in} = 10.85 \text{ j/s and } E_{out} = 10.84$$

$$E_{eff} = E_{out}/E_{in} = 0.9990 \quad \text{(B.13)}$$

B.3. PROX reactor calculations

In this system, PROX operates at 398 K temperature. Here, the reactions are:

$$CO + ½\ O_2 \rightarrow CO_2 \quad \text{(B.14)}$$

$$H_2 + ½\ O_2 \rightarrow H_2O \quad \text{(B.15)}$$

As a result of %100 CO conversion and 50% CO selectivity, outlet stream of PROX consists of this flow rate values of 4.191 µmol/s O_2, 27.46 µmol/s N_2, 64.42 µmol/s H_2O, 9.583 µmol/s CO_2, 21.06 µmol/s H_2 and 5.892 µmol/s CH_4.

Table B.7. h_d^0, c_p^h, c_p^E values for T=398 K and PROX reactant and product flow rates

T=398 K	H_2O	O_2	N_2	H_2	CH_4	CO	CO_2
n_{in} (µmol/s)	64.18	4.431	27.46	21.30	5.892	0.2402	9.343
n_{out} (µmol/s)	64.42	4.191	27.46	21.06	5.892	0	9.583
h_d^0 (kj/kmol)	-241814	0	0	0	-74520	110530	393510
c_p^h(kj/kmol*K)	33.50	28.41	29.39	28.90	38.45	29.38	39.88
c_p^E (kj/kmol)	4.57	3.99	4.06	3.98	5.41	4.06	5.6

As clearly seen here, CO is completely consumed. Exergy inlet and outlet streams of PROX are:

$$E_{in} = 10.64 \text{ j/s}; E_{out} = 10.59 \text{ j/s and } E_{eff} = E_2/E_1 = 0.9895$$

Enthalpy values are calculated via energy balance:

$$H_{in} = -19.23 \text{ j/s}; H_{out} = -19.36 \text{ j/s}$$

B.4. PEM reactor calculations

In PEM reactor, hydrogen conversion is taken as 75% and operation temperature is 349 K. Here, hydrogen is reacted with excess oxygen from air (stoichiometry of air is 3). The composition of mean constituents of air are:

$$n_{(O2)}: 19.02 \text{ µmol/s and } n_{(N2)}: 71.52 \text{ µmol/s}$$

The enthalpy of atmospheric air is zero and enthalpy will be calculated by a procedure similar to that used earlier and using values of h_d^0 and c_p^E (for T = 349 K) from tables of Kotas:

Table B. 8. Values of c_p^h and c_p^E for T = 349 K

T=349 K	H_2O	O_2	N_2	H_2	CH_4	CO_2
n_i (µmol/s)	80.22	15.31	98.98	5.266	5.892	9.583
c_p^h(kj/kmol*K)	33.21	27.43	29.25	28.81	37.08	38.61
c_p^E (kj/kmol)	2.450	2.100	2.210	2.180	2.830	2.950

Using these values:

$$H_{(T=349 \text{ K})}: -23.26 \text{ j/s}$$

$$\text{Enthalpy difference} = H_{(T=349 \text{ K})} - H_{(T=398 \text{ K})} = -3.907 \text{ j/s} \qquad \text{(B.16)}$$

60% of the enthalpy difference which is approximately equal to heat of reaction is produced as electricity:

$$\text{Electricity} = 0{,}6*3.907464 = 2.34478 \text{ j/s}$$

40% of the enthalpy difference is rejected as heat:

$$\text{Waste heat} = 0.4*3.907464 = 1.562985 \text{ j/s}$$

20% of the total heat produced by the fuel cell is assumed to be lost via convection and radiation from the fuel cell:

$$\text{Lost} = 0.2*1.562985 = 0.312597 \text{ j/s}$$

The remainder is removed at the radiator.

$$\text{Waste heat from radiator: } 0.8*1.562985 = 1.250388 \text{ j/s}$$

Exergy will be calculated by a similar procedure. Using the tabulated data:

$$E_{(T=349\ K)} = 6.812 \text{ j/s}$$

$$E_{eff} = \text{Electricity} / [E_{(T=349\ K)} - [E_{(T=398\ K)} + E_{(T=298\ K)}]] \qquad (B.17)$$

$$E_{eff} = 2.344 / [6.812 - [10.53 + 0.0117]] = 0.6282$$

B.5. Cooler calculations

Outlet stream of PEM is sent to cooler for cooling output stream of WGS. Here, to find outlet temperature of cooler which is heated by this flow, values of c_p^h extracted from tables of Kotas for a trial value of outlet temperature can be used in the energy balance in order to calculate outlet temperature by iteration.

The following table gives values of c_p^h (for T=431 K) and h_d^0 for the components of the mixture.

Table B.9. c_p^h and c_p^E (for T=431 K) values of components of the mixture

T=431 K	H_2O	O_2	N_2	H_2	CH_4	CO_2
n_i (µmol/s)	80.22	15.31	98.98	5.266	5.892	9.583
c_p^h(kj/kmol*K)	33.68	28.92	29.48	28.95	39.35	40.62
c_p^E (kj/kmol)	5.784	5.106	5.098	5.002	6.971	7.168

And then, here, we can use energy balance:

$$H_{(T=523\ K)} + H_{(T=349\ K)} = H_{(T=?)} + H_{(T=398\ K)} \quad \text{(B.18)}$$

-18.67 + 23.26 = $H_{(T=?)}$ -22.70 j/s ➔T= 431 K is found by iteration.

After that, by using c_p^E, exergy value is calculated at 431 K. From the tabulated values; E = 6.944 j/s at 431 K and E_{eff} = 0.9960.

B.6. Burner calculations

After passing through the cooler, outlet stream of PEM is fed to burner. Here, this stream is combusted by oxygen from air. However, if the oxygen within the stream is enough, it is not essential to use oxygen of atmospheric air. In this sample, oxygen within the stream is sufficient in order to combust methane and hydrogen. Reactions are:

$$CH_4 + 2O_2 \rightarrow CO_2 + 2H_2O \quad \text{(B.19)}$$

$$H_2 + ½\ O_2 \rightarrow H_2O \quad \text{(B.20)}$$

By iteration, we can determine the outlet temperature.

Table B.10. c_p^h and c_p^E values for T=1208 K

T=1208 K	H_2O	O_2	N_2	CO_2
n_i (µmol/s)	97.26	0.8980	98.98	15.47
c_p^h(kj/kmol*K)	37.88	33.28	31.42	49.93
c_p^E (kj/kmol)	20.87	18.43	17.25	28.01

As clearly seen here, methane and hydrogen are consumed completely. As a result of energy balance;

$$H_{(T=431\ K)} = H_{(T=1208)} \quad (B.21)$$

➔ at T=1208, H = -22.70 j/s value is obtained, so outlet temperature of burner is found as 1208 K. And then exergy balance is carried out. By using the table,

E=4,847 j/s at T=1208 K and exergy efficiency is calculated: $E_{eff} = 0.6980$

B.7. Heat exchanger 2 calculations

After burner, this stream is sent to heat exchanger 2 so as to provide heat to heat exchanger 2. In this system, heat exchanger 2 is installed between heat exchanger 1 and IPOX. By iteration, we can determine outlet temperature from the exchanger, using tabulated values:

Table B.11. c_p^h and c_p^E values (for T=1161 K) for mixture components

T=1161 K	H_2O	O_2	N_2	CO_2
n_i (µmol/s)	97.26	0.8980	98.98	15.47
c_p^h(kj/kmol*K)	37.63	33.17	31.31	49.59
c_p^E (kj/kmol)	20.29	17.99	16.82	27.23

$$H_{(T=573\ K)} + H_{(T=1208\ K)} = H_{(T=661\ K)} + H_{(T=?)} \quad (B.22)$$

By utilizing energy balance, T = 1161 K is found. $H_{(T=1161\ K)} = -23.09$ j/s.

Similarly, using tabulated values,

$E_{(T=1161\ K)} = 4.555$ j/s and E_{eff}(H.E.2) = 0.9950

B.8. Evaporator calculations

Output stream of H.E.2 is sent to evaporator for heating water. This stream is utilized in order to bring water temperature from 298 K to 383 K. While enthalpy of water at 298 K is -22.11 j/s, this value at 383 K becomes -18.49 j/s.

Stream which consists of O_2, N_2, H_2O and CO_2 passes from evaporator and its exit temperature is found as 702 K by iteration.

Table B.12. c_p^h and c_p^E values (for T=702 K) of output stream

T=702 K	H_2O	O_2	N_2	CO_2
n_i (μmol/s)	97.26	0.8980	98.98	15.47
c_p^h(kj/kmol*K)	35.21	31.43	30.20	45.17
c_p^E (kj/kmol)	13.06	11.88	11.20	17.20

After that, we can calculate exergy values. Water possesses 0.2414 j/s at 298 K and 0.9320 j/s at 383 K.

Outlet stream which is at 702 K has 2.110 j/s exergy. Finally, exergy efficiency is:

$$E_{eff} = 0.6340$$

B.9. Mixer calculations

Water, which is removed from evaporator, goes to mixer in order to mix with propane, n-butane, oxygen and nitrogen. Here, these components except water are at 298 K. Outlet temperature of mixture is found as 352 K by an energy balance. Enthalpy of propane – n-butane mixture is -0.5095 j/s and the enthalpy of atmospheric air is zero.

Enthalpy of mixture which consists of propane, n-butane, oxygen, nitrogen and water is found as -19.01 j/s.

By using cp^E values from tables of Kotas, exergies are also calculated:

exergy of fuel gas is 11.01 j/s; exergy of air is 0.0045 j/s; exergy of mixture at 352 K is 11.71 j/s.

After these values are found, exergy efficiency is calculated by using exergy balance:

$$E_{eff} = E_{(T=352\ K)} / [E_{air} + E_{fuel\ gas} + E_{H2O}] = 0.981 \quad (B.23)$$

This mixture is sent to H.E.1 and exergy balance is written:

$$H_{(T=352)} + H_{(T=723)} = H_{(T=523)} + H_{(T=?)} \quad (B.24)$$

By iteration, temperature of outlet stream is found as T=573 K and at this temperature: H= -18.06 j/s and E = 12.04 j/s. And then, exergy efficiency is found:

$$E_{eff} = [E_{(T=523)} + E_{(T=573)}] / [E_{(T=352)} + E_{(T=723)}] = 0.9930 \quad (B.25)$$

B.10. Overall system efficiency

Finally, the rational efficiency of the system can be expressed as:

$$\Psi = \text{Electricity} / [E_{fuel\ gas} + E_{air} + E_{water}] \quad (B.26)$$

$$\Psi = 2.344 / [11.01 + 0.0045 + 0.2414] = 20.83\ j/s$$

And, maximum exergy efficiency can be calculated:

$$\text{Max } \Psi = [\text{Electricity} + \text{Waste Heat}*(1 - T_0 / T_{Fuel\ Cell}) + E_{exhaust}] / [E_{fuel\ gas} + E_{air} + E_{water}] \quad (B.27)$$

$$\text{Max } \Psi = [2.344 + 1.250*(1 - 298 / 349) + 2.110] / [11.01 + 0.0045 + 0.2414]$$

$$\text{Max } \Psi = 41.21$$

APPENDIX C: FUEL PROCESSOR/FUEL CELL OPERATION

Table C.1. Exergy efficiencies of all system units

		Exergy Efficiencies													
IPOX T	FEED	Evaporator	Mixer	H.E.1	H.E.2	IPOX	WGS	Cooler	PROX	PEM (75% conversion)	Burner	Electricity	Lost	Waste heat	ψ
(K)												(j/s)	(j/s)	(j/s)	%
663	pure	0.7550	0.9853	0.9953	-	0.8267	0.9993	0.9970	0.9924	0.6049	0.6954	2.665	0.3553	1.421	12.50
723	pure	0.7370	0.9854	0.9945	-	0.8442	0.9985	0.9960	0.9844	0.5973	0.6640	3.544	0.4725	1.890	16.62
623	50%-50%	0.6433	0.9810	0.9953	-	0.7827	0.9997	0.9960	0.9965	0.6265	0.6850	2.213	0.2951	1.180	10.29
643	50%-50%	0.6590	0.9810	0.9945	-	0.8876	0.9996	0.9970	0.9955	0.6502	0.6860	2.974	0.3966	1.586	13.82
663	50%-50%	0.6490	0.9810	0.9931	-	0.8559	0.9995	0.9960	0.9947	0.6333	0.6907	3.048	0.4065	1.626	14.17
683	50%-50%	0.6510	0.9810	0.9938	-	0.8750	0.9995	0.9966	0.9945	0.6393	0.6894	3.111	0.4149	1.659	14.46
703	50%-50%	0.6489	0.9810	0.9932	0.9920	0.9396	0.9993	0.9967	0.9930	0.6483	0.6911	3.847	0.5129	2.052	17.88
723	50%-50%	0.6340	0.9810	0.9930	0.9950	0.9260	0.9990	0.9960	0.9895	0.6282	0.6980	4.482	0.5977	2.391	20.83
743	50%-50%	0.6280	0.9810	0.9925	-	0.8719	0.9987	0.9955	0.9872	0.6125	0.6653	4.405	0.5873	2.349	20.47
643	75%-25%	0.6630	0.9830	0.9952	-	0.8660	0.9997	0.9968	0.9967	0.6262	0.6844	2.440	0.3254	1.301	11.35
663	75%-25%	0.6555	0.9830	0.9942	-	0.8563	0.9996	0.9960	0.9960	0.6160	0.6889	2.677	0.3570	1.428	12.45
683	75%-25%	0.6676	0.9830	0.9945	-	0.9248	0.9995	0.9970	0.9953	0.6340	0.6908	3.089	0.4119	1.647	14.36
703	75%-25%	0.6618	0.9829	0.9938	-	0.9183	0.9993	0.9970	0.9932	0.6259	0.6942	3.258	0.4344	0.7672	15.15

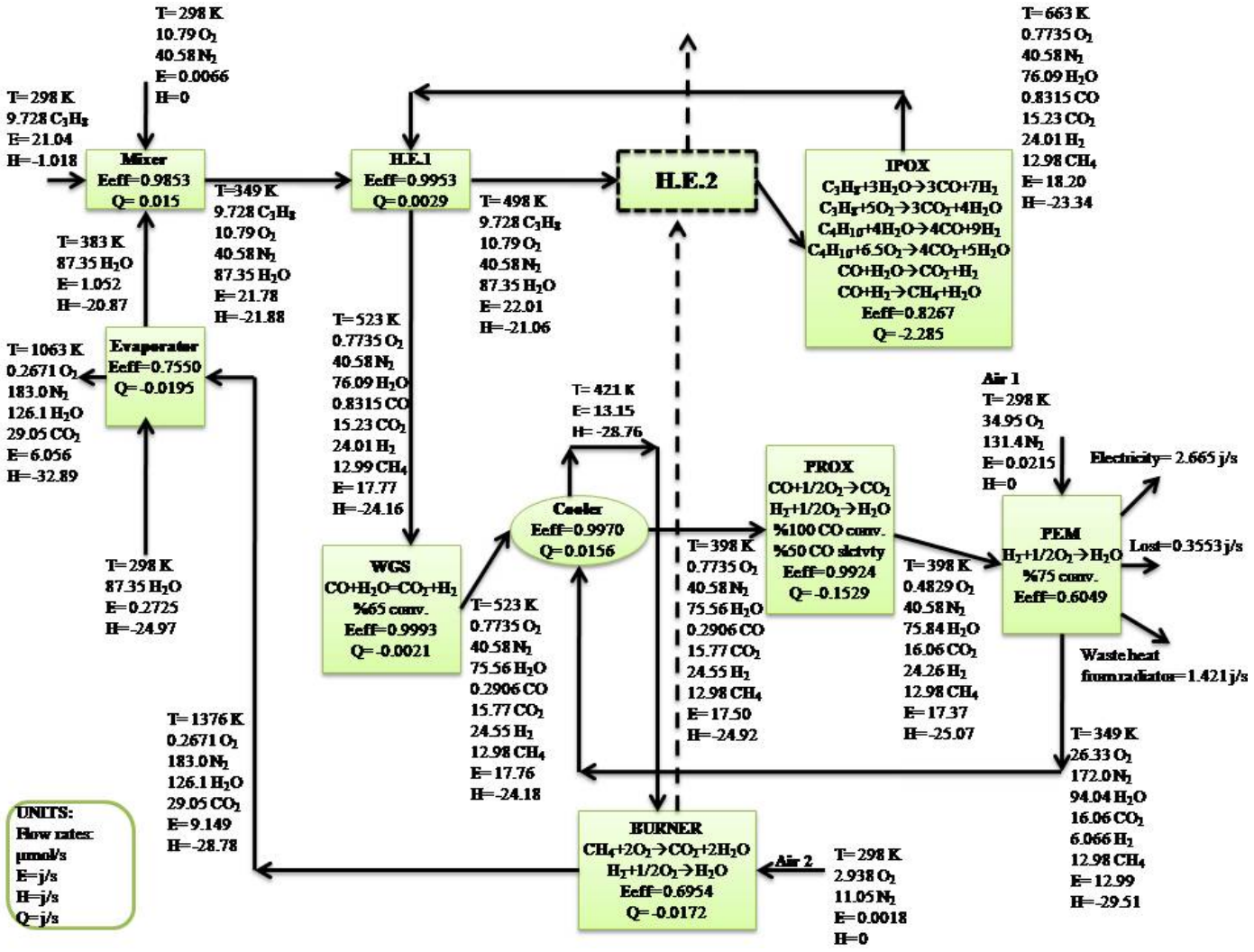

Figure C.1. Fuel processor/fuel cell operation for pure propane feed at 663 K IPOX temperature

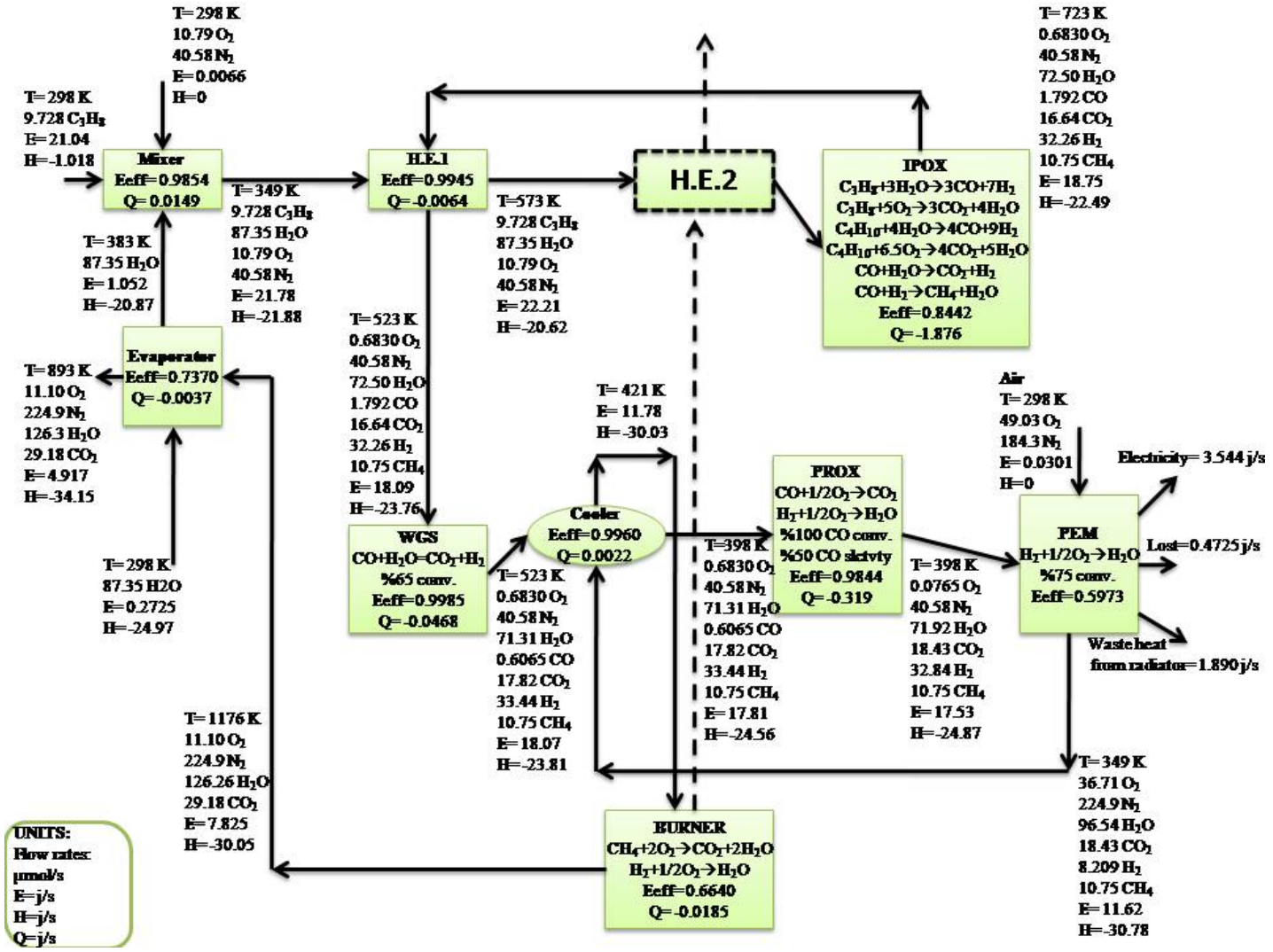

Figure C.2. Fuel processor/fuel cell operation for pure propane feed at 723 K IPOX temperature

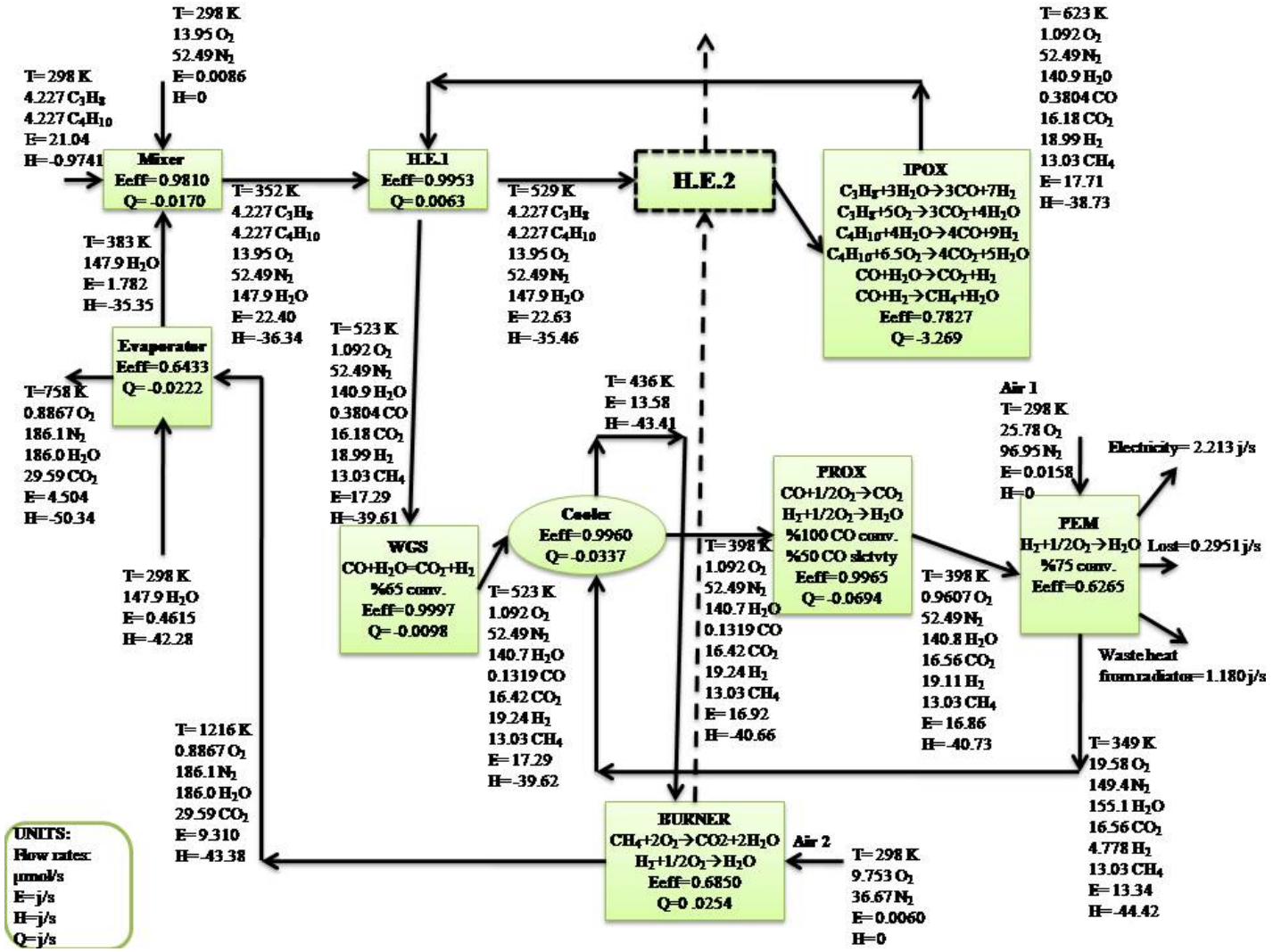

Figure C.3. Fuel processor/fuel cell operation for 50% propane – 50% butane feed at 623 K IPOX temperature

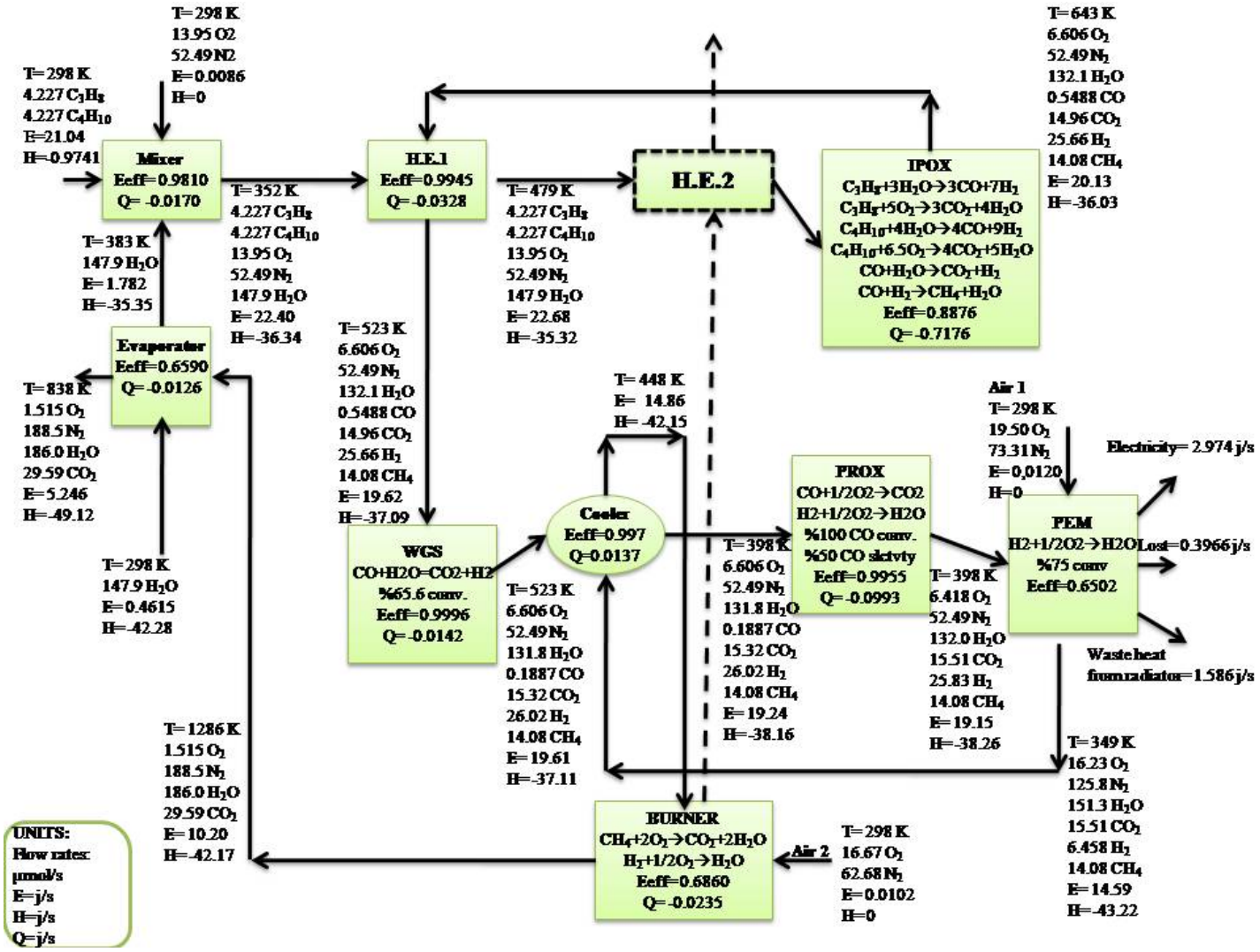
T= 298 K
13.95 O2
52.49 N2
E= 0.0086
H=0
T= 298 K
4.227 C3H8
4.227 C4H10
E=21.04
H=-0.9741
Mixer
Eeff= 0.9810
Q= -0.0170
T= 352 K
4.227 C3H8
4.227 C4H10
13.95 O2
52.49 N2
147.9 H2O
E= 22.40
H=-36.34
H.E.1
Eeff=0.9945
Q= -0.0328
T= 479 K
4.227 C3H8
4.227 C4H10
13.95 O2
52.49 N2
147.9 H2O
E= 22.68
H=-35.32
H.E.2
IPOX
C3H8+3H2O→3CO+7H2
C3H8+5O2→3CO2+4H2O
C4H10+4H2O→4CO+9H2
C4H10+6.5O2→4CO2+5H2O
CO+H2O→CO2+H2
CO+H2→CH4+H2O
Eeff=0.8876
Q= -0.7176
T= 643 K
6.606 O2
52.49 N2
132.1 H2O
0.5488 CO
14.96 CO2
25.66 H2
14.08 CH4
E= 20.13
H=-36.03
T= 383 K
147.9 H2O
E= 1.782
H=-35.35
Evaporator
Eeff=0.6590
Q= -0.0126
T= 838 K
1.515 O2
188.5 N2
186.0 H2O
29.59 CO2
E= 5.246
H=-49.12
T= 298 K
147.9 H2O
E= 0.4615
H=-42.28
T= 523 K
6.606 O2
52.49 N2
132.1 H2O
0.5488 CO
14.96 CO2
25.66 H2
14.08 CH4
E= 19.62
H=-37.09
WGS
CO+H2O=CO2+H2
%65.6 conv.
Eeff=0.9996
Q= -0.0142
T= 523 K
6.606 O2
52.49 N2
131.8 H2O
0.1887 CO
15.32 CO2
26.02 H2
14.08 CH4
E= 19.61
H=-37.11
Cooler
Eeff=0.997
Q=0.0137
T= 448 K
E= 14.86
H=-42.15
T= 398 K
6.606 O2
52.49 N2
131.8 H2O
0.1887 CO
15.32 CO2
26.02 H2
14.08 CH4
E= 19.24
H=-38.16
PROX
CO+1/2O2→CO2
H2+1/2O2→H2O
%100 CO conv.
%50 CO sletvty
Eeff=0.9955
Q= -0.0993
T= 398 K
6.418 O2
52.49 N2
132.0 H2O
15.51 CO2
25.83 H2
14.08 CH4
E= 19.15
H=-38.26
Air 1
T= 298 K
19.50 O2
73.31 N2
E= 0,0120
H=0
PEM
H2+1/2O2→H2O
%75 conv
Eeff=0.6502
Electricity= 2.974 j/s
Lost=0.3966 j/s
Waste heat
from radiator= 1.586 j/s
T= 349 K
16.23 O2
125.8 N2
151.3 H2O
15.51 CO2
6.458 H2
14.08 CH4
E= 14.59
H=-43.22
T= 1286 K
1.515 O2
188.5 N2
186.0 H2O
29.59 CO2
E= 10.20
H=-42.17
BURNER
CH4+2O2→CO2+2H2O
H2+1/2O2→H2O
Eeff=0.6860
Q= -0.0235
Air 2
T= 298 K
16.67 O2
62.68 N2
E= 0.0102
H=0
UNITS:
Flow rates:
µmol/s
E=j/s
H=j/s
Q=j/s

Figure C.4. Fuel processor/fuel cell operation for 50% propane – 50% butane feed at 643 K IPOX temperature

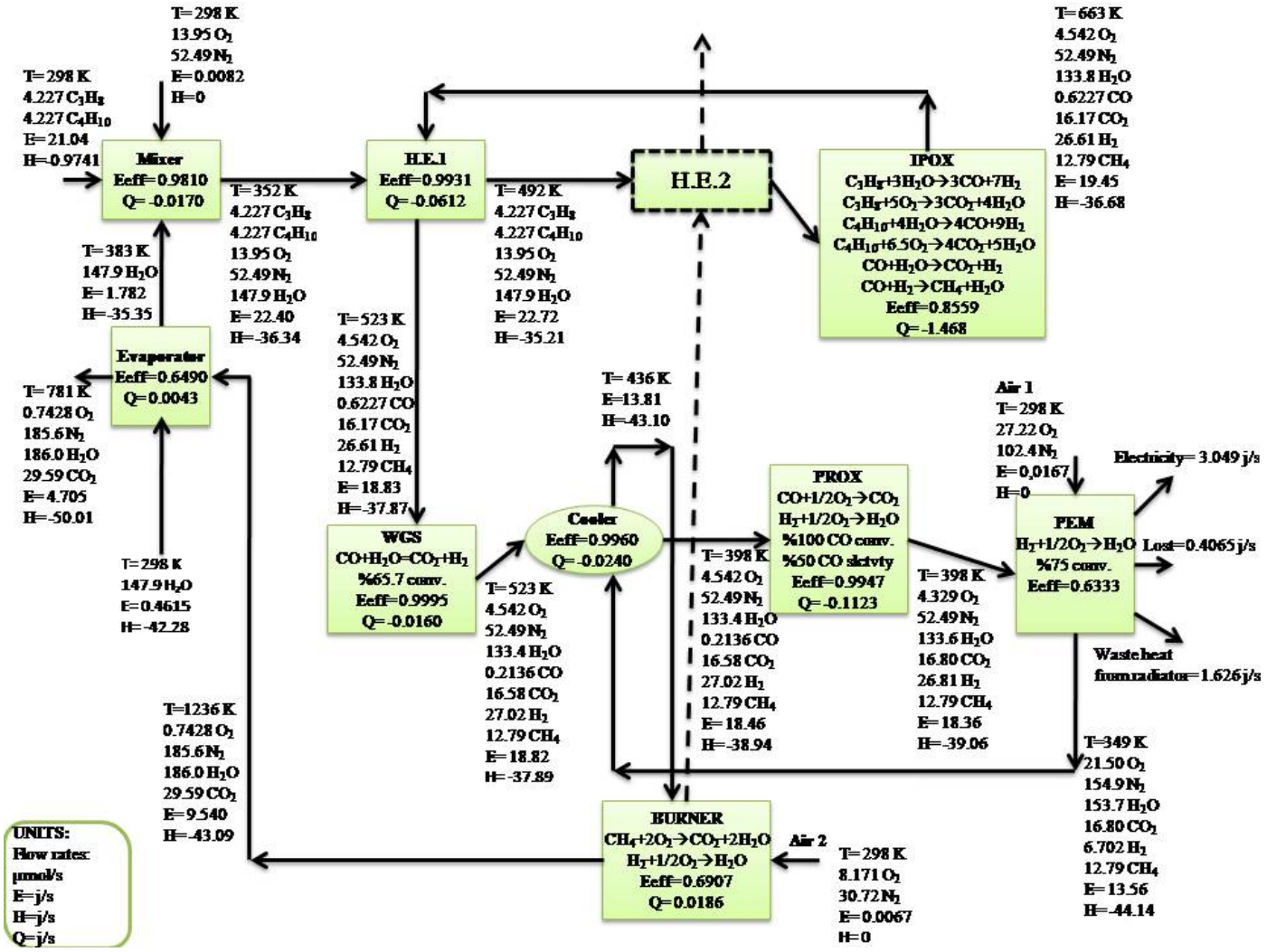

Figure C.5. Fuel processor/fuel cell operation for 50% propane – 50% butane feed at 663 K IPOX temperature

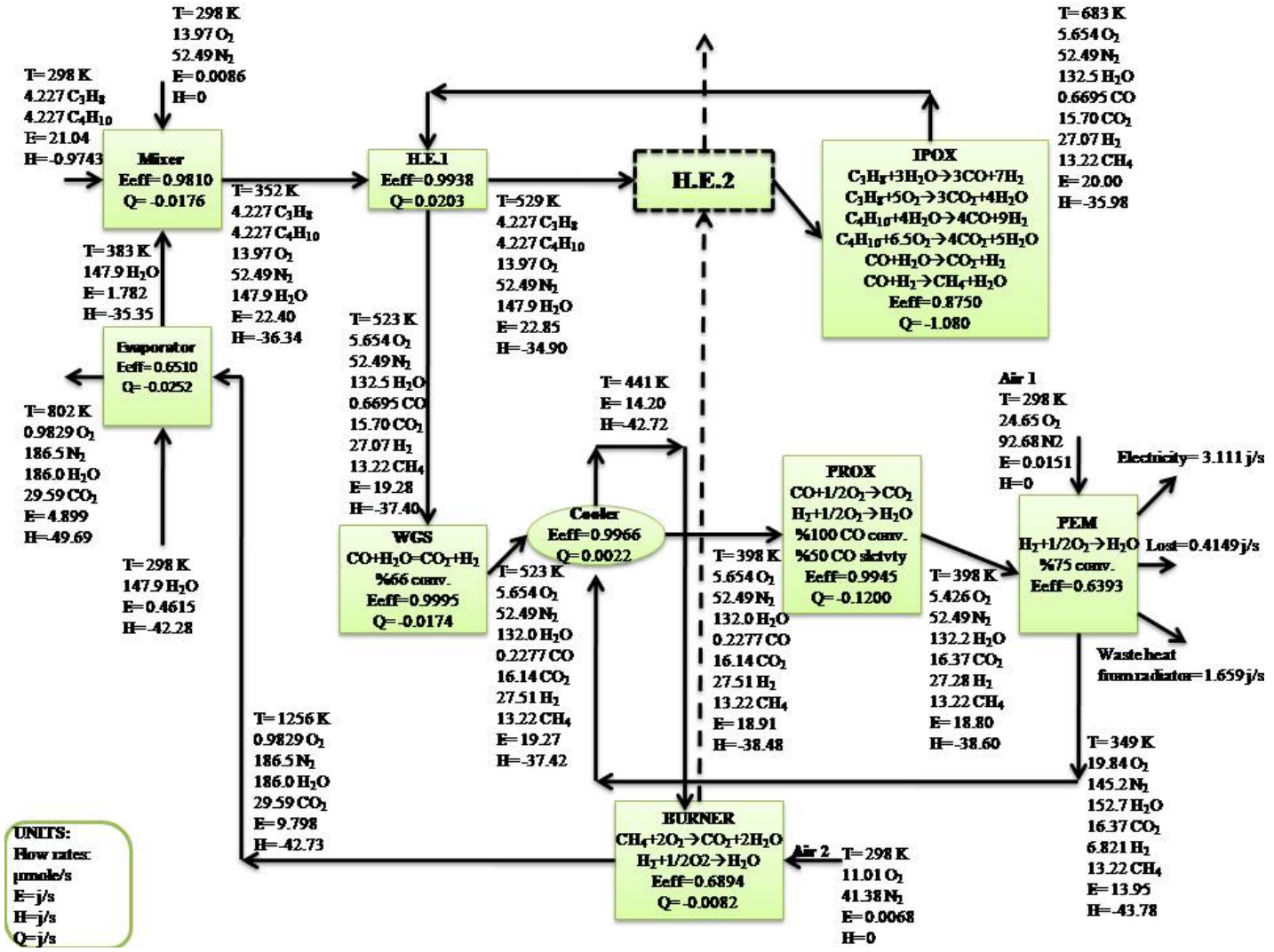

Figure C.6. Fuel processor/fuel cell operation for 50% propane – 50% butane feed at 683 K IPOX temperature

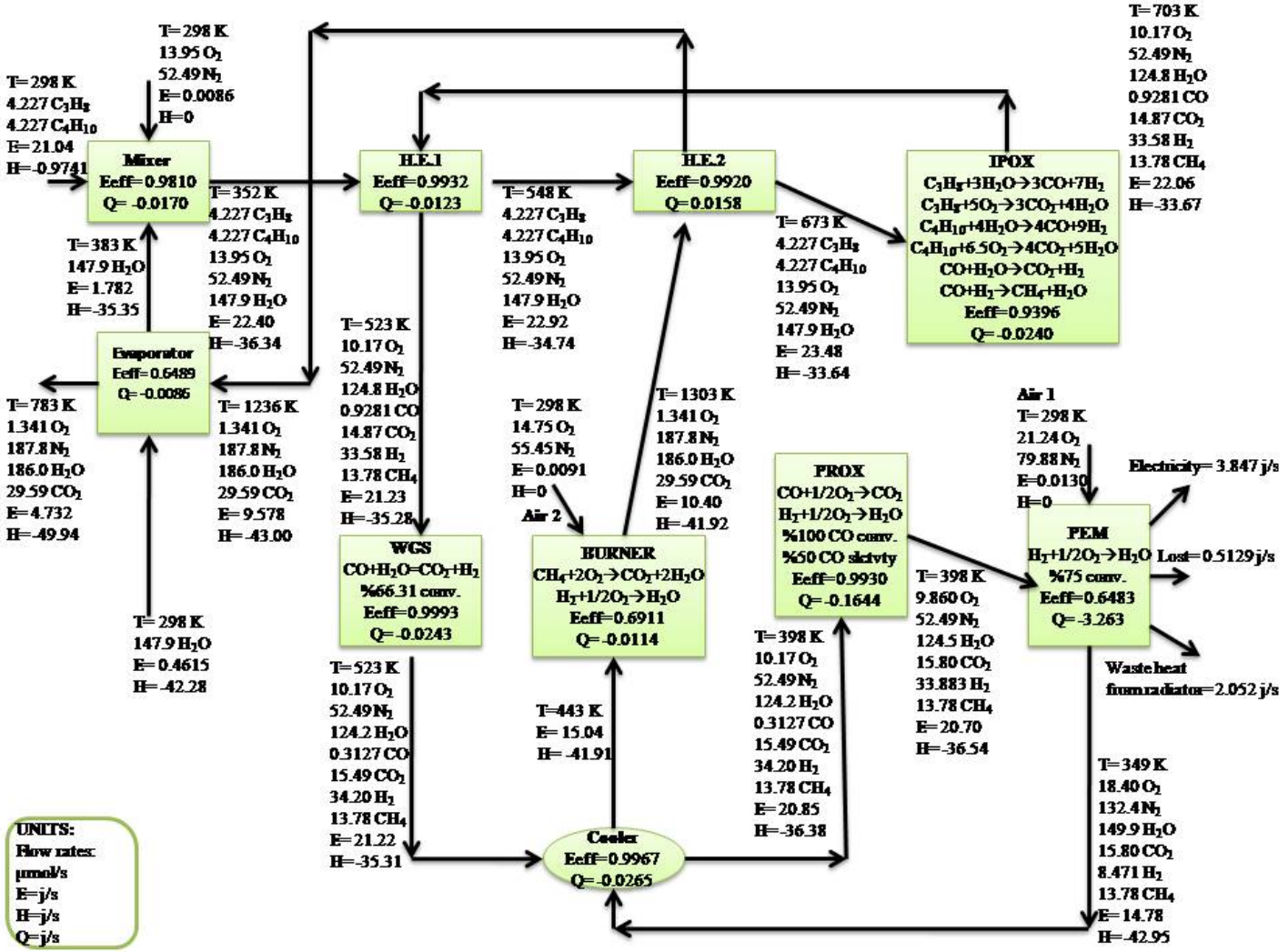

Figure C.7. Fuel processor/fuel cell operation for 50% propane – 50% butane feed at 703 K IPOX temperature

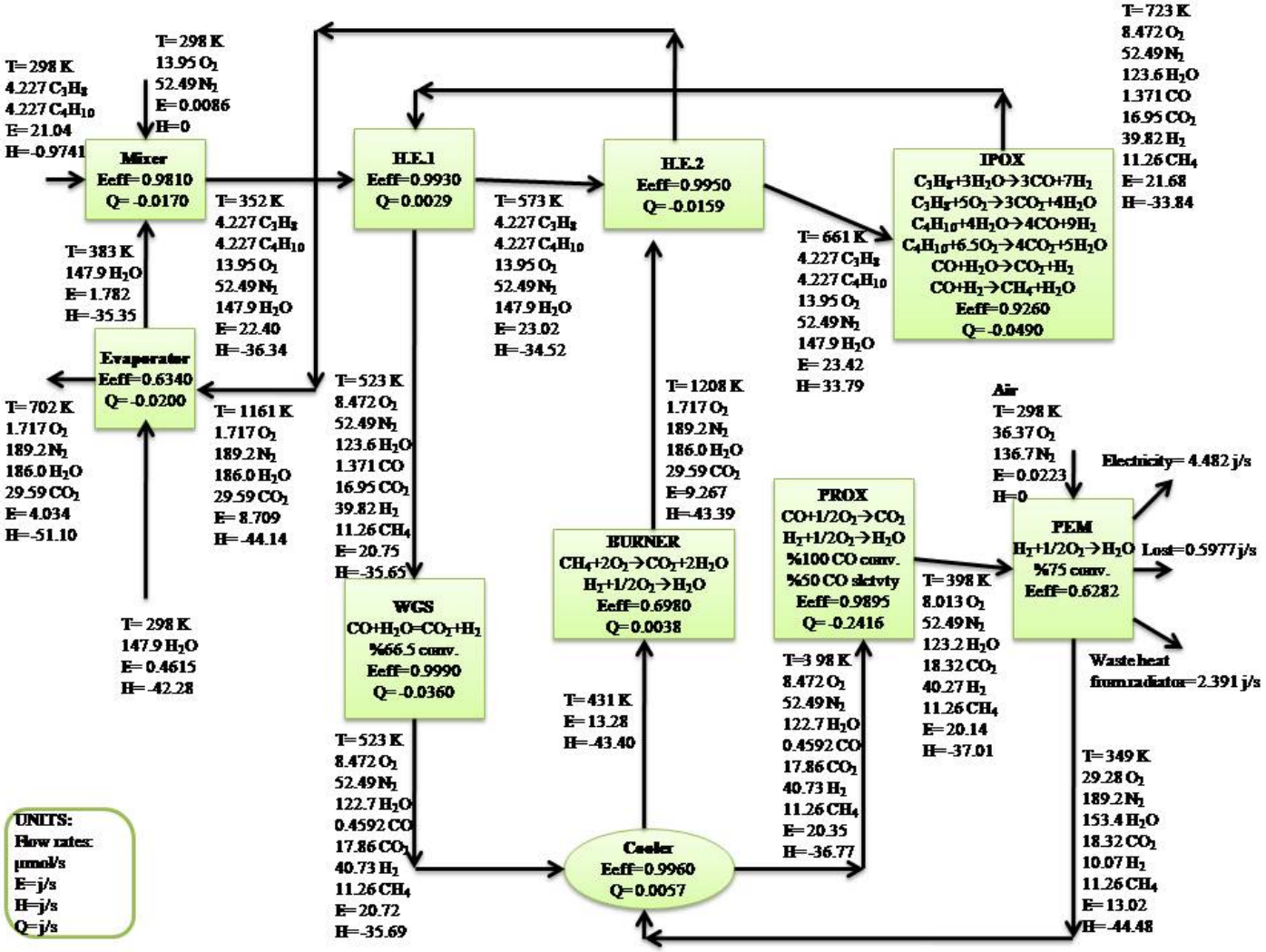

Figure C.8. Fuel processor/fuel cell operation for 50% propane – 50% butane feed at 723 K IPOX temperature

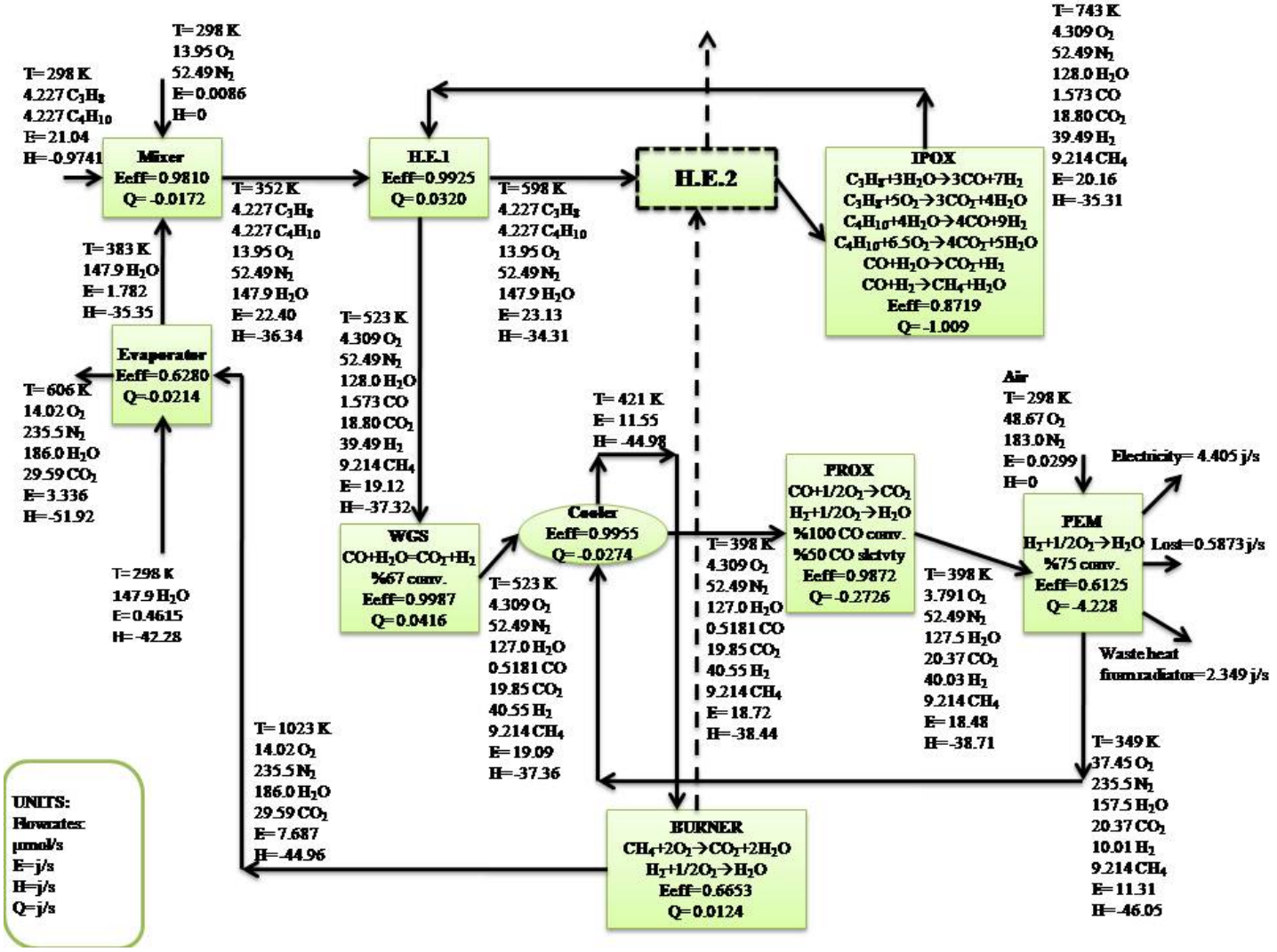

Figure C.9. Fuel processor/fuel cell operation for 50% propane – 50% butane feed at 743 K IPOX temperature

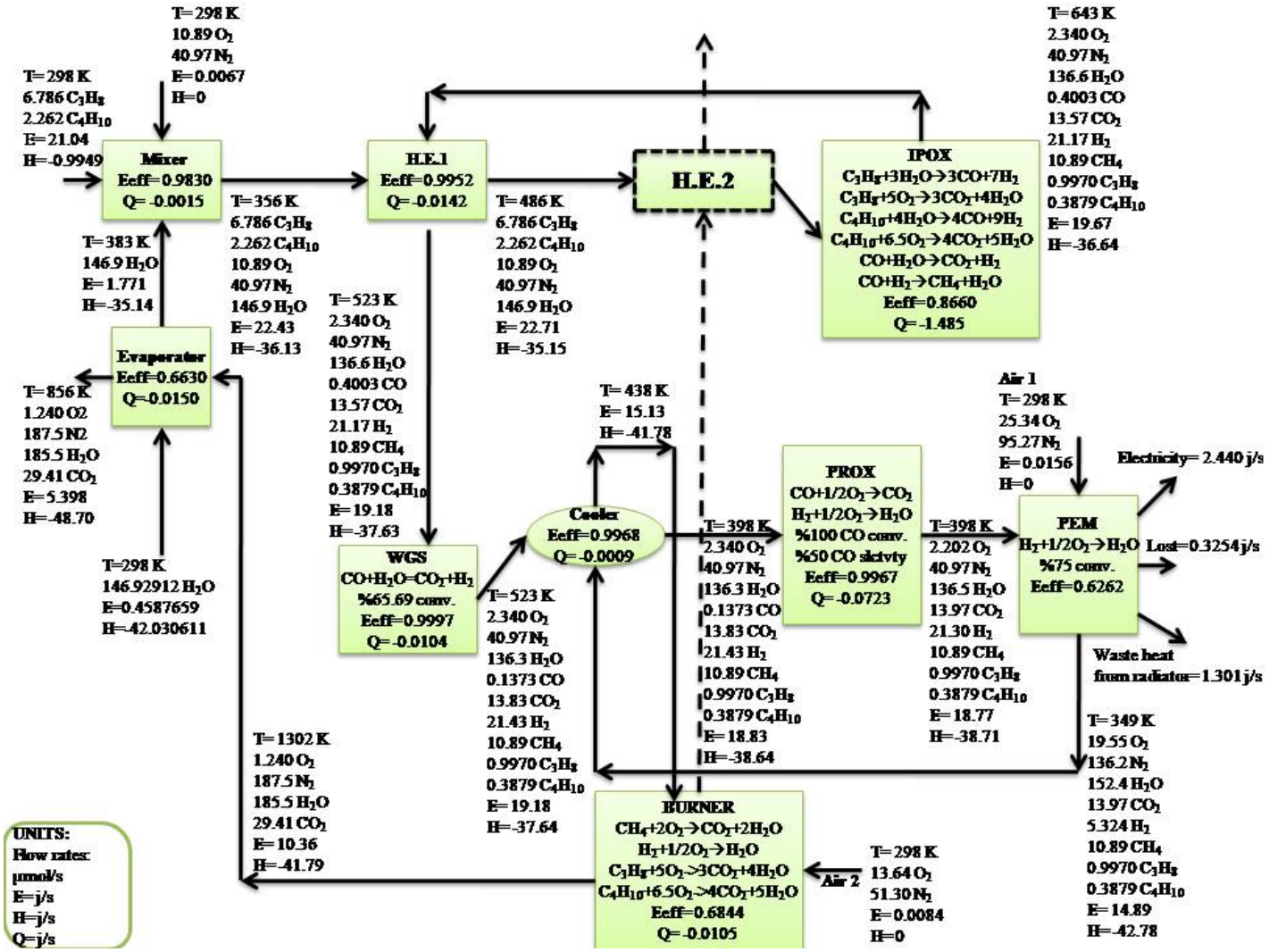

Figure C.10. Fuel processor/fuel cell operation for 75% propane – 25% butane feed at 643 K IPOX temperature

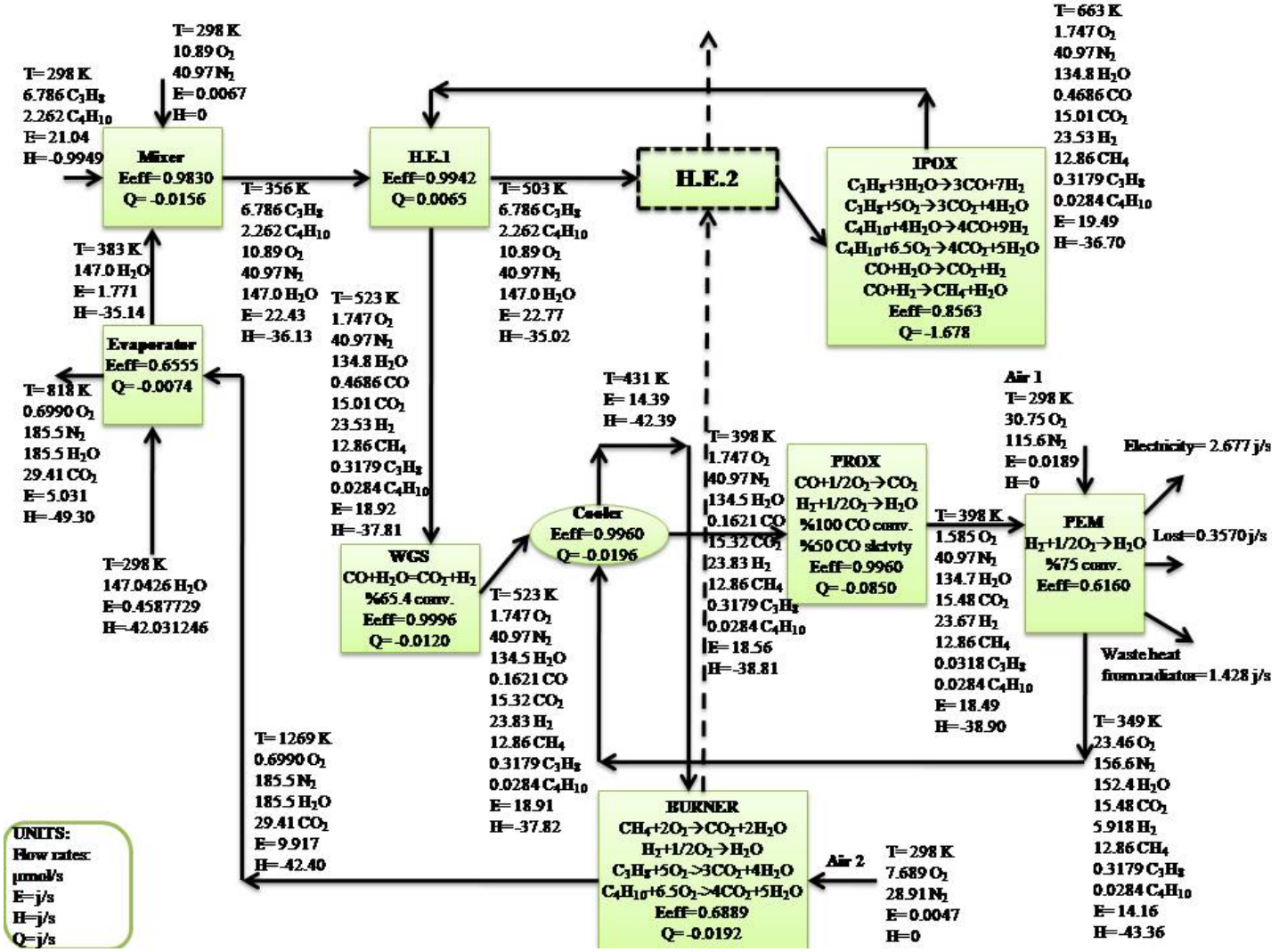

Figure C.11. Fuel processor/fuel cell operation for 75% propane – 25% butane feed at 663 K IPOX temperature

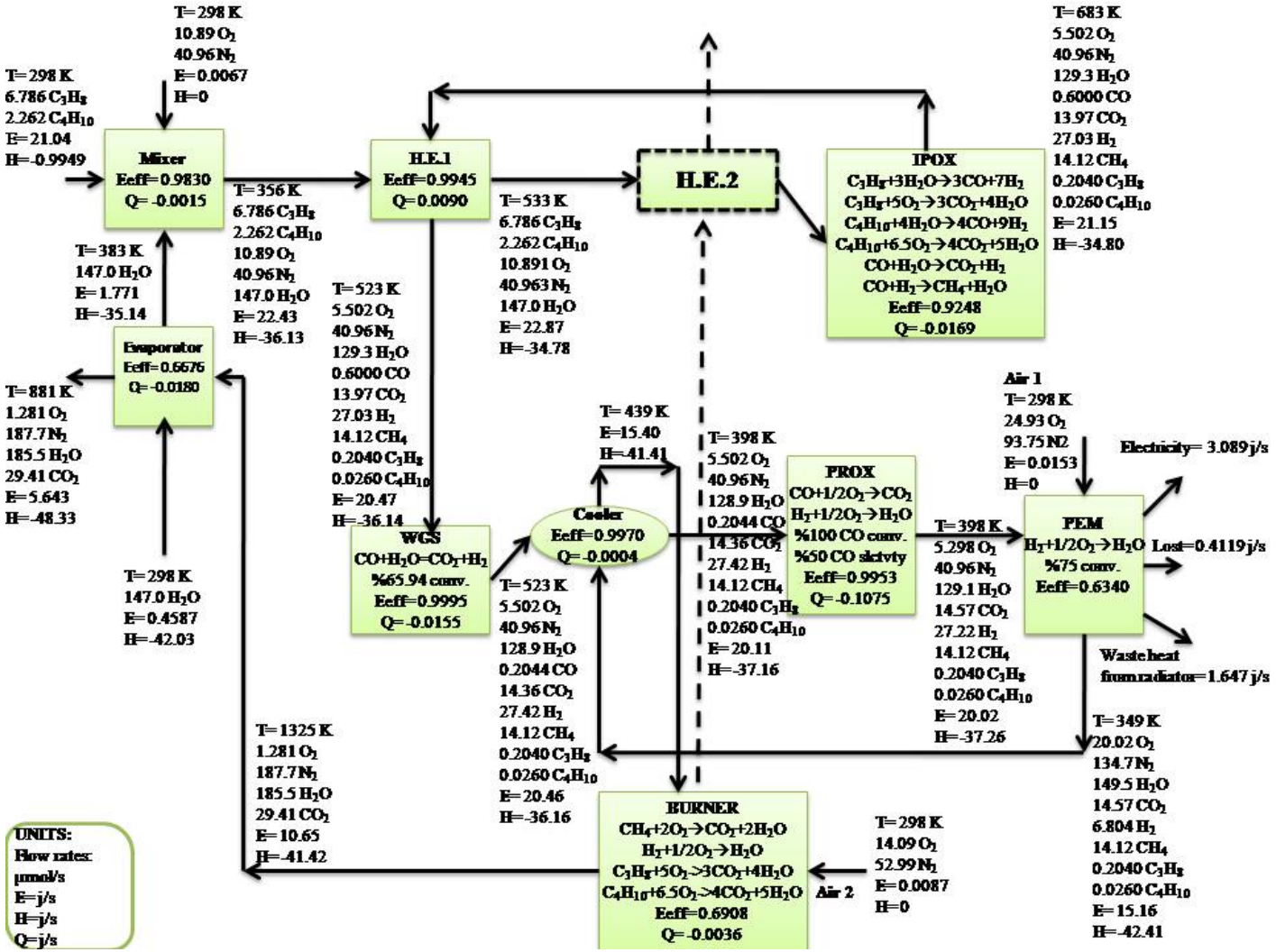

Figure C.12. Fuel processor/fuel cell operation for 75% propane – 25% butane feed at 683 K IPOX temperature

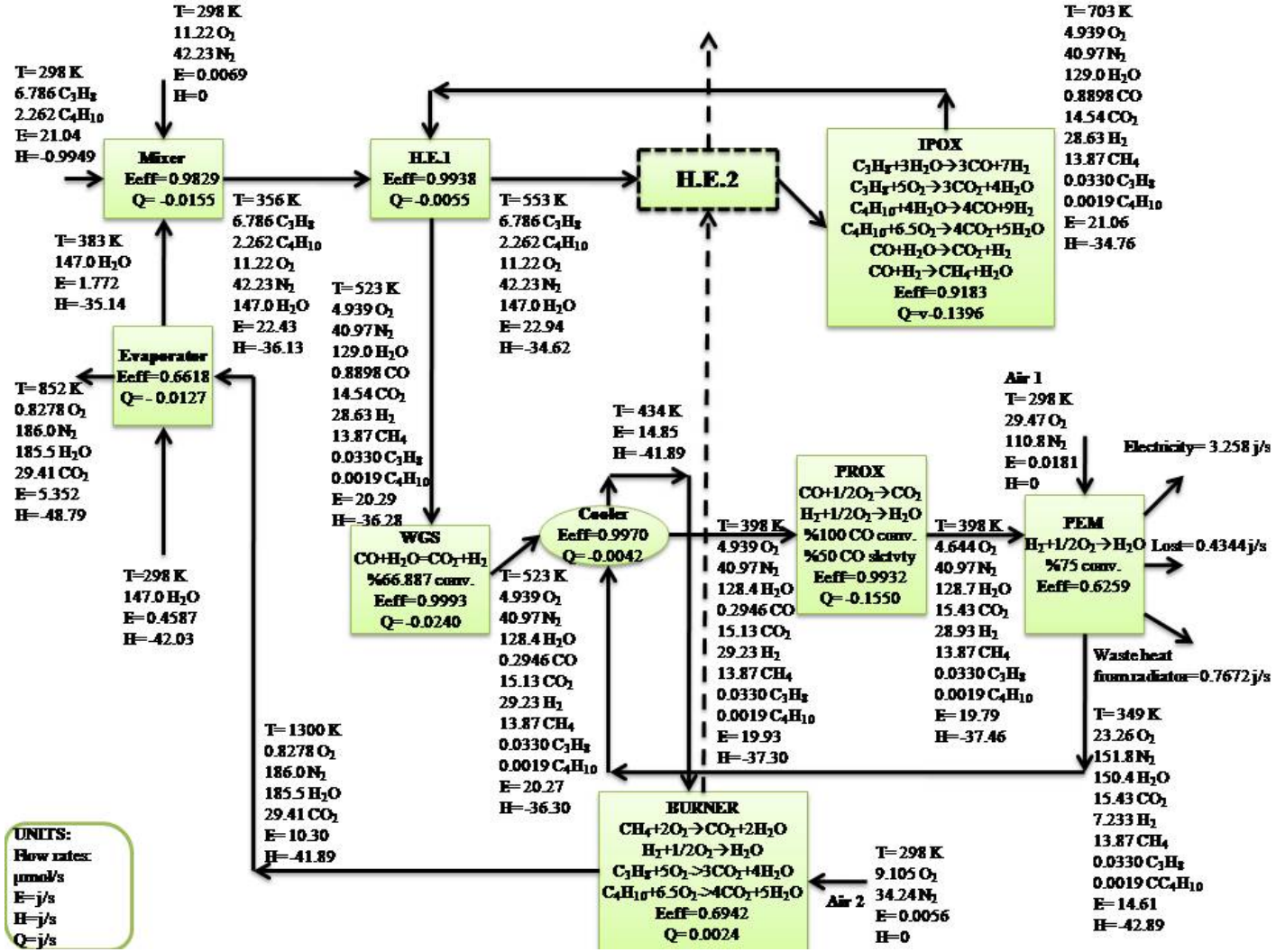

Figure C.13. Fuel processor/fuel cell operation for 75% propane – 25% butane feed at 703 K IPOX temperature

Table C.2. Reference environment according to Kotas

Chemical element	Standard state of the element	Chemical exergy: Reference substance	Concentrationf of reference substance in Standard environment		Standard chemical exergy, E_0/[kj/kmol]
1	**2**	**3**	**4**		**5**
Ag	S	$AgCl_2^-$, i	2.7×10^{-9}	(w)	73 700
Al	S	Al_2SiO_5, s Sillimanite	2×10^{-3}	(c)	887 890
Ar	G	Ar, g	0.907	(a)	11 690
As	S	$HAsO_4^{2-}$, i	1.5×10^{-8}	(w)	477 040
Au	S	$AuCl_2^-$, i	5.8×10^{-11}	(w)	18 900
B	S	$H_2BO_3^-$, i	4.6×10^{-6}	(w)	615 920
Ba	s, II	Ba^{2+} , i	5×10^{-8}	(w)	760 050
Bi	S	Bi_2O_3, s	7×10^{-10}	(c)	271 370
Br_2	I	Br^-, i	6.5×10^{-5}	(w)	91 770
C	s, graphite	Ca^{2+}, i	0.03	(a)	410 820
Ca	s, II	$CaCO_3$, s.	4×10^{-4}	(w)	717 400
Cd	s, α	Cd^{2+}, i	5×10^{-11}	(w)	290 920
Cl_2	G	Cl^-, i	19×10^{-3}	(w)	117 520
Co	s, III	Co^{2+}, i	9×10^{-11}	(w)	260 520
Cr	S	Cr_2O_3, s	4×10^{-7}	(c)	538 610
Cs	S	Cs^+, i	2×10^{-9}	(w)	408 530
Cu	S	Cu^{2+}, i	5×10^{-9}	(w)	134 400
D_2	G	D_2O, g	0.00014	(a)	266 220
F_2	G	F^-, i	1.4×10^{-6}	(w)	448 820
Fe	S	Fe_2O_3, s.	2.7×10^{-4}	(c)	377 740
H_2	G	H_2O, g	0.9	(a)	238 490
He	G	He, g	0.0005	(a)	30 290
Hg	L	$HgCl_4^{2-}$, u	3.4×10^{-10}	(w)	122 700
J_2	S	JJ_2^-, i	5×10^{-8}	(w)	184 190
K	S	K^+, i	3.8×10^{-4}	(w)	371 520
Kr	G	Kr, g	0.0001	(a)	34 280
Li	S	Li^+, i	1×10^{-7}	(w)	396 170
Mg	S	Mg^{2+}, i	12.7×10^{-4}	(w)	626 710
Mn	s, α, IV	MnO_2, s	2×10^{-4}	(c)	483 240
Mo	S	MoO_3, s	2×10^{-8}	(c)	715 540
N_2	g	N_2, g	75.83	(a)	720
Na	s	Na^+, i	10.56×10^{-3}	(w)	343 830
Ne	g	Ne, g	0.0018	(a)	27 120
Ni	s	Ni^{2+}, i	9×10^{-11}	(w)	252 800
O_2	g	O_2, g	20.40	(a)	3 970
P	s, white	HPO_4^{2-}, i	5×10^{-8}	(w)	859 600
Pb	s	Pb^{2+}, i	4×10^{-9}	(w)	226 940
Rb	s	Rb^{2+}, i	2×10^{-7}	(w)	398 800
S	s, rhombic	SO_4^{2-} , i	8.84×10^{-4}	(w)	598 850
Sb	s, III	Sb_2O_5, s	7×10^{-10}	(c)	359 190
Se	s	SeO_4^{2-}, i	4×10^{-9}	(w)	326 960
Si	s	SiO_2, s,	4.72×10^{-1}	(c)	803 010
Sn	s, white	SnO_2, s	2×10^{-5}	(c)	542 660
Sr	s	Sr^{2+}, i	1.3×10^{-5}	(w)	737 650
Ti	s, II	TiO_2, s, III	9×10^{-5}	(c)	876 000
U	s, III	UO_3, s	2×10^{-8}	(c)	1 224 180
V	s	V_2O_5, s	2×10^{-6}	(c)	725 880
W	s	WO_3, s,	4×10^{-8}	(c)	799 680
Xe	g	Xe, g	0.000 0009	(a)	40 250
Zn	s	Zn2-, i	5×10^{-10}	(w)	353 160

Key: s-solid, l-liquid, g-gaseous, i-ionic, aq-in aqueous solution, (a) Standard partial pressure in air, kPa, (c) Standard mass fraction in the Earth's crust, (w) Standard mass fraction in sea water.

REFERENCES

Ahmed, S. and M. Krumpelt, 2001, "Hydrogen from Hydrocarbon Fuels for Fuel Cells", *International Journal of Hydrogen Energy*, Vol. 26, pp. 291-301.

Alejo, L., R. Lago, M. A. Pena, and J. L. G. Fierro, 1997, "Partial Oxidation of Methanol to Produce Hydrogen over Cu-Zn-Based Catalysts", *Applied Catalysis A: General*, Vol. 162, pp. 281-297.

Avcı, A. K., 2003, "Computational and Experimental Investigation of Catalytic Hydrocarbon Fuel Processing for Autothermal Hydrogen Production", Ph. D. Thesis, Boğaziçi University.

Avcı, A. K., D. L. Trimm and Z. İ. Önsan, 2002, "Quantitative Investigation of Catalytic Natural Gas Conversion for Hydrogen Fuel Cell Applications", *Chemical Engineering Journal,* Vol. 90, pp. 77-87.

Avcı, A. K., D. L. Trimm, A. E. Aksoylu and Z. İ. Önsan, 2003, "Ignition Characteristics of Propane and n-Butane over Supported Pt, Ni, Pt-Ni Catalysts", *Catalysis Letters,* Vol. 88, pp. 17-22.

Avcı, A. K., D. L. Trimm, A. E. Aksoylu, Z. İ. Önsan, 2004, "Hydrogen Production by Steam Reforming of *n*-butane over Supported Ni and Pt-Ni Catalysts", *Applied Catalysis A: General*, Vol. 258, pp. 235-240.

Breen, J. P. and J. R. H. Ross, 1999, "Methanol Reforming for Fuel-Cell Applications: Development of Zirconia-Containing Cu-Zn-Al Catalysts", *Catalysis Today*, Vol. 51, pp. 521-233.

Brown, L. F., 2001, "A Comparative Study of Fuels for On-board Hydrogen Production for Fuel-Cell-Powered Automobiles", *International Journal of Hydrogen Energy,* Vol. 26, pp. 382-397.

Çengel, Y. A, and M. A. Boles, 2002, "Thermodynamics: An Engineering Approach", 4th edn, Dubuque, Iowa: McGraw-Hill.

Choudhary, V. R., B. S. Uphade, A. S. Mamman, 1998, "Partial Oxidation of Methane to Syngas with or without Simultaneous $C0_2$ and Steam Reforming Reactions over Ni/AlPO4", *Microporous and Mesoporous Materials,* Vol. 23, pp. 61-66.

Colpan, C. O., I. Dincer, F. Hamdullahpur, 2007, "Exergy Analysis of a SOFC Based Cogeneration System for Buildings", Summer Course on Exergy and its Applications, Proceedings, *Institute of Energy* Istanbul Technical University, 10-12 July (Coord: Aydın, M.).

Cownden, R., M. Nahon, M. A. Rosen, "Exergy Analysis of A Fuel Cell Power System for Transportation Applications", *Exergy Internat. J.*, Vol. 1, No. 2, pp. 112-121.

Çağlayan, B. C., A. K. Avcı, Z. İ. Önsan, A. E. Aksoylu, 2005, "Production of Hydrogen over Bimetallic Pt-Ni/δ-Al_2O_3 I. Indirect Partial Oxidation of Propane*", Applied Catalysis A: General,* Vol. 280, pp. 181-188.

Delsman, E.R., C.U. Uju, M.H.J.M. de Croon, J.C. Schouten and K.J. Ptasinski, 2006, "Exergy Analysis of An Integrated Fuel Processor and Fuel Cell (FP–FC) System", *Energy*, Vol. 31, pp. 3300-3309.

Ghenciu, A. F., 2002, "Review of Fuel Processing Catalysts for Hydrogen Production in PEM Fuel Cell Systems", *Current Opinion in solid state & Materials Science*, Vol. 6, pp. 389-399.

Gigliucci, G., L. Petruzzi, E. Cerelli, A. Garzisi and A. La Mendola, 2004, "Demonstration of A Residential CHP System Based on PEM Fuel Cells", *Journal of Power Sources*, Vol. 131, pp. 62-68.

Gökaliler, F., 2005, "Steam Reforming and Indirect Partial Oxidation of Light Hydrocarbons over Bimetallic Catalysts", M.S. Thesis, Boğaziçi University.

Hakkarainen, R., T. Salmi, and R. L. Keiski, 1994, "Comparison of the Dynamics of the High-Temperature Water-Gas Shift Reaction on the Oxide Catalysts", *Catalysis Today*, Vol. 20, pp. 395-408.

Haynes, C. L. and W. J. Wepfer, 2002, ""Enhancing the Performance Evaluation and Process Design of A Commercial-Grade Solid Oxide Fuel Cell Via Exergy Concept", *ASME J. Energy Resourc. Technol.,* Vol. 124, pp. 95-104.

Hohn, K.L. and L. D. Schmidt, 2001, "Partial Oxidation of Methane to Syngas at High Space Velocities Over Rh-coated Spheres", *Applied Catalysis A: General,* Vol. 211, pp. 52-68.

Hussain, M. M., J. J. Baschuk, X. Li, I. Dincer, 2005, "Thermodynamic Analysis of A PEM Fuel Cell Power System", *International Journal of Thermal Sciences,* Vol. 44, pp. 903-911.

Iwasa, N., T. Mayanagi, N. Ogawa, K. Sakata, and N. Takezawa, 1998, "New Catalytic Functions of Pd-Zn, Pd-Ga, Pd-In, Pt-Zn, Pt-Ga and Pt-In Alloys in the Conversion of Methanol", *Catalysis Letters*, Vol. 54, pp. 119-123.

Jacobs, G., L. Williams, U. Graham, G.A. Thomas, D. E. Sparks, B. H. Davis, 2003, "Low Temperature Water-Gas Shift: In Situ DRIFTS-Reaction Study of Ceria Surface Area on the Evolution of Formates on Pt/CeO_2 Fuel Processing Catalysts for Fuel Cell Applications", *Applied Catalysis A: General,* Vol. 252, pp. 107-118.

Joensen, F., and J. R. Rostrup-Nielsen, 2001, "Conversion of Hydrocarbons and Alcohols for Fuel Cells", *Journal of Power Sources,* Vol. 4566, pp, 1-7.

Karyobkina, N. A., A. A. Phatak, W. F. Ruettinger, R. J. Farrauto, and F. H. Ribeiro, 2003, "Determination of Kinetic Parameters for the Water-Gas Shift Reaction on Copper

Catalysts under Realistic Conditions for Fuel Cell Applications", *Journal of Catalysis*, Vol. 217, pp. 233-239.

Kazim, A., 2004, "Exergy Analysis of A PEM Fuel Cell at Variable Operating Condition", *Energy Conversion and Management*, Vol. 45, pp. 1949-1961.

Kepinski, L., B. Statinska, T. Borowiecki, 2000, "Carbon Deposition on Ni/Al_2O_3 Catalysts Doped with Small Amounts of Molybdenum", *Carbon,* Vol. 38, pp. 1845-1856.

Kotas, T. J., 1984, "The Exergy Method of Thermal Plant Analysis", *Queen Mary College,* London.

Lattner, J. R. and M. P. Harold, 2004, "Comparison of Conventional and Membrane Reactor Fuel Processors for Hydrocarbon-Based PEM Fuel Cell Systems", *International Journal of Hydrocarbon Energy*, Vol. 29, pp. 393-417.

Ledjeff- Hey, K., V. Formanski, T. Kalk, and K. J. Roes, 1998, "Compact Hydrogen Production Systems for Solid Polymer Fuel Cells", Journal of Power Sources, Vol. 71, pp. 199-207.

Levenspiel, O., 1972, "Chemical Reaction Engineering", *Wiley*, Newyork.

Li, Y., X. Li, L. Chang, D. Wu, Z. Fang, and Y. Shi, 1999, "Understanding on the Scattering Property of the Mechanical Strength Data of Solid Catalysts: A Statistical Analysis of Ion-Based High-Temperature Water-Gas Shift Catalysts", *Catalysis Today*, Vol. 51, pp. 73-84.

Lima, A. A. G., M. Nele, E. L. Moreno, and H. M. C. Andrade, 1998, "Composition Effects on the Activity of $Cu\text{-}ZnO\text{-}Al_2O_3$ Based Catalysts for the Water Gas Shift Reaction: A Statistical Approach", *Applied Catalysis A: General*, Vol. 171, pp. 31-43.

Ma, L., 1995, "Hydrogen Production from Steam Reforming Light Hydrocarbons in Autothermic System", Ph.D. Thesis, University of New South Wales.

Ma, L. and D. L. Trimm, 1996, "Alternative Catalyst Bed Configurations for the Autothermic Conversion of Methane to Hydrogen", *Applied Catalysis A: General,* Vol. 138, pp. 265-273.

Mert, S. O., I. Dıncer, Z. Ozcelik, 2007, "Exergoeconomic Analysis of a Vehicular PEM Fuel Cell system", *Journal of Power Souces*, Vol. 165, pp. 244-252.

Nagata, Y., 2005, "Quantitative Analysis of CO_2 Emissions Reductions Through Introduction of Stationary-Type PEM-FC Systems in Japan", *Energy*, Vol. 30, pp. 2636-2653.

Natesakhawat, S., X. Wang, L. Zhang, U. S. Ozkan, 2006, "Development of Chromium-Free Iron-Based Catalysts for High-Temperature Water-Gas Shift Reaction", *Journal of Molecular Catalysis A: Chemical,* Vol. 260, pp. 82-94.

O'Connor, R. P., E. J. Klein and L. D. Schmidt, 2000, "High Yields of Synthesis Gas by Millisecond Partial Oxidation of Higher Hydrocarbons", *Catalysis Letters*, Vol. 70, pp. 99-107.

Özkara, Ş., and A. E. Aksoylu, 2003, "Selective Low Temperature Carbon Monoxide Oxidation in H_2-Rich Gas Streams over Activated Carbon Supported Catalysts", *Applied Catalysis A: General*, Vol. 251, pp. 75-83.

Pokojski, M., 2000, "The First Demonstration of the 250-kW Polymer Electrolyte Fuel Cell for Stationary Application (Berlin)", *Journal of Power Sources*, Vol. 86, pp. 140-144.

Ralph, T. R., 1999, "Clean Fuel Cell Energy for Today", *Platinum Metals Review,* Vol. 43, pp. 14-17.

Ralph, T. R. and G. A. Hards, 1998, "Powering the Cars and Homes of Tomorrow", *Chemistry & Industry*, Vol. 9, pp. 337-342

Selen, B., 2003, "Production of Hydrogen from Light Hydrocarbons Via Indirect Partial Oxidation on Bimetallic Catalysts", M.S. Thesis, Boğaziçi University.

Sinnott, R. K., J. M. Coulson, J. F. Richardson, 1983, "Chemical Engineering", *Pergamon,* Oxford.

Song, C., 2002, "Fuel Processing for Low-Temperature and High-Temperature Fuel Cells: Challenges, and Opportunities for Sustainable Development in the 21st Century", *Catalysis Today*, Vol. 77, pp. 17-49.

Şimşek, E., 2005, "Preferential CO Oxidation over Activated Carbon Supported Noble Metal Reducible Oxide Catalysts", M.S. Thesis, Boğaziçi University.

Şimşek, E., Ş. Özkara, A. E. Aksoylu and Z. I. Önsan, 2007, "Preferential CO Oxidation over Activated Carbon Supported Catalysts in H_2-Rich Gas Streams Containing CO_2 and H_2O", *Applied Catalysis A: General*, Vol. 316, pp. 169-174

Trimm, D. L. and Z. İ. Önsan, 2001, "On-Board Fuel Conversion for Hydrogen-Fuel-Cell-Driven Vehicles", *Catalysis Reviews: Science and Engineering*, Vol. 43, pp. 31-84.

Tsai, A. P. and M. Yoshimura, 2001, "Highly Active Quasicrystalline Al-Cu-Fe Catalyst for Steam Reforming of Methanol", *Applied Catalysis A: General*, Vol. 214, pp. 237-241.